

SuFEx-enabled, agnostic discovery of covalent inhibitors of human neutrophil elastase

Qinheng Zheng^{a,1} Jordan L. Woehl^{b,1} Seiya Kitamura^b, Diogo Santos-Martins^c, Christopher J. Smedley^d, Gencheng Li^a, Stefano Forli^c, John E. Moses^d, Dennis W. Wolan^{b,2}, and K. Barry Sharpless^{a,2}

^aDepartment of Chemistry; ^bDepartment of Molecular Medicine; ^cDepartment of Integrative Structural and Computational Biology, Scripps Research, La Jolla, California 92037, United States; ^dLa Trobe Institute for Molecular Science, La Trobe University, Bundoora, Melbourne, VIC 3086, Australia

¹Q.Z. and J.L.W. contributed equally to this work.

²To whom correspondence may be addressed. Email: wolan@scripps.edu or sharples@scripps.edu.

This PDF file includes:

Supplementary text

Figs. S1 to S10

Tables S1 to S3

References for SI reference citations

Table of Contents

<i>Contents</i>	<i>Page</i>
1. General	S-4
2. Synthetic procedures and characterizations of new compounds	S-6
2.1. General procedures	S-6
2.2. Naphthalene-1,3,6-trisulfonyl trifluoride (2)	S-8
2.3. Naphthalene-2,3-disulfonyl difluoride (3)	S-9
2.4. Methyl 3-(fluorosulfonyl)thiophene-2-carboxylate (4)	S-11
2.5. 2,6-dichlorobenzenesulfonyl fluoride (5)	S-12
2.6. 3,4-dichlorobenzenesulfonyl fluoride (7)	S-13
2.7. 2-Iodobenzenesulfonyl fluoride (11)	S-13
2.8. [1,1'-biphenyl]-2-sulfonyl fluoride (18)	S-14
2.9. (<i>E</i>)-2-(2-(fluorosulfonyl)vinyl)benzenesulfonyl fluoride (19)	S-15
2.10. 2-(Morpholinosulfonyl)benzenesulfonyl fluoride (20)	S-16
2.11. 4-((2-(Fluorosulfonyl)phenyl)sulfonyl)piperazine-1-sulfonyl fluoride (21)	S-18
2.12. 2-((Trifluoromethyl)sulfonyl)benzenesulfonyl fluoride (22)	S-20
2.13. 2-((Perfluoropropyl)sulfonyl)benzenesulfonyl fluoride (23)	S-20
2.14. 2-(Fluorosulfonyl)phenyl fluorosulfate (24)	S-21
3. Protease activity assays and library screen	S-23
3.1. Methods	S-23
3.2. Screen results	S-23
3.3. Validation of permanent binding	S-35
3.4. Inhibitory activity of hit molecules against hCG.	S-36
4. Mass Spectrometry	S-38
4.1. Methods	S-38
4.2. Results	S-38
5. X-ray crystal structure	S-39
5.1. Methods	S-39
5.2. Results	S-40
6. Reactive docking	S-41
6.1. Methods	S-41

6.2. Results and discussion	S-41
7. Reactivities of SuFExable functional groups	S-43
8. Stability of sulfur fluoride probes against potentially reactive amino acids	S-44
9. “Refluxing aniline” test on electrophilic covalent reactive groups.	S-46
10. NMR spectra	S-49
10.1. Naphthalene-1,3,6-trisulfonyl trifluoride (2)	S-49
10.2. Naphthalene-2,3-disulfonyl difluoride (3)	S-52
10.3. Methyl 3-(fluorosulfonyl)thiophene-2-carboxylate (4)	S-55
10.4. 2,6-dichlorobenzenesulfonyl fluoride (5)	S-58
10.5. 3,4-dichlorobenzenesulfonyl fluoride (7)	S-61
10.6. 2-Iodobenzenesulfonyl fluoride (11)	S-64
10.7. [1,1'-biphenyl]-2-sulfonyl fluoride (18)	S-67
10.8. (<i>E</i>)-2-(2-(fluorosulfonyl)vinyl)benzenesulfonyl fluoride (19)	S-70
10.9. 2-(Morpholinosulfonyl)benzenesulfonyl fluoride (20)	S-73
10.10. 4-((2-(Fluorosulfonyl)phenyl)sulfonyl)piperazine-1-sulfonyl fluoride (21)	S-76
10.11. 2-((Trifluoromethyl)sulfonyl)benzenesulfonyl fluoride (22)	S-79
10.12. 2-((Perfluoropropyl)sulfonyl)benzenesulfonyl fluoride (23)	S-82
10.13. 2-(Fluorosulfonyl)phenyl fluorosulfate (24)	S-86
11. References	S-89

1. General

Synthetic reagents, catalysts, and solvents were used as purchased without further purification, unless otherwise indicated. The extent of reaction was monitored by thin-layer chromatography (TLC), performed on 250 μm silica gel G plates with F254 indicator. The TLC plates were visualized by ultraviolet light (254 nm) and treatment with potassium permanganate stain followed by gentle heating. Flash chromatography was performed using 40–63 μm (230–400 mesh) silica gel.

Unless otherwise noted, ^1H , ^{13}C , and ^{19}F NMR spectra were recorded on Bruker DRX-500, Bruker DRX-600, Bruker AMX-400 instruments. Data for ^1H NMR spectra is reported as follows: chemical shift (ppm, referenced to residual solvent peak), coupling constant (Hz), and integration. Data for ^{13}C NMR is reported in terms of chemical shift, δ (ppm) relative to residual solvent peak (CDCl_3 singlet at 77.0 ppm, DMSO multiplet at 39.5 ppm). Data for ^{19}F NMR is reported in terms of chemical shift (ppm) relative to added internal standard (CFCl_3 at 0.65 ppm) (1). Accurate mass spectrometry (a.k.a. HRMS) spectra were recorded using electrospray ionization (ESI) or atmosphere-pressure chemical ionization (APCI) with a time-of-flight (TOF) analyzer. For some entries (compounds **5**, **7**, **11**, and **18**), soft ionization like ESI and APCI failed to give a molecular ion signal. Hence, GC-MS with electron impact ionization (EI) and quadrupole analyzer was used and gave strong signals at $[\text{M}]^+$ for these compounds. Melting points were measured on a Barnstead Electrothermal 9300 digital capillary melting point apparatus and are uncorrected.

Abbreviations:

TEA	triethylamine
DCM	dichloromethane
ESF	ethenesulfonyl fluoride
iPr	isopropyl
TFA	trifluoroacetic acid
HMPA	hexamethylphosphoramide
TLC	thin-layer chromatography
EA	ethyl acetate
THF	tetrahydrofuran
DMSO	dimethyl sulfoxide

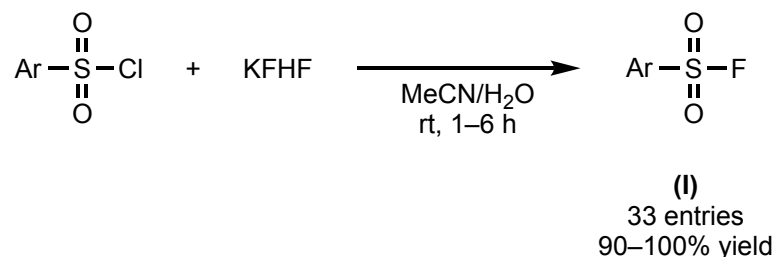
TMS	trimethylsilyl
hNE	human neutrophil elastase
hCG	human cathepsin G
rt	room temperature
MALDI	matrix-assisted laser desorption/ionization
TOF	time-of-flight
PMSF	phenylmethyl sulfonyl fluoride
DBU	1,8-diazabicyclo(5.4.0)undec-7-ene
PBS	phosphate-buffered saline
APCI	atmosphere-pressure chemical ionization
AcOH	acetic acid
MeCN	acetonitrile

2. Synthetic procedures and characterizations of new compounds

2.1. General procedures

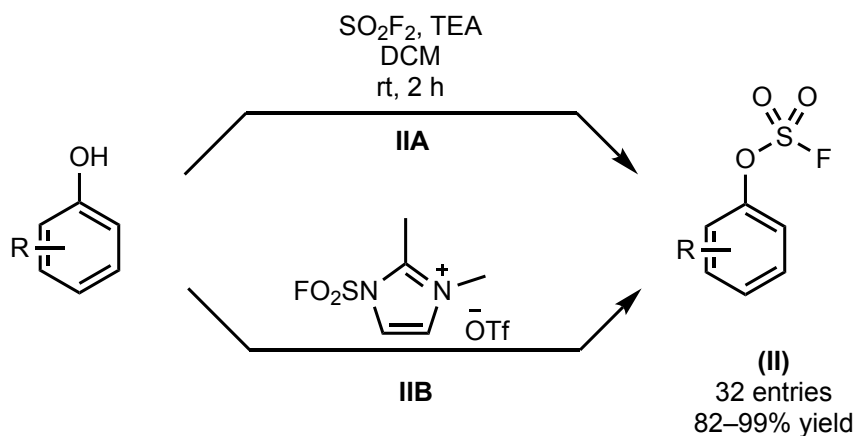
Unless otherwise noted, compounds in the SuFEx library were synthesized by the following general procedures (I, II, III, IV). Synthesis and characterizations of compounds **1**, **6**, **8–10**, and **12–17** have been reported in the literature (2-6).

(I) Synthesis of aryl sulfonyl fluorides



Procedure I (2): Aryl sulfonyl chloride (from commercial sources or synthesized by established methods) dissolved in acetonitrile (MeCN, 0.5–1 M) was treated with saturated potassium bifluoride aqueous solution (KFHF, ~5 M, 1.5–2.5 equiv). The emulsion was stirred vigorously for 1–4 h before partitioned between ethyl acetate and water. The organic solution was collected, dried over anhydrous sodium sulfate, concentrated and purified by column chromatography, if necessary, to yield desired aryl sulfonyl fluoride (33 examples, 90–100% isolated yield).

(II) Synthesis of aryl fluorosulfates

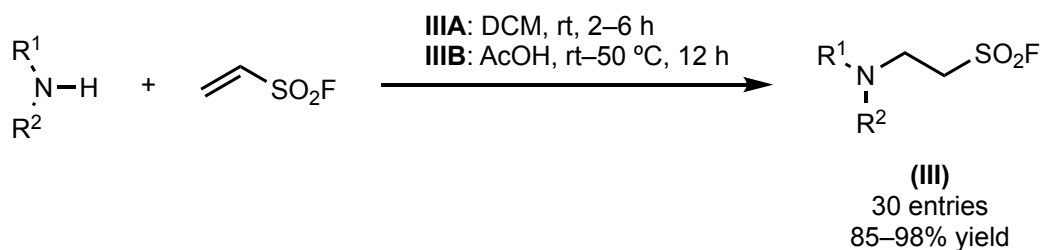


Procedure IIA (2): (CAUTION: the reaction must be performed in a well vented fume hood. Sulfuryl fluoride gas is toxic.) Phenols (from commercial sources), and triethylamine (TEA, 1.5 equiv) were dissolved in DCM. The flask sealed with a rubber septum was evacuated, and a balloon filled with sulfuryl fluoride gas was introduced to the flask *via* a needle. The reaction was stirred

vigorously for 2 h. Upon completion, solvent was removed *in vacuo*. The residue was partitioned between ethyl acetate and water. The organic phase was washed with brine, dried over anhydrous sodium sulfate, then concentrated and purified by flash column chromatography to give desired aryl fluorosulfate (32 examples, 82–99% isolated yield).

Procedure IIB (7): Phenols (from commercial sources), and *N*-fluorosulfonyl *N'*-methyl-2-methylimidazolium triflate (1.2 equiv) were dissolved in MeCN (0.1–1 M). TEA (1.5 equiv) was added dropwise *via* a syringe. The reaction was stirred at room temperature for 1 h. Upon completion, solvent was removed *in vacuo*. The residue was partitioned between ethyl acetate and water. The organic phase was washed with brine, dried over anhydrous sodium sulfate, then concentrated and purified by flash column chromatography to give desired aryl fluorosulfate (32 examples, 82–99% isolated yield).

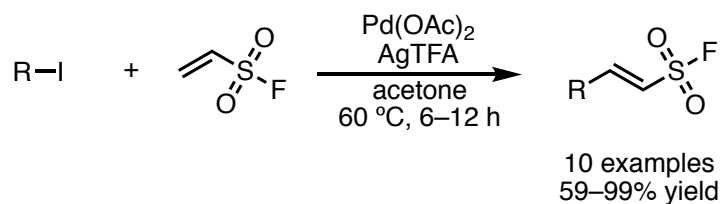
(III) Synthesis of alkyl sulfonyl fluorides by Michael addition



Procedure IIIA (2, 8): To a solution of primary or secondary alkyl amine in DCM (0.5–1 M), ethenesulfonyl fluoride (ESF, 2.2 equiv) was added dropwise (exotherm). The mixture was stirred at autogenous temperature for 6–12 h. Upon completion, volatiles were removed *in vacuo*. The residue was purified by flash column chromatography to give desired sulfonyl fluoride adducts of primary or secondary amines. (30 examples, 85–98% isolated yield).

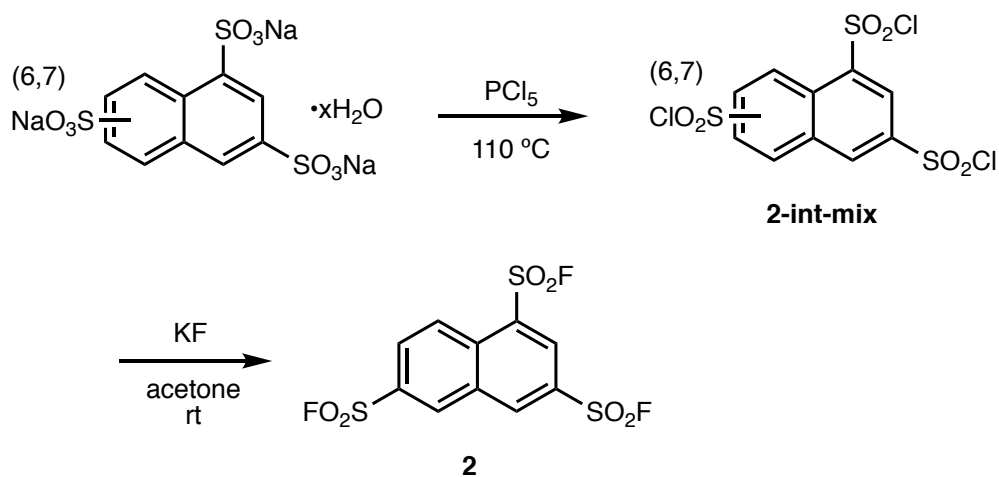
Procedure IIIB (2, 8): Anilines and ESF (2.2 equiv) were dissolved (or suspended at starting point) in glacial acetic acid (AcOH, 10 mmol per 1 mmol). The mixture was heated to 50 °C (or 80 °C if necessary) for 12 h. Upon completion, volatiles were removed *in vacuo*. The residue was purified by either recrystallization in ethanol or flash column chromatography to give desired sulfonyl fluoride adducts of anilines (30 examples, 85–98% isolated yield).

(IV) Synthesis of vinyl sulfonyl fluorides



Procedure IV (9): An oven-dried vessel was charged with (hetero)aryl iodide, silver (I) trifluoroacetate (AgTFA, 1.2 equiv), palladium (II) acetate (Pd(OAc)₂, 2 mol%), acetone, and ESF (2 equiv). The resulting mixture was refluxed at 60 °C. Upon full conversion of (hetero)aryl iodide (6–12 h), solvent was removed *in vacuo*. The crude was purified by flash column chromatography to give the desired product (10 examples, 59–99% yield).

2.2. Naphthalene-1,3,6-trisulfonyl trifluoride (2)



A 100-mL round bottom flask equipped with a condenser was charged with naphthalene-1,3,(6,7)-trisulfonic acid trisodium salt hydrate (mixture of two regio-isomers, 4.34 g, < 10 mmol), and phosphorus pentachloride (PCl₅, 21 g, 100 mmol). Upon shaking of the flask, fume evolution and exotherm were observed. The mixture liquefied after heated at 110 °C for about 0.5 h. The reaction was stirred at 110 °C overnight and cooled to room temperature. The yellow suspension was poured with care onto crushed ice (200 g). The mixture was extracted with chloroform (150 mL x 3). The combined organic phase was washed by brine and dried over anhydrous sodium sulfate before evaporated to a yellow solid crude (**2-int-mix**).

The crude sulfonyl chloride was mixed with potassium fluoride (11.6 g, 200 mmol) in a 500-mL round bottom flask. Acetone (200 mL) was added and the resulting suspension was stirred overnight. Volatiles were removed in *vacuo*, and the solid was partitioned with chloroform/water. The organic phase was collected, concentrated and purified by column chromatography (SiO₂,

eluted with hexanes to 20% ethyl acetate (EA) in hexanes). The titled compound was isolated as a white crystalline (**2**, 1.53 g, 41% yield over 2 steps, not corrected for the contamination of water in starting material).

$^1\text{H NMR}$ (500 MHz, CDCl_3) δ 9.17 (d, $J = 1.3$ Hz, 1H), 9.01 (d, $J = 1.9$ Hz, 1H), 8.99 (d, $J = 1.8$ Hz, 1H), 8.96 (dd, $J = 9.1, 1.8$ Hz, 1H), 8.50 (dd, $J = 9.1, 2.0$ Hz, 1H).

$^{13}\text{C NMR}$ (126 MHz, CDCl_3) δ 139.6, 134.8 (d, $J_{\text{CF}} = 27.7$ Hz), 133.5, 133.1, 132.9, 132.2, 132.0, 131.1 (d, $J_{\text{CF}} = 2.5$ Hz), 130.1, 127.6.

$^{19}\text{F NMR}$ (377 MHz, CDCl_3) δ 67.7, 66.8, 64.9.

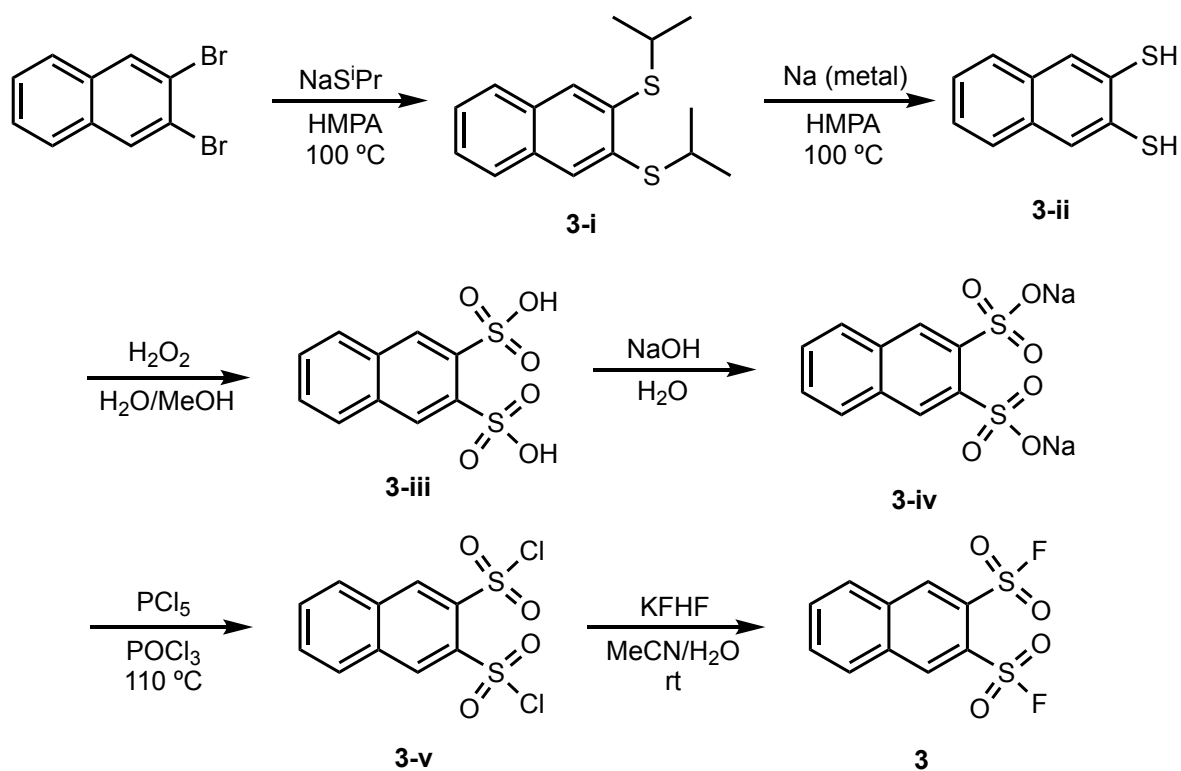
TLC $R_f = 0.65$ (17% EA in hexanes).

Melting point 124 – 126 °C.

Mass Spectrometry APCI-TOF accurate mass calculated for $\text{C}_{10}\text{H}_5\text{F}_3\text{O}_6\text{S}_3$ $[\text{M}]^-$ 373.9206, found 373.9213.

HPLC purity (280 nm) 96.8% ($t_R = 5.320$ min).

2.3. Naphthalene-2,3-disulfonyl difluoride (**3**)



A 250-mL round bottom flask equipped with a stir bar was charged with 2,3-dibromonaphthalene (1.1 g, 3.82 mmol), and sodium 2-propylthiolate (NaSⁱPr, 90% tech. grade,

1.66 g, 15.3 mmol). Hexamethylphosphoramide (HMPA, 20 mL, anhydrous, stored over 4 Å molecular sieves) was added under N₂. Upon heating to 100 °C, the suspension was rapidly stirred and turned into an orange solution, and about 15 min later to another suspension. The suspension was stirred for 8 h and cooled to room temperature. The mixture was partitioned between ether (100 mL) and water (100 mL). The aqueous phase was further extracted by ether (50 mL x 2). All the organic phase was combined, washed with water (150 mL x 2) and brine (150 mL). Solvent was removed *in vacuo* giving crude thioether (**3-i**). ¹H NMR (500 MHz, Chloroform-*d*) δ 7.76 (s, 2H), 7.72 (dd, *J* = 6.2, 3.3 Hz, 2H), 7.42 (dd, *J* = 6.2, 3.2 Hz, 2H), 3.59 (hept, *J* = 6.7 Hz, 2H), 1.39 (d, *J* = 6.7 Hz, 12H). ¹³C NMR (126 MHz, CDCl₃) δ 135.8, 132.3, 129.2, 127.0, 126.2, 37.4, 23.0.

The crude product (>95 % purity by ¹H NMR) was dissolved in HMPA (20 mL). Under N₂ stream, freshly cut sodium strips (about 0.3 g, 10 mmol) were added with care over 15 min. A dark solution was obtained, which was further stirred at 100 °C overnight. The reaction gradually turned light-yellow. The mixture was cooled to room temperature, and concentrated HCl was added dropwise (Be very careful!) to adjust the pH lower than 3. The resulting suspension was partitioned between tert-butyl methyl ether (100 mL) and water (100 mL). The organic phase was washed by water (100 mL x 2) and brine (100 mL) and concentrated to a yellow solid crude (**3-ii**, 0.83 g, 4.3 mmol, >100% over 2 steps, HMPA contaminated). ¹H NMR (400 MHz, CDCl₃) δ 7.90 (s, 2H), 7.66 (dd, *J* = 6.3, 3.2 Hz, 2H), 7.41 (dd, *J* = 6.3, 3.2 Hz, 2H), 3.88 (s, 2H).

The yellow solid was suspended on methanol (10 mL). Gentle heating at 50 °C helped to dissolve the thiophenol. After cooling to room temperature, hydrogen peroxide (H₂O₂, 30% wt., 10 mL, ~ 40 equiv) was added into the solution. This process was found to be exothermic, and precipitates formed instantly. The yellow suspension was stirred at room temperature, turned into a thick porridge after 3 h, and then a clear yellow solution overnight. After 24 h, the clean conversion to **3-iii** was determined by ¹H NMR. ¹H NMR (400 MHz, Methanol-*d*₄) δ 8.68 (s, 1H), 8.01 (dd, *J* = 6.1, 3.2 Hz, 1H), 7.67 (dd, *J* = 6.2, 3.2 Hz, 1H).

The pH of the acid solution was adjusted with 2 M NaOH (3 mL) to over 8 (exothermic process). Catalytic amount of manganese dioxide (25 mg) was added to digest the excess H₂O₂ (10). When oxygen gas evolution ceased (usually at least 4 h), the solvent was removed *in vacuo*, and the crude product being azeotropically dried by toluene (25 mL x 3).

Naphthalene-2,3-disulfonic acid disodium salt, with MnO₂ contaminated, was mixed with PCl₅ (1.5 g, 7.2 mmol) in a 100-mL round bottom flask. Reaction occurred instantly releasing heat and fume (CAUTION!). The mixture was heated at 110 °C for 6 h, then cooled to room temperature and poured onto crushed ice (50 g). The precipitated sulfonyl chloride was extracted by CHCl₃ (100 mL) and washed sequentially by cold water (100 mL), brine (100 mL). The crude product was not stable on silica gel (i.e., TLC or column). ¹H NMR showed > 90% purity. ¹H NMR (400 MHz, CDCl₃) δ 8.98 (s, 1H), 8.21 (dd, *J* = 6.2, 3.3 Hz, 1H), 7.98 (dd, 1H).

Naphthalene-2,3-disulfonyl chloride (**3-v**) was dissolved in acetone (20 mL, insoluble in MeCN) and treated by finely powdered potassium fluoride (KF, 464 mg, 8.00 mmol). The suspension was stirred overnight, and then concentrated. The crude was partitioned between CHCl₃ and water. The organic phase was collected, concentrated, and purified by column chromatography (SiO₂, 10% to 33% EA in hexanes) to give the titled compound as a yellow solid (**3**, 208 mg, 0.711 mmol, 19% over 6 steps).

¹H NMR (600 MHz, CDCl₃) δ 9.00 – 8.96 (m, 2H), 8.20 (dt, *J* = 6.4, 3.2 Hz, 2H), 8.02 – 7.97 (m, 2H).

¹³C NMR (151 MHz, CDCl₃) δ 137.2, 133.7, 132.9, 130.2, 126.8 (d, *J*_{CF} = 30.2 Hz).

¹⁹F NMR (377 MHz, CDCl₃) δ 72.8.

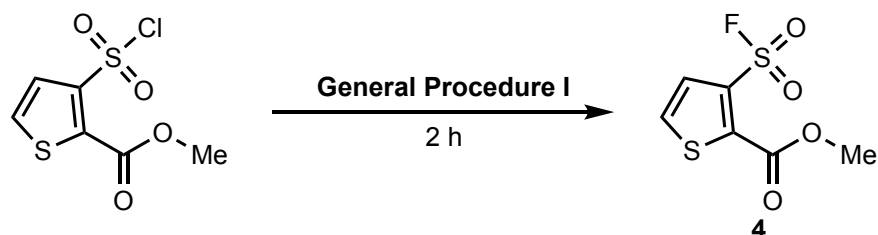
TLC *R*_f = 0.52 (33% EA in hexanes, UV).

Melting point 156 – 158 °C (ether).

Mass spectrometry APCI-TOF accurate mass calculated for C₁₀H₆F₂O₄S₂NH₄ [M + NH₄]⁺ 310.0014, found 310.0013.

HPLC purity (280 nm) 92.3% (*t*_R = 5.210 min).

2.4. Methyl 3-(fluorosulfonyl)thiophene-2-carboxylate (**4**)



The title compound was synthesized by **General Procedure I**. Saturated KFHF solution effected the conversion of methyl 3-(chlorosulfonyl)thiophene-2-carboxylate (Combi-Blocks,

1.20 g, 5.00 mmol) to methyl 3-(fluorosulfonyl)thiophene-2-carboxylate (**4**, 1.06 g, 4.73 mmol, 95%) as a brown solid.

¹H NMR (600 MHz, CDCl₃) δ 7.65 (dd, *J* = 5.3, 0.6 Hz, 1H), 7.61 (d, *J* = 5.3 Hz, 1H), 3.99 (s, 3H).

¹³C NMR (151 MHz, CDCl₃) δ 159.1, 137.3, 134.6 (d, *J*_{CF} = 30.2 Hz), 130.9 (d, *J*_{CF} = 1.5 Hz), 130.6 (d, *J*_{CF} = 1.5 Hz), 53.6.

¹⁹F NMR (377 MHz, CDCl₃) δ 63.0.

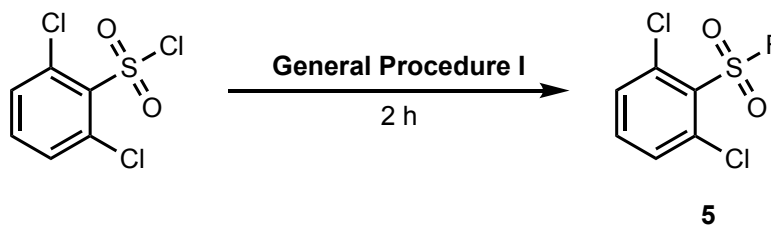
TLC *R*_f = 0.26 (17% EA in hexanes, UV).

Melting point 78 – 80 °C (decomposed).

Mass spectrometry ESI-TOF accurate mass calculated for C₆H₅FO₄S₂Na [M + Na]⁺ 246.9505, found 246.9505.

HPLC purity (254 nm) 100% (*t*_R = 4.307 min).

2.5. 2,6-dichlorobenzenesulfonyl fluoride (**5**)



The title compound was synthesized by General Procedure I. Saturated potassium bifluoride solution effected the conversion of 2,6-dichlorobenzenesulfonyl chloride (Combi-Blocks, 1.23 g, 5.00 mmol) to 2,6-dichlorobenzenesulfonyl fluoride (**5**, 1.11 g, 4.85 mmol, 97%) as a yellow crystalline.

¹H NMR (600 MHz, CDCl₃) δ 7.63 – 7.44 (m, 3H).

¹³C NMR (151 MHz, CDCl₃) δ 136.2, 135.0, 131.6, 131.0 (d, *J*_{CF} = 24.2 Hz).

¹⁹F NMR (377 MHz, CDCl₃) δ 68.2.

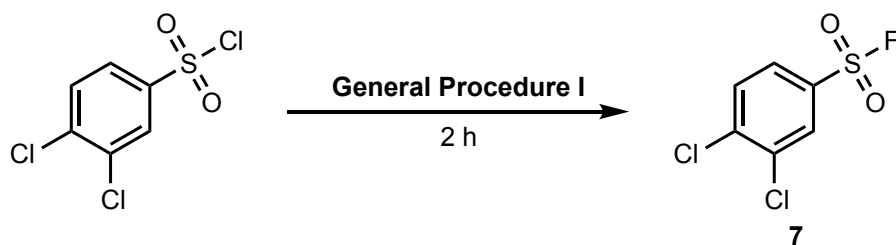
TLC *R*_f = 0.47 (17% EA in hexanes, UV).

Melting point 70 – 72 °C (hexane/EA).

Mass spectrometry EI-Q mass calculated for C₆H₃Cl₂FO₂S [M]⁺ 227.92, found 227.9 (100), 132.9 (80), 229.9 (78), 109.0 (61), 74.0 (53), 160.9 (38), 144.9 (43).

HPLC purity (280 nm) 97.8% (*t*_R = 4.775 min).

2.6. 3,4-dichlorobenzenesulfonyl fluoride (**7**)



The title compound was synthesized by **General Procedure I**. Saturated KFHF solution effected the conversion of 3,4-dichlorobenzenesulfonyl chloride (Combi-Blocks, 1.23 g, 5.00 mmol) to 3,4-dichlorobenzenesulfonyl fluoride (**7**, 1.03 g, 4.50 mmol, 90%) as a colorless liquid. $^1\text{H NMR}$ (600 MHz, CDCl_3) δ 8.10 (d, $J = 2.2$ Hz, 1H), 7.85 (dd, $J = 8.5, 2.2$ Hz, 1H), 7.73 (dd, $J = 8.5, 1.0$ Hz, 1H).

$^{13}\text{C NMR}$ (151 MHz, CDCl_3) δ 140.7, 134.2, 132.0 (d, $J_{\text{CF}} = 27.2$ Hz), 131.3, 129.8, 126.9.

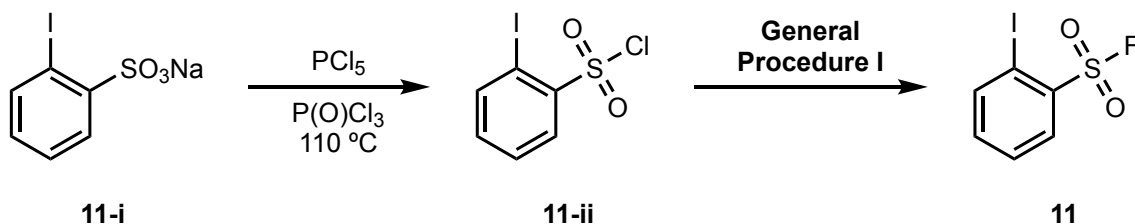
$^{19}\text{F NMR}$ (377 MHz, CDCl_3) δ 66.89, 0.65.

TLC $R_f = 0.50$ (9% EA in hexanes, UV).

Mass spectrometry EI-MS calculated for $\text{C}_6\text{H}_3\text{Cl}_2\text{FO}_2\text{S}$ $[\text{M}]^+$ 227.92, found 227.9.

HPLC purity (254 nm) 98.0% ($t_R = 4.977$ min).

2.7. 2-Iodobenzenesulfonyl fluoride (**11**)



Commercially available 2-iodobenzene sulfonic acid hydrate (Alfa-Aesar) was neutralized with sodium bicarbonate (NaHCO_3) and gave 2-iodobenzene sulfonic acid sodium salt (**11-i**) as a brown crystalline. A 100-mL round bottom flask equipped with a condenser and a tail gas absorbing water tank was charged with 2-iodobenzene sulfonic acid sodium salt (5.00 g, 16.3 mmol) and PCl_5 (5.10 g, 24.5 mmol). The solid mixture liquefied partially after being shaken with strong exotherm. Phosphoryl chloride ($\text{P}(\text{O})\text{Cl}_3$, 2 mL) was added to help the stirring of the syrup-like viscous mixture. The reaction was heated at 110 °C for 4 h then cooled to room temperature. The dark red

mixture was poured onto ice (150 g) and was extracted with ether (100 mL x 3). The organic phase was washed with cold water and dried over anhydrous Na₂SO₄. TLC indicated the purity of the crude product (**11-ii**) about 90%. The ether solution was concentrated, and the remaining thick oil was re-dissolved into MeCN (10 mL). Saturated KFHF solution (~ 5 mol L⁻¹, 6.5 mL) was added, and the resulting biphasic mixture being stirred into an emulsion for 3 h. The mixture was partitioned between water (100 mL) and EA (100 mL). The organic phase was concentrated and purified by column chromatography (SiO₂, hexanes to 17% EA in hexanes) to give an off-white crystalline (**11**, 2.73 g, 9.54 mmol, 59% over 3 steps).

¹H NMR (500 MHz, CDCl₃) δ 8.18 (dd, *J* = 7.9, 1.1 Hz, 1H), 8.15 (dd, *J* = 8.0, 1.5 Hz, 1H), 7.59 (tt, *J* = 7.9, 1.3 Hz, 1H), 7.38 (td, *J* = 7.7, 1.6 Hz, 1H).

¹³C NMR (126 MHz, CDCl₃) δ 143.3, 137.8 (d, *J*_{CF} = 28.7 Hz), 135.8, 132.1 (d, *J*_{CF} = 1.3 Hz), 128.8, 92.3.

¹⁹F NMR (377 MHz, CDCl₃) δ 56.9.

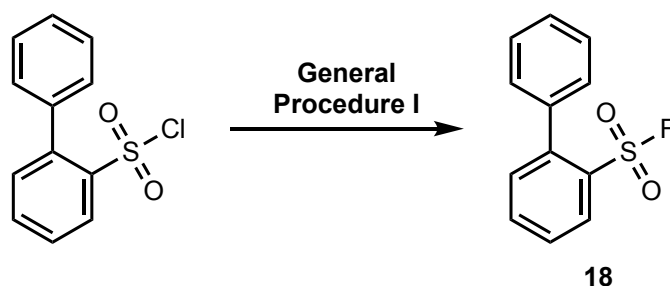
TLC *R*_f = 0.58 (17% EA in hexanes, UV).

Melting point 61 – 62 °C (MeOH).

Mass spectrometry EI-MS calculated for C₆H₄FIO₂S [M]⁺ 285.9, found 285.6.

HPLC purity (280 nm) 96.2% (*t*_R = 5.088 min).

2.8. [1,1'-biphenyl]-2-sulfonyl fluoride (**18**)



The title compound was synthesized by **General Procedure I**. Saturated KFHF solution effected the conversion of [1,1'-biphenyl]-2-sulfonyl chloride (Alfa-Aesar, 1.25 g, 5.00 mmol) to [1,1'-biphenyl]-2-sulfonyl fluoride (**18**, 1.10 g, 4.66 mmol, 93%) as a white crystalline.

¹H NMR (600 MHz, CDCl₃) δ 8.19 (d, *J* = 8.0 Hz, 1H), 7.76 (t, *J* = 7.6 Hz, 1H), 7.60 (t, *J* = 7.8 Hz, 1H), 7.51 – 7.43 (m, 5H), 7.41 – 7.35 (m, 3H).

¹³C NMR (151 MHz, CDCl₃) δ 143.2, 138.0, 134.9, 133.2 (d, *J*_{CF} = 1.5 Hz), 132.5 (d, *J*_{CF} = 22.7 Hz), 130.1 (d, *J*_{CF} = 1.5 Hz), 129.1 (d, *J*_{CF} = 1.5 Hz), 128.7, 128.2 (d, *J*_{CF} = 10.6 Hz).

^{19}F NMR (377 MHz, CDCl_3) δ 67.6.

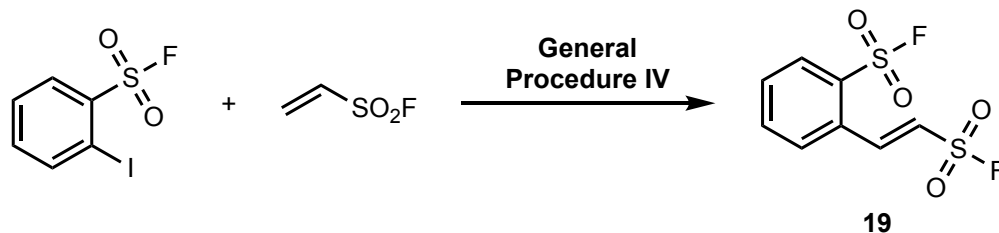
TLC R_f = 0.60 (17% EA in hexanes).

Melting point 76 – 77 °C (EA).

Mass spectrometry EI-MS calculated for $\text{C}_{12}\text{H}_9\text{FO}_2\text{S}$ $[\text{M}]^+$ 236.0, found 235.8.

HPLC purity (280 nm) 98.8% (t_R = 5.320 min).

2.9. (*E*)-2-(2-(fluorosulfonyl)vinyl)benzenesulfonyl fluoride (**19**)



The title compound was synthesized by **General Procedure IV**. $\text{Pd}(\text{OAc})_2/\text{AgTFA}$ effected the conversion of **11** (286 g, 1.00 mmol) and ESF (220 mg, 2.00 mmol) to (*E*)-2-(2-(fluorosulfonyl)vinyl) benzenesulfonyl fluoride (**19**, 173.8 mg, 0.648 mmol, 65%) as a white crystalline.

^1H NMR (600 MHz, CDCl_3) δ 8.50 (d, J = 15.3 Hz, 1H), 8.22 (d, J = 7.9 Hz, 1H), 7.88 (t, J = 7.6 Hz, 1H), 7.78 (dd, J = 12.8, 7.7 Hz, 3H), 6.98 – 6.91 (m, 1H).

^{13}C NMR (151 MHz, CDCl_3) δ 143.2, 136.1, 132.8 (d, J_{CF} = 25.7 Hz), 132.3, 131.6, 131.3, 129.7, 124.8 (d, J_{CF} = 30.2 Hz), 117.4 (d, J_{CF} = 336.73 Hz).

^{19}F NMR (377 MHz, CDCl_3) δ 67.1, 61.6.

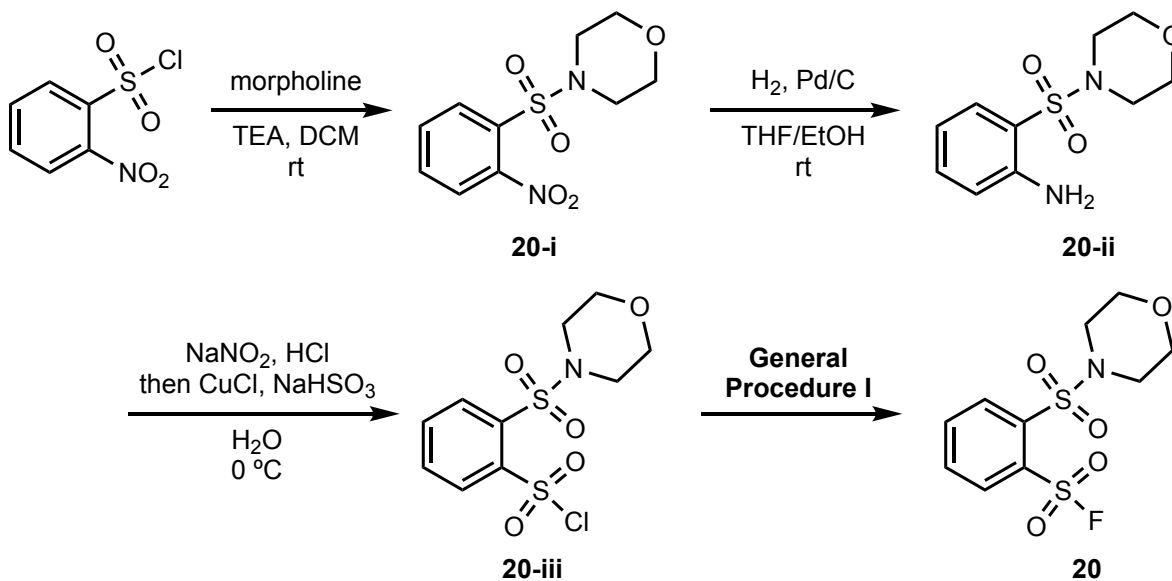
TLC R_f = 0.50 (33% EA in hexanes, UV).

Melting point 91 – 92 °C (hexanes/EA).

Mass spectrometry APCI-TOF accurate mass calculated for $\text{C}_8\text{H}_6\text{F}_2\text{O}_4\text{S}_2$ $[\text{M}]^-$ 267.9681, found 267.9678.

HPLC purity (280 nm) 98.3% (t_R = 5.013 min).

2.10. 2-(Morpholinosophonyl)benzenesulfonyl fluoride (**20**)



A 4-mL vial equipped with an egg-shape stir bar was charged with 2-nitrobenzenesulfonyl chloride (222 mg, 1.00 mmol), morpholine (95.8 mg, 1.10 mmol), and DCM (1.0 mL). TEA (152 mg, 1.50 mmol) was added dropwise to give a yellow suspension. The mixture was stirred at room temperature for 4 h, before being partitioned between HCl (1 M, 50 mL) and EA (50 mL). The organic phase was collected and concentrated to give virtually pure sulfonamide (**20-i**, 270 mg, 0.99 mmol).

Into a reaction tube, the crude sulfonamide (270 mg), palladium on carbon (27 mg, 10% wt.), tetrahydrofuran (THF, 2 mL) and EtOH (2 mL) were added. Hydrogen gas (balloon) was introduced *via* a syringe, and bubbled for 10 min. The suspension was stirred under hydrogen for another 6 h, before being diluted with MeOH (50 mL). The methanolic solution was passed through a pad of Celite and concentrated to give a yellow oil (**20-ii**).

A 20-mL scintillation vial was charged with the crude aniline. Concentrated hydrochloric acid (0.4 mL) was added, and the suspension was cooled to 0 °C. At the same temperature, sodium nitrite solution (NaNO₂, 40% wt., 0.4 mL) was added dropwise via a syringe. The diazotization process took 30 min to complete at 0 °C. In another 20-mL scintillation vial, copper(I) chloride (CuCl, 30 mg, 0.31 mmol) was dissolved in concentrated HCl (1 mL), and to which, sodium bisulfite solution (40%, 1 mL) was added dropwise to make a yellow suspension. The diazonium solution was added to the SO₂ solution at 0 °C *via* a glass pipette dropwise. The resulting mixture was allowed to be warmed to 5–10 °C and was stirred for an additional 30 min, before being

extracted by DCM (20 mL). Concentration of the DCM solution gave crude sulfonyl chloride (**20-iii**, ~ 80% purity).

The crude sulfonyl chloride was dissolved into MeCN (2 mL) and treated with saturated KFHF solution (1 mL). The biphasic mixture was stirred at room temperature for 2 h and partitioned between EA (50 mL) and water (50 mL). The organic phase was concentrated and purified by chromatography to give the titled compound as a yellow solid (**20**, 142 mg, 0.459 mmol, 46% over 4 steps).

¹H NMR (600 MHz, CDCl₃) δ 8.35 (dd, $J = 7.9, 1.4$ Hz, 1H), 8.24 (dd, $J = 7.9, 1.4$ Hz, 1H), 7.91 (td, $J = 7.7, 1.4$ Hz, 1H), 7.84 (tt, $J = 7.7, 1.3$ Hz, 1H), 3.75 – 3.71 (m, 4H), 3.34 – 3.29 (m, 4H).

¹³C NMR (151 MHz, CDCl₃) δ 138.5, 135.4, 133.5, 133.2, 132.9 (d, $J = 1.5$ Hz), 132.1 (d, $J = 27.2$ Hz), 66.46, 46.14.

¹⁹F NMR (377 MHz, CDCl₃) δ 64.0.

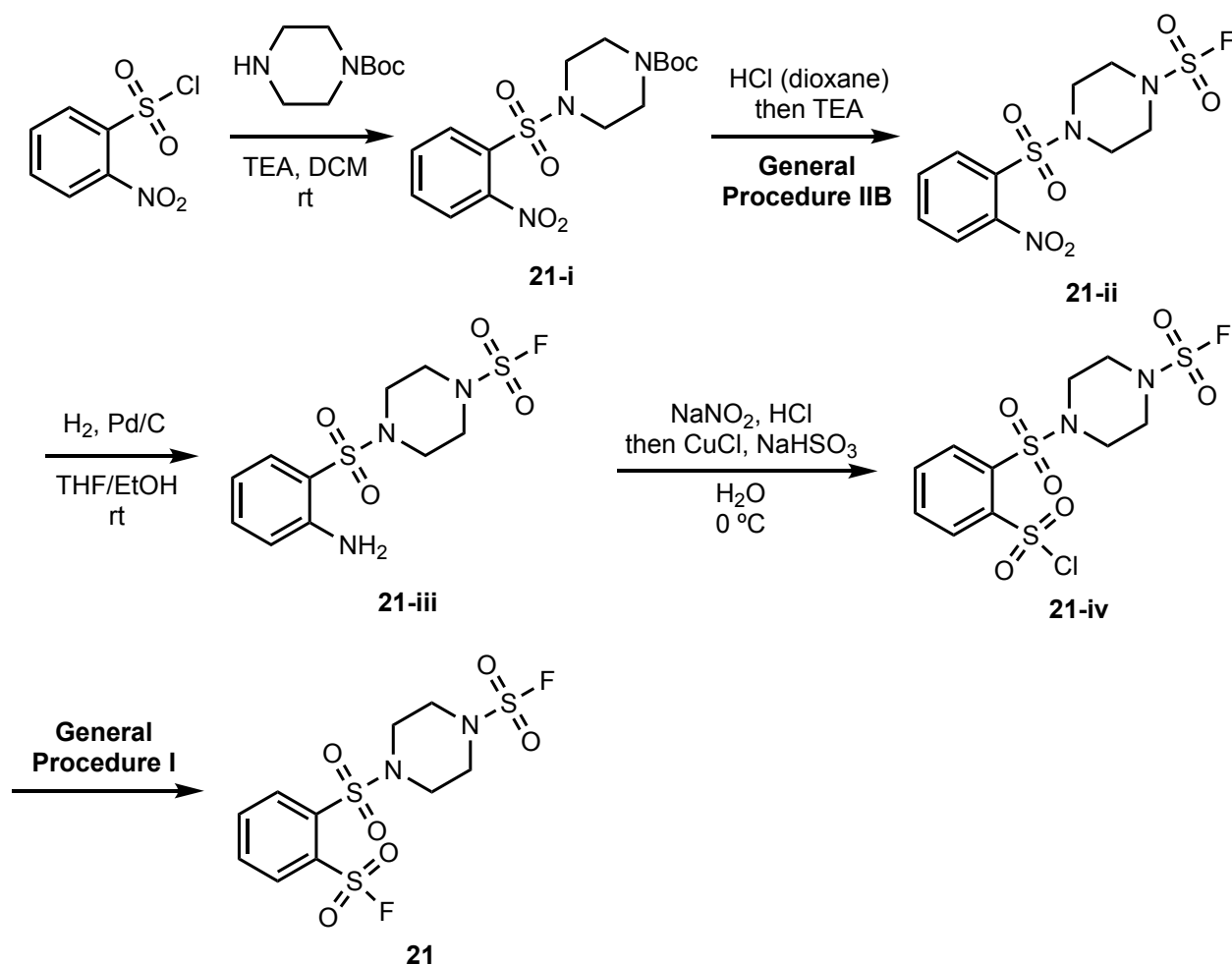
TLC $R_f = 0.32$ (50% EA in hexanes, UV).

Melting point 135 – 138 °C.

Mass spectrometry Accurate mass (ESI-TOF) calculated for C₁₀H₁₃FNO₅S₂ [M + H]⁺ 310.0214, found 310.0212.

HPLC purity (280 nm) 96.8% ($t_R = 4.257$ min).

2.11. 4-((2-(Fluorosulfonyl)phenyl)sulfonyl)piperazine-1-sulfonyl fluoride (**21**)



A 4-mL vial equipped with an egg-shape stir bar was charged with 2-nitrobenzenesulfonyl chloride (222 mg, 1.00 mmol), *N*-Boc-piperazine (205 mg, 1.10 mmol), and DCM (1.0 mL). TEA (152 mg, 1.50 mmol) was added dropwise to give a yellow suspension. The mixture was stirred at room temperature for 4 h, before being partitioned between HCl (0.1 mol L⁻¹, 50 mL) and EA (50 mL). The organic phase was collected and concentrated to give virtually pure sulfonamide product (**21-i**, 364 mg, 0.98 mmol).

The crude sulfonamide was treated with HCl in 1,4-dioxane (4 M, 10 mL) overnight, and the Boc group was cleanly cleaved. The resulting hydrochloride salt was obtained in >98% purity by evaporation, and then mixed with 2,3-dimethyl-1-fluorosulfonylimidazolium triflate (492 mg, 1.50 mmol) in a 20-mL scintillation vial. Acetonitrile (5 mL) and triethylamine (303 mg, 3.00 mmol) were added, and the solution was stirred for 3 h at room temperature before being quenched with water. The sulfamoyl fluoride (**21-ii**) was isolated by column chromatography as a white

crystalline (328 mg, 0.921 mmol, 92% over 2 steps). The structure of this compound was determined by NMR and LRMS.

Into a reaction tube, the crude sulfamoyl fluoride (328 mg, 0.921 mmol), palladium on carbon (27 mg, 10% wt.), tetrahydrofuran (2 mL) and ethanol (2 mL) were added. Hydrogen gas was introduced by a balloon, and bubbled for 10 min. The suspension was stirred under hydrogen for another 6 h, before being diluted by methanol (50 mL). The methanolic solution was passed through a pad of Celite and concentrated to give a yellow solid (**21-iii**).

A 20-mL scintillation vial was charged with the crude aniline (**21-iii**). Concentrated hydrochloric acid (0.4 mL) was added, and the suspension was cooled to 0 °C. At the same temperature, sodium nitrite solution (40%, 0.4 mL) was added dropwise via a syringe. The diazotization process took 30 min to complete at 0 °C. In another 20-mL scintillation vial, copper(I) chloride (30 mg, 0.31 mmol) was dissolved in hydrochloric acid (1 mL), and to which, sodium bisulfite solution (40%, 1 mL) was added dropwise to make a yellow suspension. The diazonium solution was added dropwise to the SO₂ solution at 0 °C *via* a glass pipette. The resulting mixture was allowed to be warmed to 5–10 °C and stirred for a further 30 min, before being extracted by dichloromethane (20 mL). Concentration of the dichloromethane solution gave crude sulfonyl chloride (**21-iv**, ~ 80% purity).

The crude sulfonyl chloride (**21-iv**) was dissolved into acetonitrile (2 mL) and treated with saturated potassium bifluoride solution (1 mL). The biphasic mixture was stirred at room temperature for 2 h and partitioned between ethyl acetate (50 mL) and water (50 mL). The organic phase was concentrated and purified by chromatography to give the titled compound as an off-white solid (**21**, 210 mg, 0.538 mmol, 58% over 3 steps).

¹H NMR (600 MHz, CDCl₃) δ 8.36 (dd, J = 7.9, 1.4 Hz, 1H), 8.31 (dd, J = 7.8, 1.4 Hz, 1H), 7.94 (td, J = 7.7, 1.4 Hz, 1H), 7.90 – 7.86 (m, 1H), 3.54 (dd, J = 7.2, 3.1 Hz, 4H), 3.51 (dd, J = 6.6, 3.6 Hz, 4H).

¹³C NMR (151 MHz, CDCl₃) δ 138.4, 135.7, 134.0, 133.4, 133.2 (d, J = 1.5 Hz), 131.8 (d, J = 25.7 Hz), 46.8, 45.0.

¹⁹F NMR (377 MHz, CDCl₃) δ 64.1, 41.4.

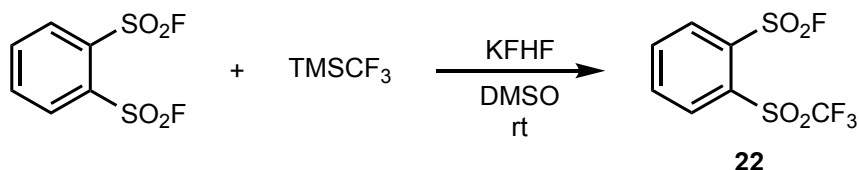
TLC R_f = 0.34 (33% ethyl acetate in hexanes, UV).

Melting point 175 – 177 °C.

Mass spectrometry APCI-TOF accurate mass calculated for $C_{10}H_{12}F_2N_2O_6S_3NH_4$ $[M + NH_4]^+$ 408.0164, found 408.0160.

HPLC purity (254 nm) 96.4% ($t_R = 4.594$ min).

2.12. 2-((Trifluoromethyl)sulfonyl)benzenesulfonyl fluoride (**22**)



The reaction condition was adapted from Smedley *et al* (11). A 10-mL vial sealed with a septum was charged with benzene-1,2-disulfonyl fluoride (242 mg, 1.00 mmol), and finely powdered $KFHF$ (1.6 mg, 0.02 mg). Under N_2 atmosphere, anhydrous dimethyl sulfoxide ($DMSO$, 4.0 mL) and trifluoromethyl trimethylsilane ($TMSCF_3$, 200 mg, 1.4 mmol) were added via syringe. The resulting mixture was stirred at room temperature for 2 h (distribution of starting material, mono-trifluoromethylated product, di-trifluoromethylated product was estimated by analytical HPLC as 41/52/7), before being directly loaded onto a prep-HPLC. The titled compound was isolated as a white crystalline (**22**, 104 mg, 0.304 mmol, 30%).

1H NMR (600 MHz, $CDCl_3$) δ 8.53 – 8.47 (m, 1H), 8.47 – 8.42 (m, 1H), 8.16 – 8.02 (m, 2H).

^{13}C NMR (151 MHz, $CDCl_3$) δ 137.0, 136.6, 136.1, 134.9 (d, $J_{CF} = 28.7$ Hz), 133.8 (d, $J_{CF} = 1.5$ Hz), 132.2 (d, $J_{CF} = 1.5$ Hz), 118.6 (qd, $J_{CF_3} = 336.7$ Hz, $J_{CF} = 359.4$ Hz).

^{19}F NMR (376 MHz, $CDCl_3$) δ 67.1 (s, 1F), -73.5 (s, 3F).

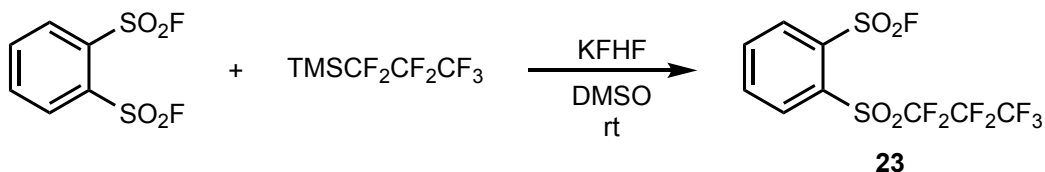
TLC $R_f = 0.45$ (33% EA in hexanes, UV)

Melting point 91 – 93 °C (MeOH).

Mass spectrometry APCI-TOF accurate mass calculated for $C_7H_4F_4O_4S_2NH_4$ $[M + NH_4]^+$ 309.9825, found 309.9821.

HPLC purity (280 nm) 97.1% ($t_R = 4.949$ min).

2.13. 2-((Perfluoropropyl)sulfonyl)benzenesulfonyl fluoride (**23**)



The reaction condition was adapted from Smedley *et al* (11). A 10-mL vial sealed with a septum was charged with benzene-1,2-disulfonyl fluoride (242 mg, 1.00 mmol), finely powdered KFHF (1.6 mg, 0.02 mg). Under N₂ atmosphere, anhydrous DMSO (2.0 mL) and perfluoropropyl trimethylsilane (TMSCF₂CF₂CF₃, 242 mg, 1.0 mmol) were added via syringe. The resulting mixture was stirred at room temperature for 2 h (distribution of starting material, mono-perfluoropropylated product, di-perfluoropropylated product was estimated by analytical HPLC as 50/45/5). The titled compound was isolated by prep-TLC (SiO₂, 33% EA in hexanes) as a white crystalline (**23**, 43 mg, 0.110 mmol, 11%).

¹H NMR (600 MHz, CDCl₃) δ 8.53 – 8.48 (m, 1H), 8.46 – 8.42 (m, 1H), 8.12 – 8.05 (m, 2H).

¹³C NMR (151 MHz, CDCl₃) δ 136.5, 136.2, 135.5, 134.46 (d, *J*_{CF} = 28.7 Hz), 133.2 (*J*_{CF} = 1.5 Hz), 131.9, 120 – 106 (m, perfluoropropyl).

¹⁹F NMR (377 MHz, CDCl₃) δ 67.1 (s, 1F), -80.8 (t, *J* = 9.3 Hz, 3F), -107.38 (qt, *J* = 8.8, 4.2 Hz, 2F), -124.78 – -124.81 (m, 2F).

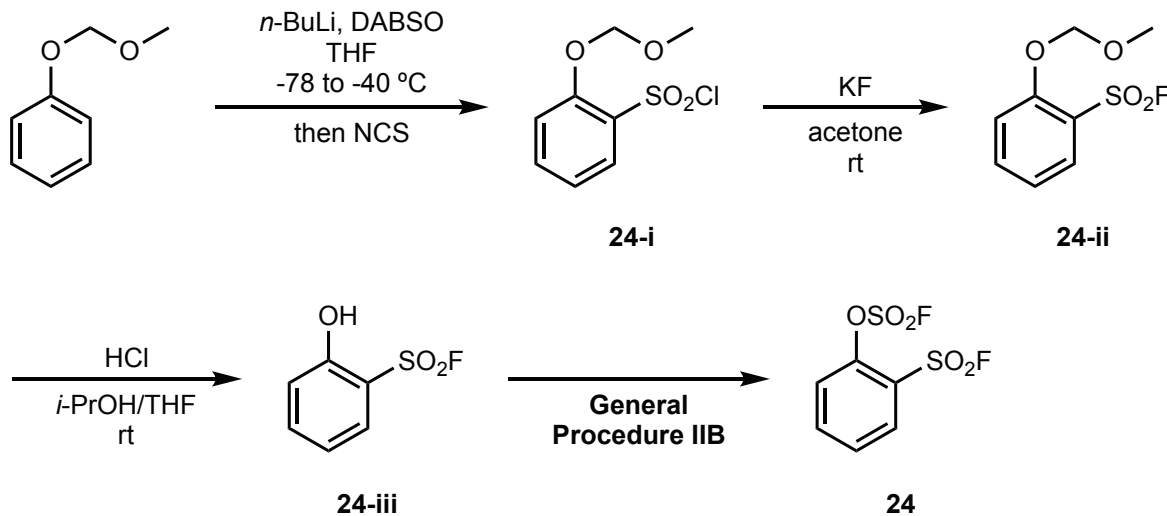
TLC *R*_f = 0.45 (33% EA in hexanes, UV).

Melting point 78 – 79 °C (hexanes/EA).

Mass spectrometry APCI-TOF accurate mass calculated for C₉H₃F₈O₄S₂ [M]⁻ 390.9350, found 390.9339.

HPLC purity (280 nm) 95.2% (*t*_R = 5.368 min).

2.14. 2-(Fluorosulfonyl)phenyl fluorosulfate (**24**)



(Methoxymethoxy)benzene (166 mg, 1.20 mmol) prepared from phenol and MOMCl was dissolved in THF (2.4 mL), and cooled to -78 °C by an acetone/dry ice bath. *n*-Butyl lithium (2.5

M in hexane, 0.55 mL, 1.3 mmol, 1.1 equiv) was added dropwise at -78 °C and the resulting orange suspension was stirred for 2 h before being cannulated into a stirred suspension of 1,4-diazabicyclo[2.2.2]octane bis(sulfur dioxide) adduct (abbr. DABSO, 720 mg, 3.0 mmol, 2.5 equiv) in THF (2.4 mL). The resulting suspension was stirred at -40 °C for 1 h before being treated with *N*-chlorosuccinimide (abbr. NCS, 641 mg, 4.80 mmol, 4 equiv) in one portion. The mixture was stirred at rt for 5 min before being quenched by saturated NH₄Cl solution. The product was extracted by diethyl ether and purified by column chromatography to give **24-i** (230.0 mg, 0.972 mmol, 81%) as a yellow oil.

Sulfonyl chloride **24-i** (224 mg, 0.946 mmol) dissolved in acetone (5 mL) was treated with anhydrous KF (164 mg, 2.84 mmol, 3 equiv). The white suspension was stirred at rt overnight. Acetone was removed *in vacuo*, the residue was partitioned between diethyl ether and water. The organic phase was collected, dried, and concentrated to give **24-ii**.

The crude sulfonyl fluoride **24-ii** (182 mg, 0.828 mmol), without purification, was dissolved in THF (4 mL). Hydrochloric acid in isopropanol (3 M, 4 mL) was added to the THF solution, and the resulting mixture was stirred at rt for 8 h. All volatiles were blown dry with a stream of N₂ giving virtually pure **24-iii** (140 mg, 0.795 mmol, 96%).

Compound **24** was prepared from **24-iii** using **General Procedure IIB**. Phenol **24-iii** (56.3 mg, 0.319 mmol) afforded fluorosulfate **24** (63.1 mg, 0.244 mmol, 77%) as a colorless oil.

¹H NMR (600 MHz, CDCl₃) δ 8.17 (dd, *J* = 7.9, 1.7 Hz, 1H), 7.93 (td, *J* = 8.2, 1.7 Hz, 1H), 7.71 (d, *J* = 8.4 Hz, 1H), 7.68 (t, *J* = 7.8 Hz, 1H).

¹³C NMR (151 MHz, CDCl₃) δ 146.8, 137.9, 132.2, 129.3, 126.4 (d, *J* = 27 Hz), 122.9 (d, *J* = 1.5 Hz).

¹⁹F NMR (377 MHz, CDCl₃) δ 65.3 (d, *J* = 3.8 Hz), 44.0 (d, *J* = 3.8 Hz).

TLC *R*_f = 0.46 (25% EA in hexanes).

Mass spectrometry GC-EI-MS *t*_R = 6.84 min, calculated for C₆H₄F₂O₅S₂ [M]⁺ 257.95, found 258.0.

HPLC purity (254 nm) 98.2% (*t*_R = 4.877 min).

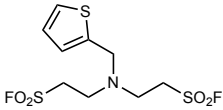
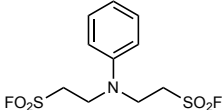
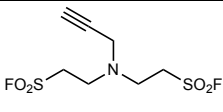
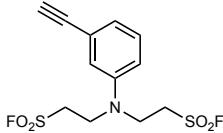
3. Protease activity assays and library screen

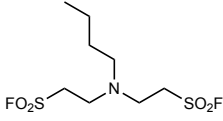
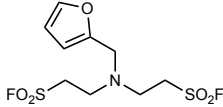
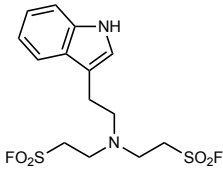
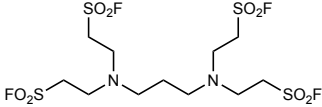
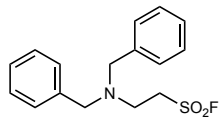
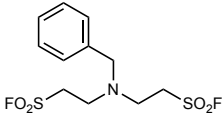
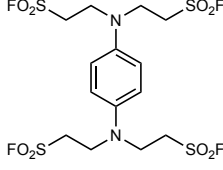
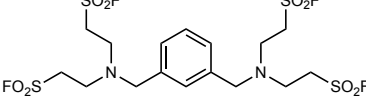
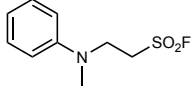
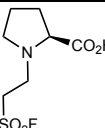
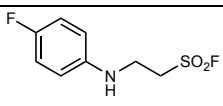
3.1. Methods

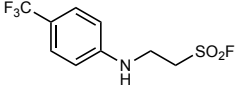
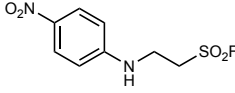
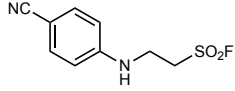
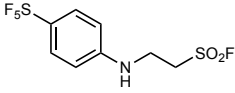
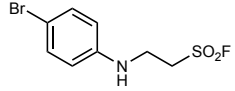
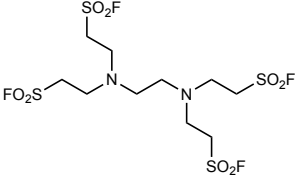
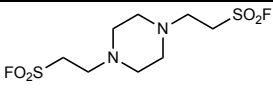
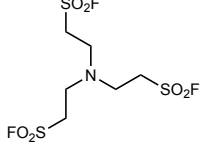

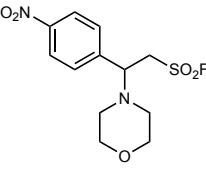
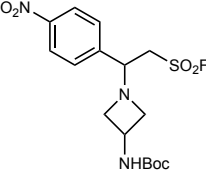
Activity of hNE was measured in a total volume of 100 μ L in a reaction buffer of PBS (pH 7.4) and 0.05% (v/v) NonidetTM P 40 Substitute (Sigma). Final composition of each reaction was 5 nM hNE (Elastin Products Corp.), 50 μ M AAPV-aminomethylcoumarin (AMC) substrate (Millipore), ~2.5% dimethyl sulfoxide (Fisher), and various concentrations of compounds as inhibitors. hNE was incubated with inhibitors for 10 min at room temperature before addition of AAPV-AMC (12, 13). Residual proteolytic activity was measured kinetically at 25 $^{\circ}$ C using an Envision microplate reader for a total of 30 min at 30 sec intervals. Only data points reflecting linear substrate conversion were used to determine relative protease activity. IC₅₀ values were obtained by fitting the data to a dose-response inhibition, log (inhibitor) vs. response – variable slope (four parameters) using GraphPad Prism. Human Cathepsin G (hCG) activity was measured in a comparable manner to hNE, except that the final concentration of protease in each reaction was 15 nM and 50 μ M of the substrate, AAPF-AMC (Millipore) (12, 13).

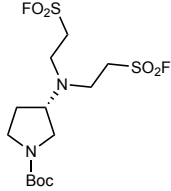
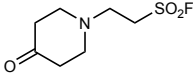
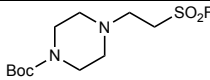
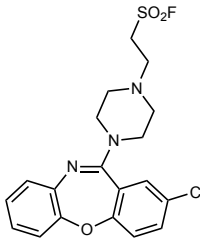
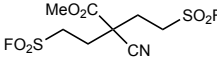
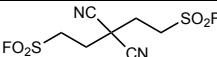
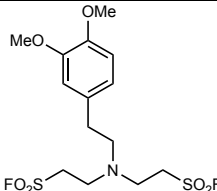
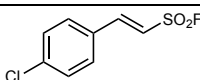
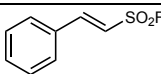
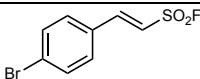
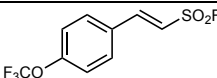
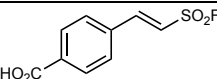
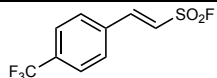
3.2. Screen results

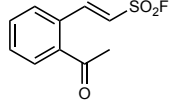
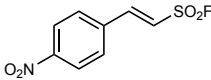
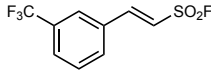
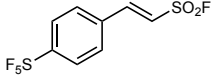
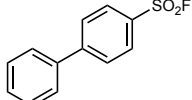
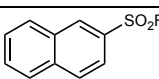
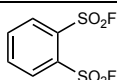
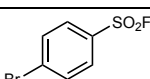
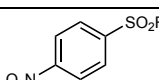
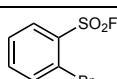
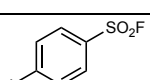
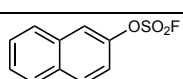
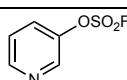
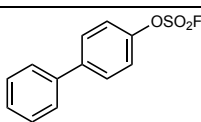
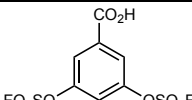
Table S1. Randomly picked SuFExable molecules and corresponding hNE inhibitory activity.

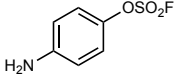
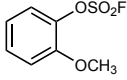
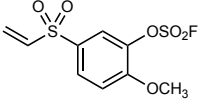
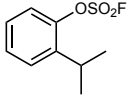
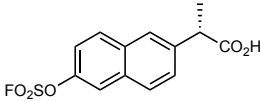
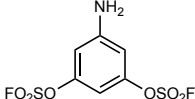
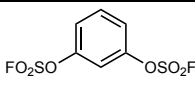
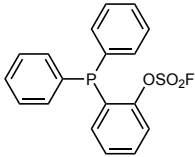
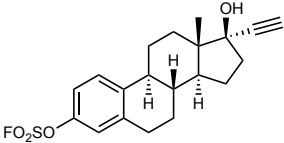
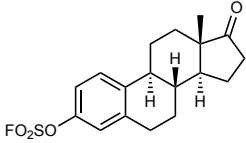
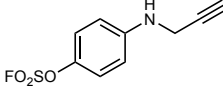
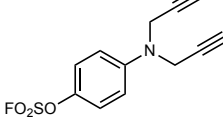
BBS Code* (cmpd # in text)	Subset	Structure	% inhibition [†] (IC ₅₀) [‡]
BBS-63	III		20%
BBS-64	III		12%
BBS-65	III		22%
BBS-66	III		17%

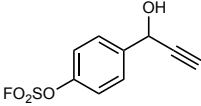
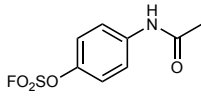
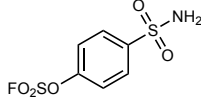
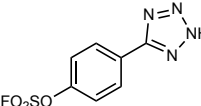
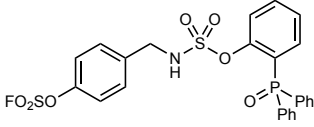
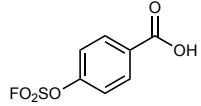
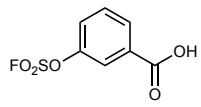
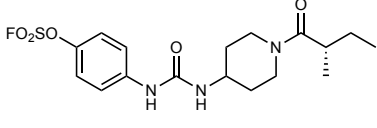
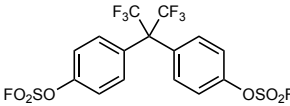
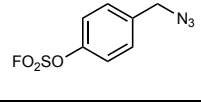
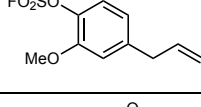
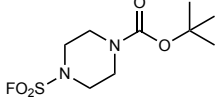
BBS-67	III		39%
BBS-68	III		19%
BBS-70	III		12%
BBS-244	III		11%
BBS-245	III		7%
BBS-246	III		37%
BBS-247	III		28%
BBS-248	III		25%
BBS-249	III		31%
BBS-250	III		10%
BBS-254	III		0%

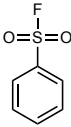
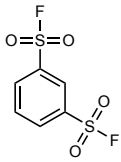
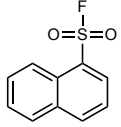
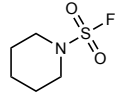
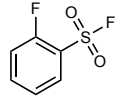
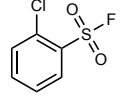
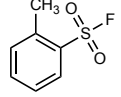
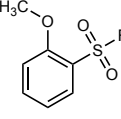
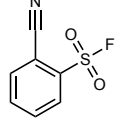
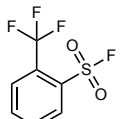
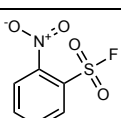
BBS-255	III		36%
BBS-256	III		36%
BBS-257	III		9%
BBS-258	III		16%
BBS-268	III		12%
BBS-297	III		5%
BBS-298	III		10%
BBS-299	III		41%
BBS-300	III		3%
BBS-310	III		40%
BBS-311	III		24%

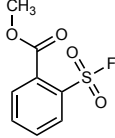
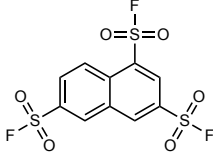
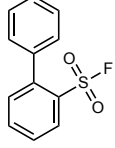
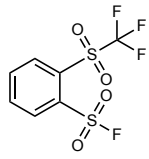
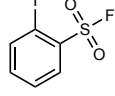
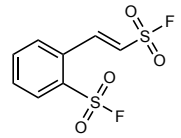
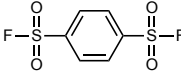
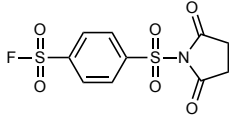
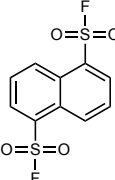
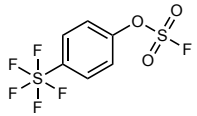
BBS-418	III		26%
BBS-421	III		1%
BBS-422	III		1%
BBS-424	III		6%
BBS-430	III		44%
BBS-432	III		14%
BBS-420	III		25%
BBS-216	III		0%
BBS-219	IV		24%
BBS-222	IV		0%
BBS-224	IV		10%
BBS-225	IV		21%
BBS-226	IV		15%

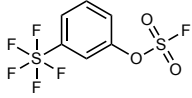
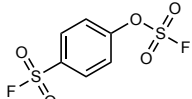
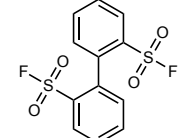
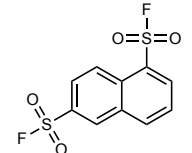
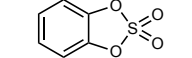
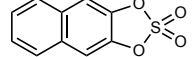
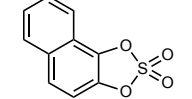
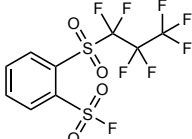
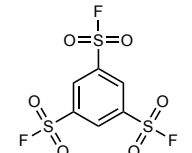
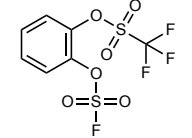
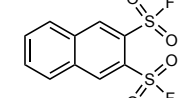
BBS-235	IV		9%
BBS-228	IV		40%
BBS-232	IV		18%
BBS-417	IV		12%
BBS-241	I		0%
BBS-295	I		(>200)
BBS-305 (1)	I		(3.3 ± 1.0)
BBS-306	I		(20 ± 10)
BBS-416	I		(>150)
BBS-433 (10)	I		(20 ± 10)
BBS-434	I		(>150)
BBS-114	II		0%
BBS-116	II		0%
BBS-240	II		0%
BBS-263	II		34%

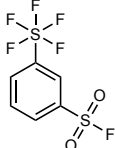
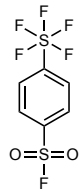
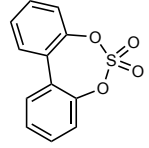
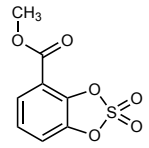
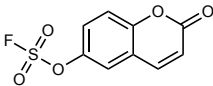
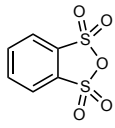
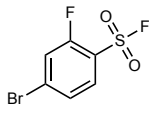
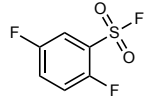
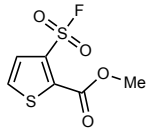
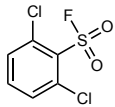
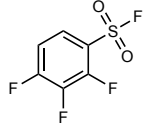
BBS-266	II		12%
BBS-272	II		0%
BBS-274	II		0%
BBS-275	II		3%
BBS-282	II		10%
BBS-290	II		10%
BBS-291	II		13%
BBS-292	II		26%
BBS-296	II		16%
BBS-312	II		12%
BBS-319	II		2%
BBS-320	II		3%

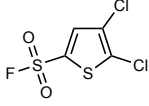
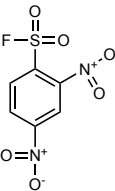
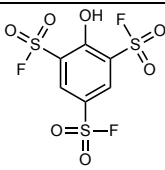
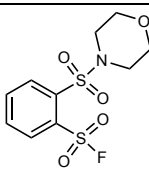
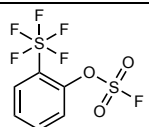
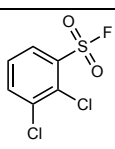
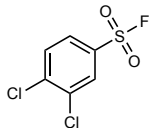
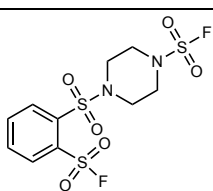
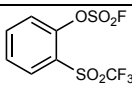
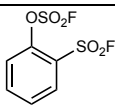
BBS-321	II		5%
BBS-413	II		8%
BBS-414	II		15%
BBS-415	II		11%
BBS-419	II		11%
BBS-423	II		11%
BBS-425	II		10%
BBS-426	II		15%
BBS-427	II		3%
BBS-428	II		7%
BBS-429	II		17%
BBS-301	II		(9.5 ± 3.5)

BBS-1001	I		(~200)
BBS-740	I		(10 ± 4)
BBS-743	I		(>200)
BBS-1002	II		(>400)
BBS-1003 (8)	I		(~120)
BBS-1004 (9)	I		(82 ± 16)
BBS-1005 (12)	I		(>200)
BBS-1006 (13)	I		(73 ± 4)
BBS-1007 (14)	I		(13.3 ± 0.5)
BBS-1008 (15)	I		(60 ± 8)
BBS-1009 (16)	I		(20 ± 1)

BBS-1010 (17)	I		(37 ± 2)
BBS-1011 (2)	I		(17.5 ± 1.1)
BBS-1012 (18)	I		(27 ± 2)
BBS-1013 (22)	I		(1.1 ± 0.1)
BBS-1014 (11)	I		(9.7 ± 1.2)
BBS-1015 (19)	I		(2.2 ± 0.7)
BBS-1016	I		(7.7 ± 0.7)
BBS-1017	I		(51 ± 7)
BBS-1018	I		(>200)
BBS-1019	II		(>200)

BBS-1020	II		(>200)
BBS-1021	I		(~200)
BBS-1022	I		(~200)
BBS-1023	I		(>200)
BBS-1024	N/A		(~200)
BBS-1025	N/A		(~200)
BBS-1026	N/A		(~200)
BBS-1027 (23)	I		(48 ± 2)
BBS-1028	I		(36 ± 3)
BBS-1029	II		(~200)
BBS-1030 (3)	I		(6.8 ± 1.1)

BBS-1031	I		(>200)
BBS-1032	I		(>200)
BBS-1033	N/A		(>200)
BBS-1034	N/A		(59 ± 15)
BBS-1035	II		(>200)
BBS-1036	N/A		(>200)
BBS-1037	I		(>200)
BBS-1038	I		(67 ± 19)
BBS-1039 (4)	I		(17 ± 2)
BBS-1040 (5)	I		(5.4 ± 0.5)
BBS-1041	I		(105 ± 17)

BBS-1042	I		(>200)
BBS-1043 (6)	I		(5.9 ± 1.1)
BBS-406	I		(89 ± 4)
BBS-1044 (20)	I		(84 ± 1)
BBS-1045	II		(>200)
BBS-1048	I		(60 ± 10)
BBS-1049 (7)	I		(49 ± 3)
BBS-1050 (21)	I		(>200)
BBS-1053	II		(176 ± 63)
BBS-1054 (24)	I		(0.235 ± 0.022)

PMSF (ref.)	N/A		(24 ± 1)
----------------	-----	--	----------

*BBS-numbering is assigned for every SuFExable compound for internal (Scripps Research) reference. †Per cent inhibition of hNE activity was measured based on a compound concentration of 200 μ M. ‡IC₅₀ values were measured based on 10 min incubation and are shown in mean \pm SD (n \geq 3).

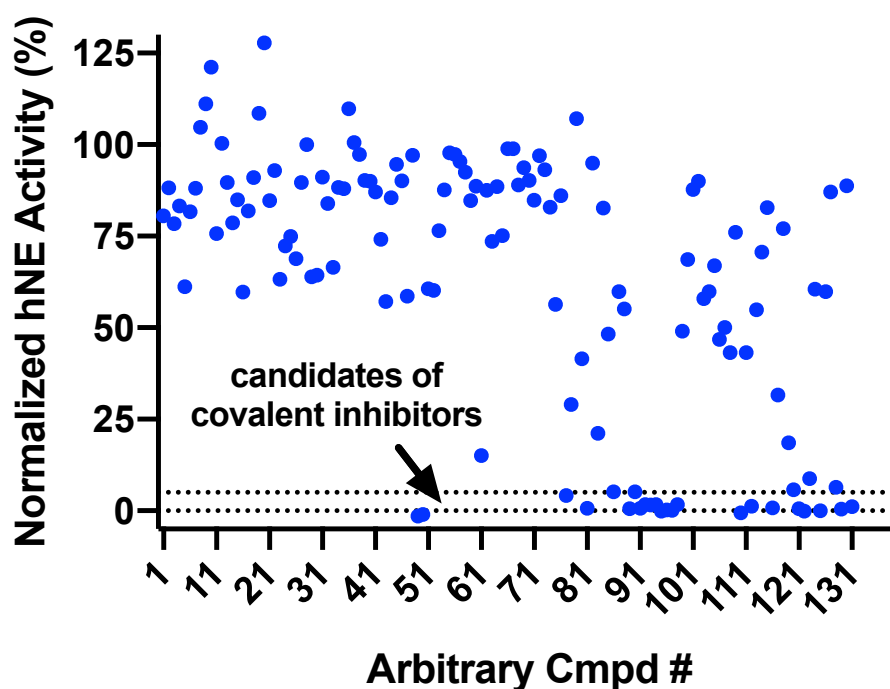


Fig S1. Scatterplot of in-house SuFEx library screened against human neutrophil elastase. Residual hNE activity toward a fluorescent-peptide substrate (AAPV-AMC) after incubation of 5 nM hNE with 200 μ M compound from a 10mM DMSO stock. Percent residual activity normalized against a positive control of hNE plus substrate and negative control of substrate alone.

3.3. Validation of permanent binding

To test for covalency and the possibility of hydrolytic activity returning to hNE over time, hNE was resuspended in the above buffer to 0.1 mg/ml. Compounds **1** and **22** were added to hNE in a 50:1 ratio and incubated for 30 min at rt. Complexes were dialyzed using 0.5 mL Slide-A-Lyzer MINI dialysis units (Thermo) in the above buffer for 24 hrs. At time points, $t = 0, 1, 2,$ and 24 h, an aliquot was removed, hNE concentration determined, two-fold dilution series of hNE in PBS

(7.4), AAPV-AMC substrate added, and residual proteolytic activity measured kinetically at 25 °C using an Envision microplate reader for a total of 30 min at 30 s intervals. Dilution series curves made using GraphPad Prism 8 and hNE activity at 5 nM determined through Michaelis-Menton kinetics for each time point (**Fig S2**).

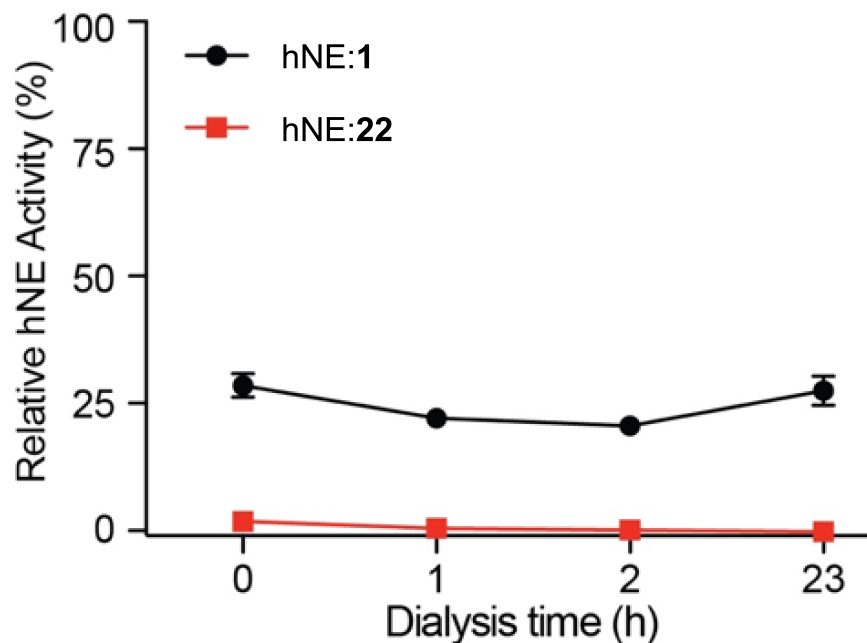


Fig S2. Covalency test, dialysis of hNE complexed with compounds 1 and 22 over time. Enzyme hNE was resuspended to 0.1 mg/mL and complexed with compounds 1 and 22 in a 50:1 (compound:hNE) ratio for 30 min at rt. Complexes were dialyzed, with hNE control, in resuspension buffer for 24 h. Aliquots taken at time points and residual hNE activity was tested at 5 nM protein concentration. No change in hNE hydrolytic activity is observed over time. Data presented here are taken from a representative trial of at least three independent experiments.

3.4. Inhibitory activity of hit molecules against hCG.

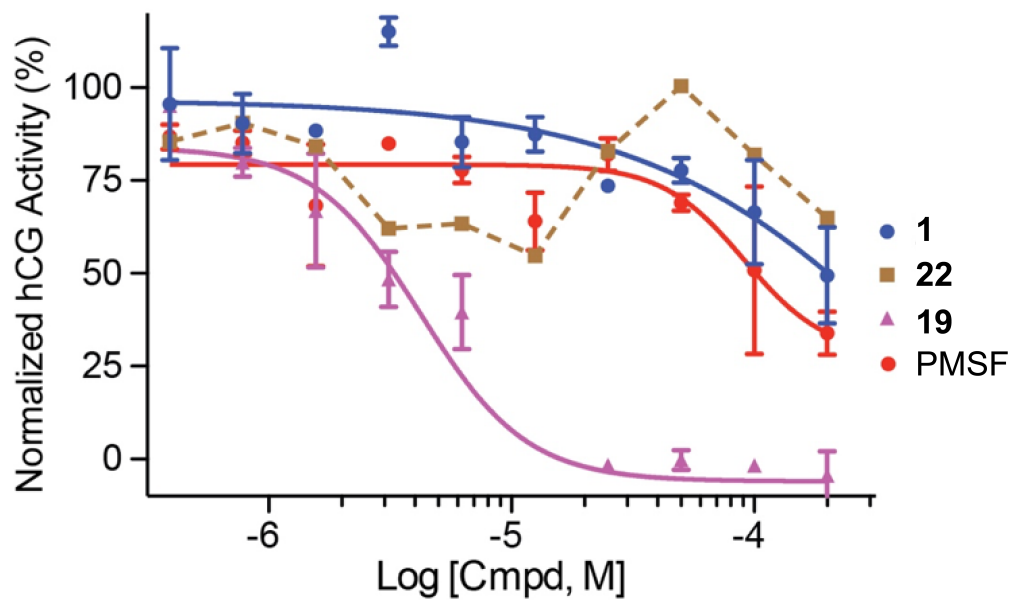


Fig S3. Dose-response curves of top hNE inhibitors against human cathepsin G. Each compound was assessed over a two-fold logarithmic dilution series. Data presented here are taken from a representative trial of at least three independent experiments. Legend is inset.

4. Mass Spectrometry

4.1. Methods

Enzyme hNE was resuspended in 50 mM sodium acetate (NaOAc, pH 4.5), 100 mM NaCl to 0.2 mg/ml final concentration. DMSO solution of each compound (10 mM) was diluted 1:10 in the above buffer, then added in a compound:hNE ratio = 3:1 and incubated at rt for 1 h prior to analysis by MALDI-TOF mass spectrometry.

4.2. Results

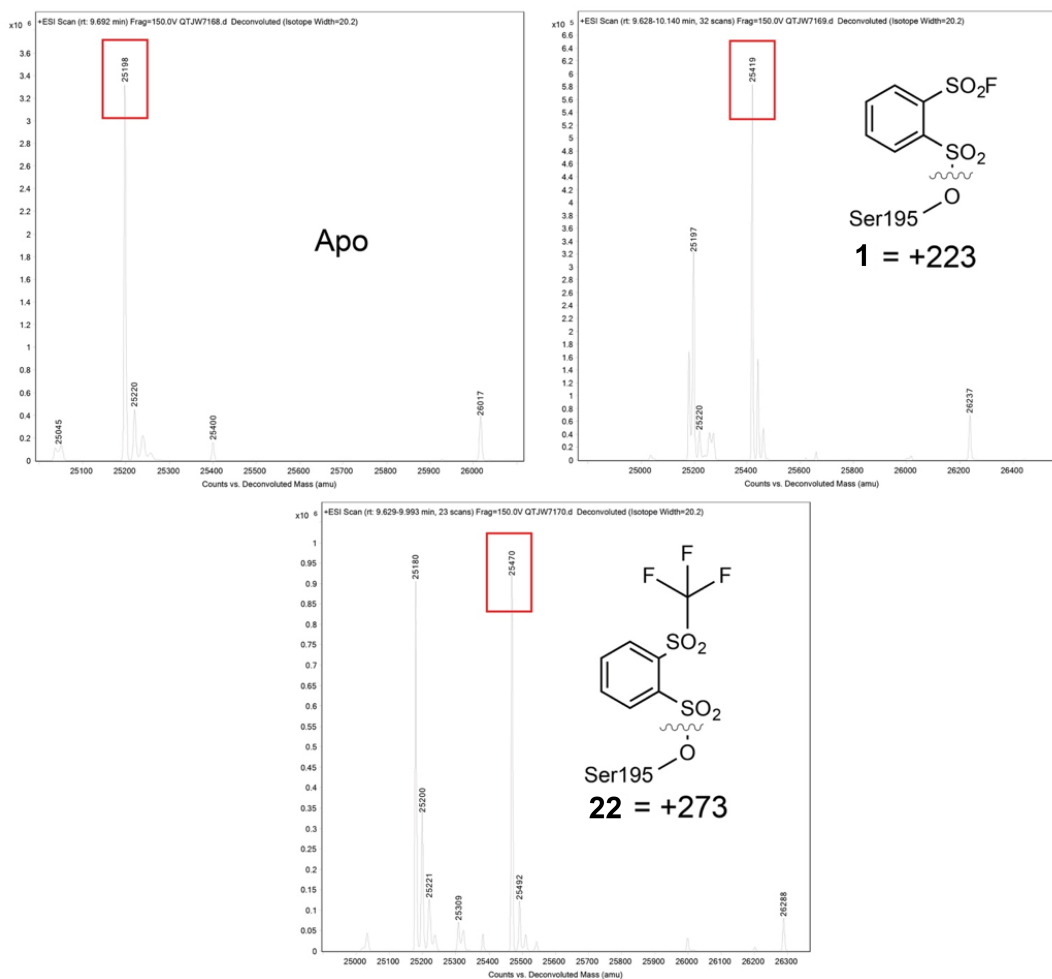


Fig S4. MALDI-TOF mass spectrometry analysis of hNE with or without compounds, 1 and 22. hNE was incubated alone (top left) and in a 1:3 ratio with compounds 1 (top right) and 22 (bottom) for 1 hr at RT and analyzed by high accuracy MALDI-TOF mass spectrometry. Peaks correspond to the mass of hNE apo and \pm compound in Da.

5. X-ray crystal structure

5.1. Methods

Crystallization and x-ray data collection. Crystallization of hNE in complex with our covalent capture agent was set up similarly to Hansen et al. and their structure of a dihydropyrimidone inhibitor (14). In short, inhibitor **1** was added in a 1.2 molar excess to human neutrophil elastase (Elastin Products Co.) [10 mg/ml in 10 mM HEPES (pH 6.5)], incubated for 1 h at 25°C and immediately used for crystallization. Crystals were grown by sitting drop-vapor diffusion by mixing equal volumes (1.5 μ L) of hNE:**1** complex and reservoir solution consisting of 0.3 M ammonium citrate (pH 5.0), 14% (w/v) PEG3350 at 25°C. Data was collected on single, flash-cooled crystals at 100 K in cryoprotectant consisting of 0.2 M ammonium citrate (pH 5.0), 20% (w/v) PEG3350, and 20% (v/v) glycerol, and were processed with HKL2000 in orthorhombic space group $P2_12_12_1$. The calculated Matthews' coefficient ($V_M = 2.77 \text{ \AA}^3\text{Da}^{-1}$) suggested four monomers per asymmetric unit with a solvent content of 56%. X-ray data was collected to 2.33 \AA resolution on beamline 12.2 at the Stanford Synchrotron Radiation Lightsource (SSRL) (Menlo Park, CA). Data collection and processing statistics are summarized in **Table S2**.

Structure solution and refinement. The hNE:**1** structure was determined by molecular replacement (MR) with Phaser (15) using the previously published apo structure (PDB ID: 5abw) as the initial search model. The structure was manually built with Coot (16) and iteratively refined using Phenix (17) with cycles of conventional positional refinement with isotropic B-factor refinement. Non-crystallographic symmetry (NCS) constraints were applied for the initial rounds of refinement. The electron density maps clearly identified that **1** was covalently attached to Ser195 within the active site (Fig. 3B-D). Water molecules were automatically positioned by Phenix using a 2.5σ cutoff in F_o-F_c maps and manually inspected. The final R_{cryst} and R_{free} are 19.3% and 24.1%, respectively (**Table S2**). The model was analyzed and validated with PROCHECK (18), WHATCHECK (19), and Molprobity (20) on the JCSG webserver. Analysis of backbone dihedral angles with the program PROCHECK indicated that all residues are located in the most favorable and additionally allowed regions in the Ramachandran plot. Coordinates and structure factors have been deposited in the PDB with accession entry 6e69. Structure refinement and statistics are shown in **Table S2**.

X-ray structure data deposition. PDB ID: 6e69.

5.2. Results

Table S2. X-ray crystallography data collection and refinement statistics.

Structure	6E69
Space group	P 2 ₁ 2 ₁ 2 ₁
Cell dimensions	
a, b, c; Å	69.5, 124.6, 126.7
α, β, γ ; °	90, 90, 90
Data Processing	
Resolution, Å (outer shell)	50.0-2.33 (2.37-2.33)
Completeness, %	96.8 (72.5)
Unique reflections	46,266 (1,697)
Redundancy	2.7 (2.6)
R _{meas} (%) [*]	6.7 (44.9)
R _{merge} (%) [†]	4.7 (31.7)
R _{p.i.m.} (%) [‡]	7.1 (31.2)
Average I / Average σ (I)	13.0 (3.2)
CC _{1/2}	87.4 (100)
Refinement	
Resolution, Å (outer shell)	50.0-2.33 (2.38-2.33)
No. reflections (test set) [§]	46,245 (2,386)
R _{cryst} (%) [¶]	19.3 (21.3)
R _{free} (%)	24.1 (28.5)
Protein atoms / Waters	6,711 / 267
CV coordinate error (Å) [#]	0.28
Rmsd bonds (Å) / angles °	0.006 / 0.9
B-values protein/waters/ligands (Å ²)	39 / 34 / 53
Ramachandran Statistics (%)	
Preferred	97.1
Allowed	2.9
Outliers	0

^{*}R_{meas} = $\sqrt{\sum_{hkl} \sum_i I_i(hkl) / \langle I_{(hkl)} \rangle}$, where I_{i(hkl)} are the observed intensities, $\langle I_{(hkl)} \rangle$ are the average intensities and N is the multiplicity of reflection hkl. [†]R_{merge} = $\sum_{hkl} \sum_i |I_i(hkl) - \langle I_{(hkl)} \rangle| / \sum_{hkl} \sum_i I_i(hkl)$ where I_{i(hkl)} is the ith measurement of reflection h and $\langle I_{(hkl)} \rangle$ is the average measurement value. [‡]R_{p.i.m.} (precision-indicating R_{merge}) = $\sum_{hkl} [1 / (N_{hkl} - 1)]^{1/2} \sum_i |I_i(hkl) - \langle I_{(hkl)} \rangle| / \sum_{hkl} \sum_i I_i(hkl)$. [§]Reflections with I > 0 were used for refinement (16). [¶]R_{cryst} = $\sum_h ||F_{obs}| - |F_{calc}|| / \sum |F_{obs}|$, where F_{obs} and F_{calc} are the calculated and observed structure factor amplitudes, respectively. R_{free} is R_{cryst} with 5.0% test set structure factors. [#]Cross-validated (CV) Luzzati coordinate errors.

6. Reactive docking

6.1. Methods

The structures of hNE (PDB ID: 6e69) and hCG (PDB ID: 1t32) (21) were superposed and prepared according to the standard AutoDock protocol (22). Hydrogens, protonation states, and side chain conformations of Gln, Asn, and His residues were calculated with Reduce (23). Ligand 3D coordinates were generated from SMILES strings using custom Python scripts based on OpenBabel (24). The reactive docking protocol was applied, as described previously (25, 26). The reactive potential was defined for the sulfonyl-fluoride sulfur and the serine O γ , with ϵ value of 0.241. For each ligand, 10 independent ga_runs were performed with the default GA settings. Results were clustered, and the lowest energy result was selected.

6.2. Results and discussion

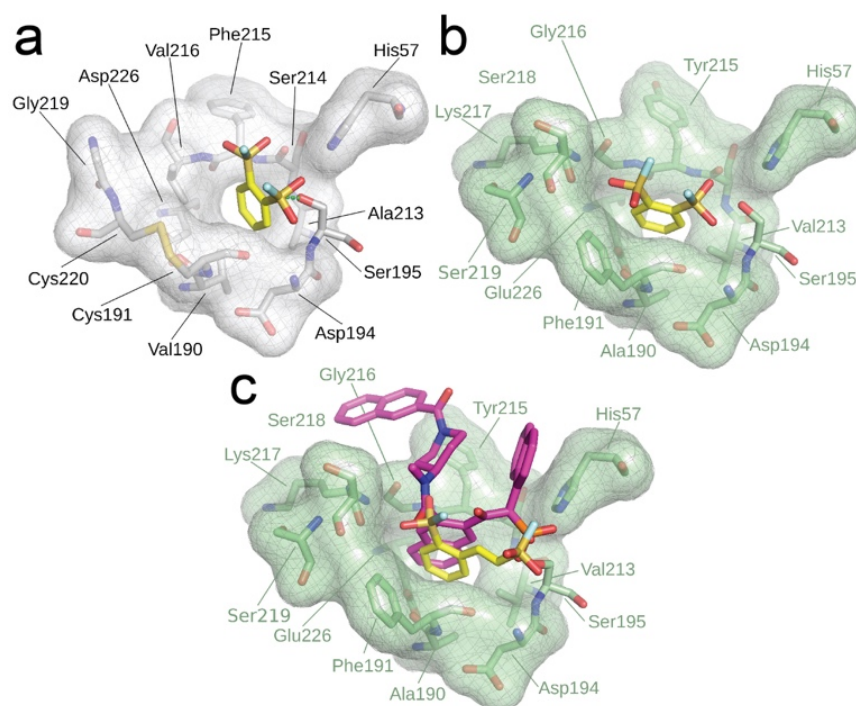


Fig S5. Reactive docking results. Residues defining binding sites are shown as sticks, and volumes represented as semi-transparent surfaces. Ligands are shown as sticks. (a) Compound **1** (yellow) docked in hNE (white; PDB ID 6e69); pseudo-covalent bond between **1** and Ser195 is shown as dashed lines (green). (b). Compound **1** (yellow) docked in hCG (green; PDB ID 1t32); (c) Compound **19** (yellow) docked in hCG (green; PDB ID 1t32), and the experimental coordinates of beta-ketophosphonate **1** (JNJ-10311795; purple), a potent non-covalent hCG inhibitor.

Superposition of hCG (PDB ID: 1t32) and our hNE:**1** co-complex (PDB ID: 6e69) crystal structures provides insight as to how **1** is selective for hNE over hCG. The active sites are conserved in shape, topography, and sequence. However, key differences in residues flanking the catalytic site are likely responsible for selectivity of **1** for hNE, including substitutions of Phe192 to Lys, Val216 to Gly, and that hCG lacks the disulfide bond formed by hNE Cys191 and Cys220 (**Fig S5a**). We applied a reactive docking protocol to identify the determinants of selectivity by **1** and the promiscuity of **19**. Modeling the near-attack conformations (NAC), which precede formation of irreversible adducts, suggests that the Val216 side chain of hNE is important for binding the free compound and stabilizing the proper reactive geometry. The side chain of Val216 engages the aromatic ring of **1** and **19** and orients the sulfonyl fluoride at an optimal distance for nucleophilic attack by Ser195. The substitutions of hNE's Val216 for a Gly in hCG and Ala213 for a Val, expand the active site cavity and promote repulsion with the compound's aromatic ring, respectively (**Fig S5b**). Our docking results suggest the combined substitutions in hCG result in a shift of the aromatic ring binding interaction away from Ser195 and a significant increase in distance for nucleophilic attack by the active site serine (from 2.2 ± 0.2 Å in hNE to 3.4 ± 0.1 Å in hCG). Importantly, compounds with the reactive warhead attached to the phenyl group via one or more carbons (i.e., **19**, and PMSF) have optimal distance between the sulfonyl fluoride and aromatic ring to react with the serine and interact with the larger hydrophobic pocket of hCG (1.8 ± 0.1 Å for **19**), respectively, as demonstrated by the orientation of the naphthyl group of JNJ-10311795 in the x-ray co-complex structure with hCG (**Fig S5c**) (21).

7. Reactivities of SuFExable functional groups

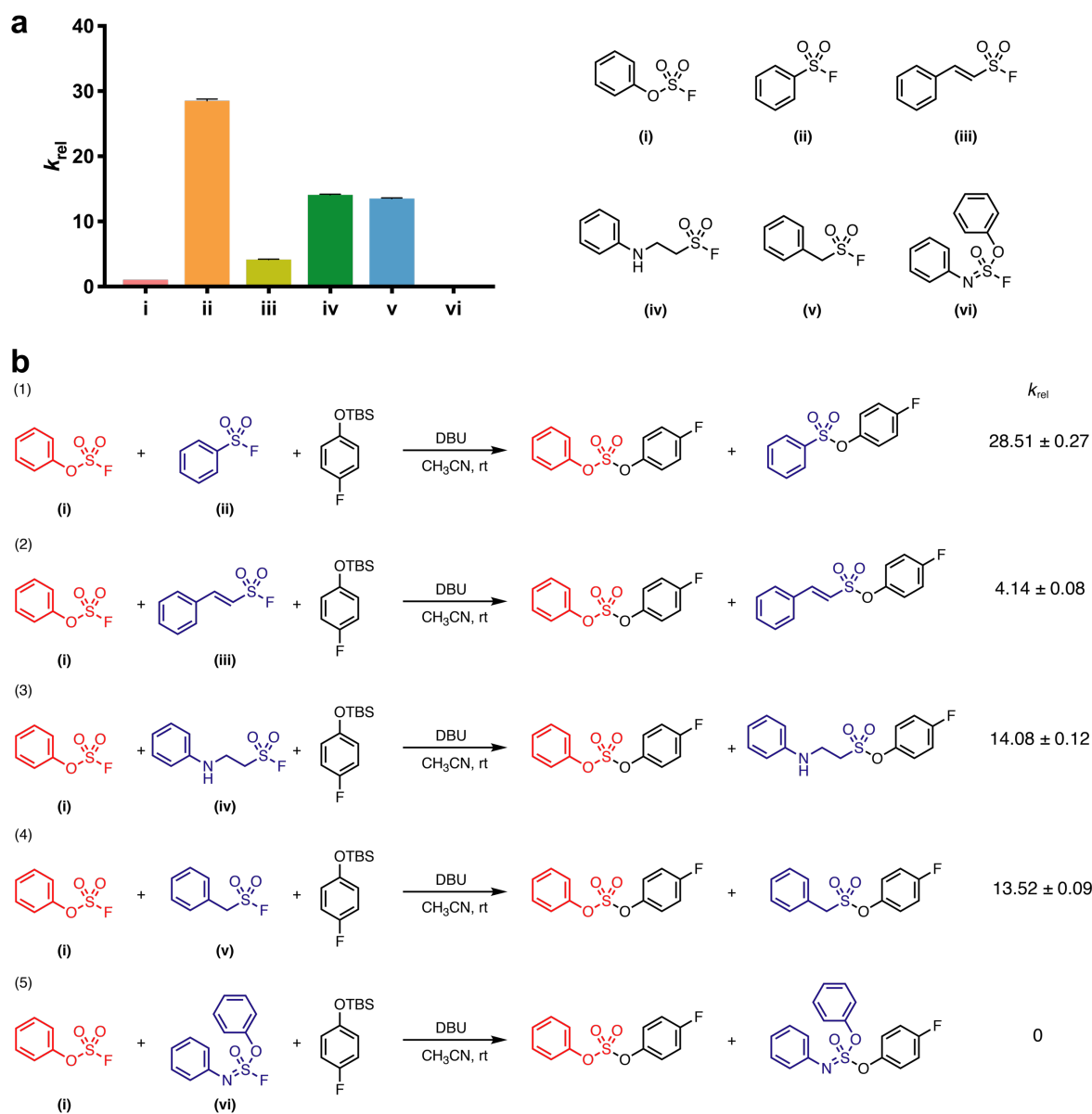


Fig S6. SuFEx reactions of various sulfur fluoride species with aryl silyl ether. a) Relative rates of various sulfur fluoride species were measured by competition with phenyl fluorosulfate. By limiting the amount of 4-phenyl tert-butyldimethylsilyl ether (5%), all reactions were carried to about 2.5% conversion (according to the amount of total “S–F” groups) in the presence of DBU catalyst. The ratio of respective product (k_{rel}) was determined by ^{19}F NMR. Relative rates of compounds **i–iv** and **v** (PMSF) in SuFEx reactions offer a general impression of the reactivity of library subsets **I–IV** and PMSF in the main text; b) reactions for determining relative rates.

8. Stability of sulfur fluoride probes against potentially reactive amino acids

The report by Wang et al. (27) prompted us to test the intrinsic reactivity of several known SuFExable amino acid sidechains with our most reactive sulfonyl fluoride probe **22**. Compound **22** as a 10 mM DMSO solution was mixed (1:1) with phosphate-buffered saline (PBS) containing 10 mM additive (glutathione, histidine hydrochloride, lysine hydrochloride, tyrosine, or serine). The DMSO/PBS mixture containing 5 mM of both compound **22** and additive was incubated at room temperature (23 °C). The remaining of the sulfonyl fluoride compound was monitored by HPLC (**Fig S7**). After 48 h, there was >80% sulfonyl fluoride remaining indicating the good hydrolytic stability. Importantly, the hydrolytic behavior of compound **22** in the presence of glutathione (GSH), histidine, or tyrosine was almost identical to it without such additive, indicating that thiol group (cysteine sidechain), imidazole (histidine sidechain), or phenol (tyrosine sidechain) was unlikely to either covalent capture sulfonyl fluoride or catalyze its hydrolysis by transient covalent attachment.

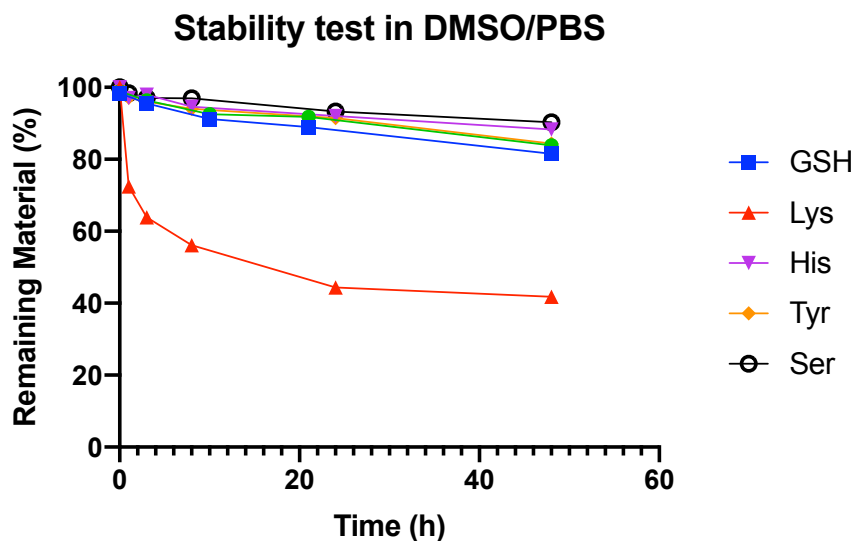


Fig S7. Stability curve of compound 22 in aqueous buffer in the presence of various amino acid additives.

Intriguingly, compound **22** was slowly eaten in the presence of a free lysine, its half-life at physiological pH being around 16 h (**Fig S8**). The fate of lysine was bifurcate, most of which being hydrolyzed into sulfonic acid, and a minor proportion (< 10%) being covalently captured by

sulfonyl fluoride probe **22**. Both products were confirmed by mass spectrometry (sulfonic acid by ESI-neg channel, sulfonamide by ESI-pos channel).

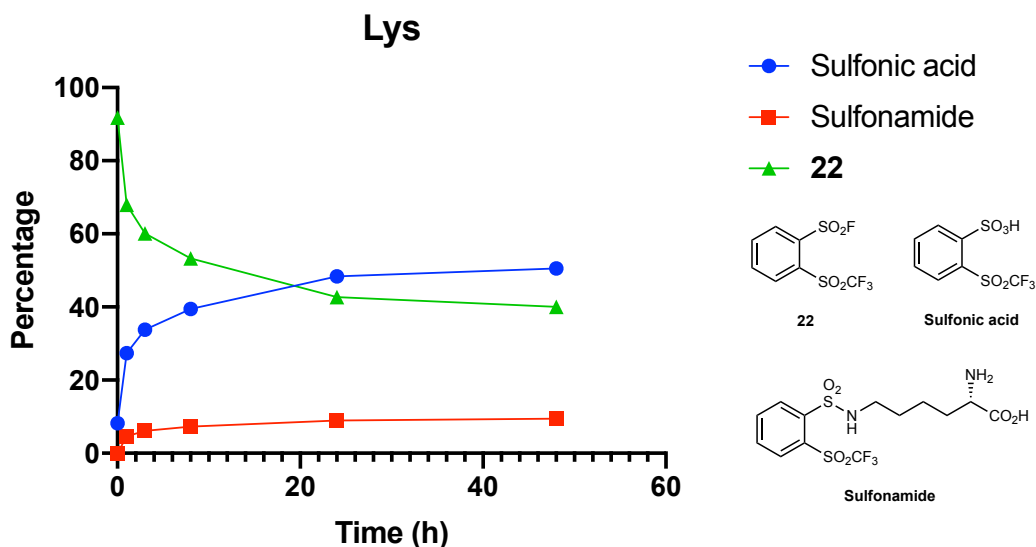


Fig S8. Fate of compound **22** in DMSO/PBS in the presence of lysine. Percentage was calculated by the integrated peak area of respective component on HPLC UV trace (254 nm) without correction.

To further demonstrate the essential role of the tertiary structure of the enzyme, we synthesized a penta-peptide identical to the AA sequence around the catalytic serine (GDSGS). A 5-mer peptide Ac-Gly-Asp-Ser-Gly-Ser-NH₂ was prepared by solid-phase peptide synthesis and purified by HPLC. Incubation of the penta-peptide (10 μM) with compound **22** (1 mM) in DMSO/PBS at room temperature overnight in the presence or absence of imidazole (1 mM). High resolution ESI-TOF mass spectrometry evidenced that no reaction occurred.

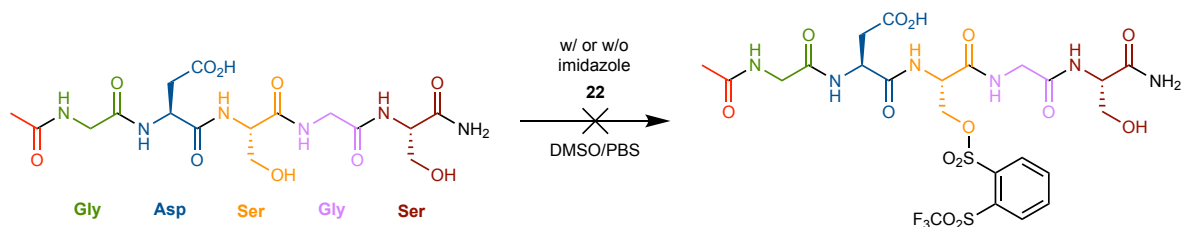


Fig S9. Peptide sequence did not effect the SuFEx reaction with the same sulfonyl fluoride probe **22**.

9. “Refluxing aniline” test on electrophilic covalent reactive groups.

The “refluxing aniline” test was adapted from Suter’s masterful book *Organic Chemistry of Sulfur* (28). Suter described the surprising observation that “benzenesulfonyl fluoride ... refluxing with aniline for several hours causes no change.” We reproduced the “refluxing aniline” experiment as follows. Fresh aniline and benzenesulfonyl fluoride were prepared by distillation under reduced pressure. No reaction occurred in the neat mixture of refluxing benzenesulfonyl fluoride (4 mL, ~33 mmol) and aniline (45 mL, ~500 mmol) at 184 °C for 3 h. Checked by both GC-MS and LC-MS, all starting materials remained.

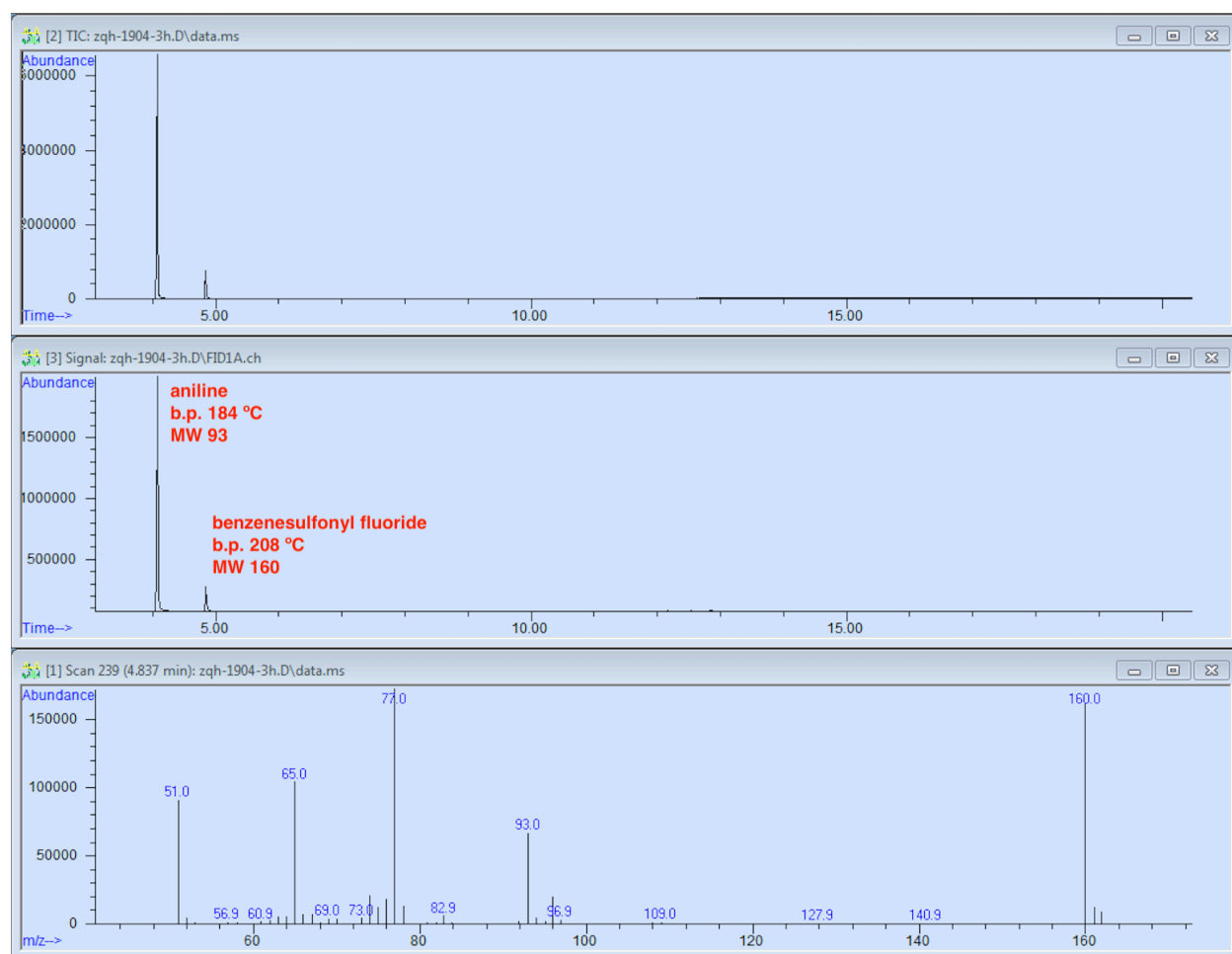
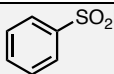
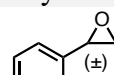
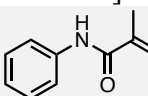
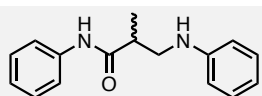
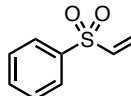
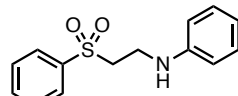
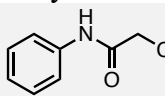
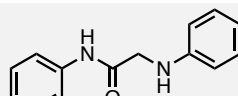
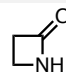


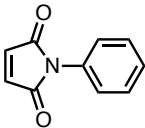
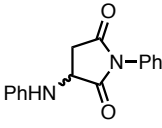
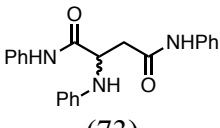
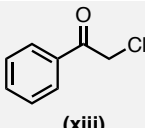
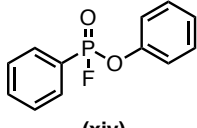
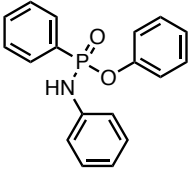
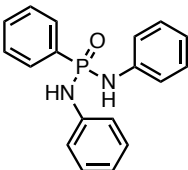
Fig S10. GC-MS results of benzenesulfonyl fluoride after “reflux aniline” test.

We then subjected various electrophilic reactive groups (epoxide, acrylamide, vinyl sulfone, chloroacetamide, chloromethyl ketone, β -lactam, maleimide, and fluorophosphate) to the same “refluxing aniline” test only at smaller scale (1 mmol electrophile, 1.3 mL freshly distilled aniline).

The results were checked by either GC-MS or LC-MS. Other than acrylamide and fluorophosphate, these “warheads” were completely converted to either proposed products or unidentifiable mess. And in the cases of acrylamide and fluorophosphate, only 59% and 11% starting material remained intact, respectively. The “refluxing aniline” test demonstrated the high inherent stability of sulfonyl fluoride.

Table S3. Fate of various reactive groups in the “refluxing aniline” test*.

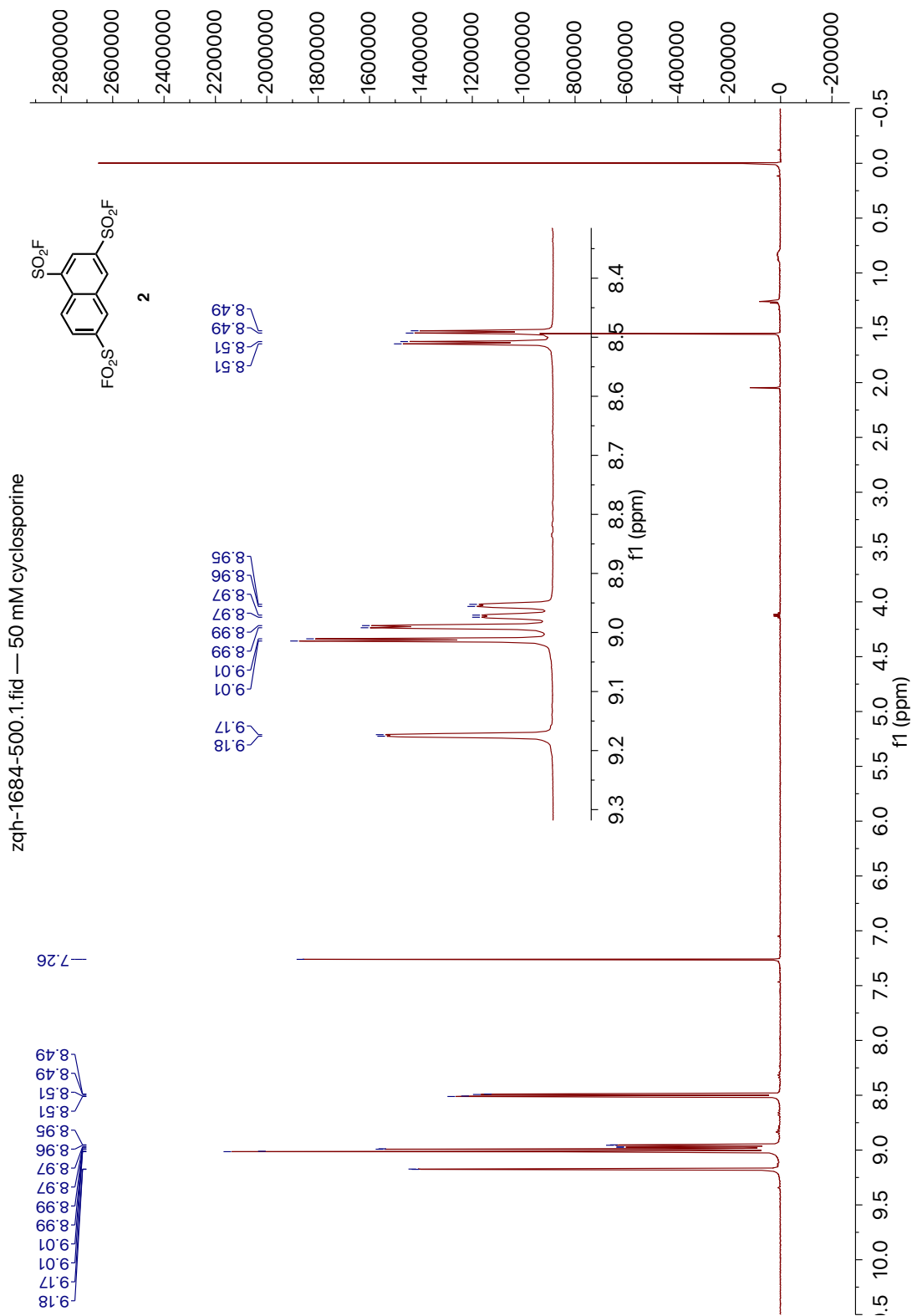
Entry	Electrophile	% remaining SM	Product (% HPLC yield)	Analytical method
1	 (ii) Sulfonyl fluoride	100	N/A	GC-MS LC-MS
2	 (vii) Epoxide [(±)-styrene oxide]	0	Unidentified mixture	GC-MS LC-MS
3	 (viii) Acrylamide	59	 (41)	LC-MS
4	 (ix) Vinyl sulfone	0	 (100)	LC-MS
5	 (x) α-chloroamide	0	 (>95)	LC-MS
6	 (xi) β-lactam	0	Unidentified mixture	GC-MS LC-MS

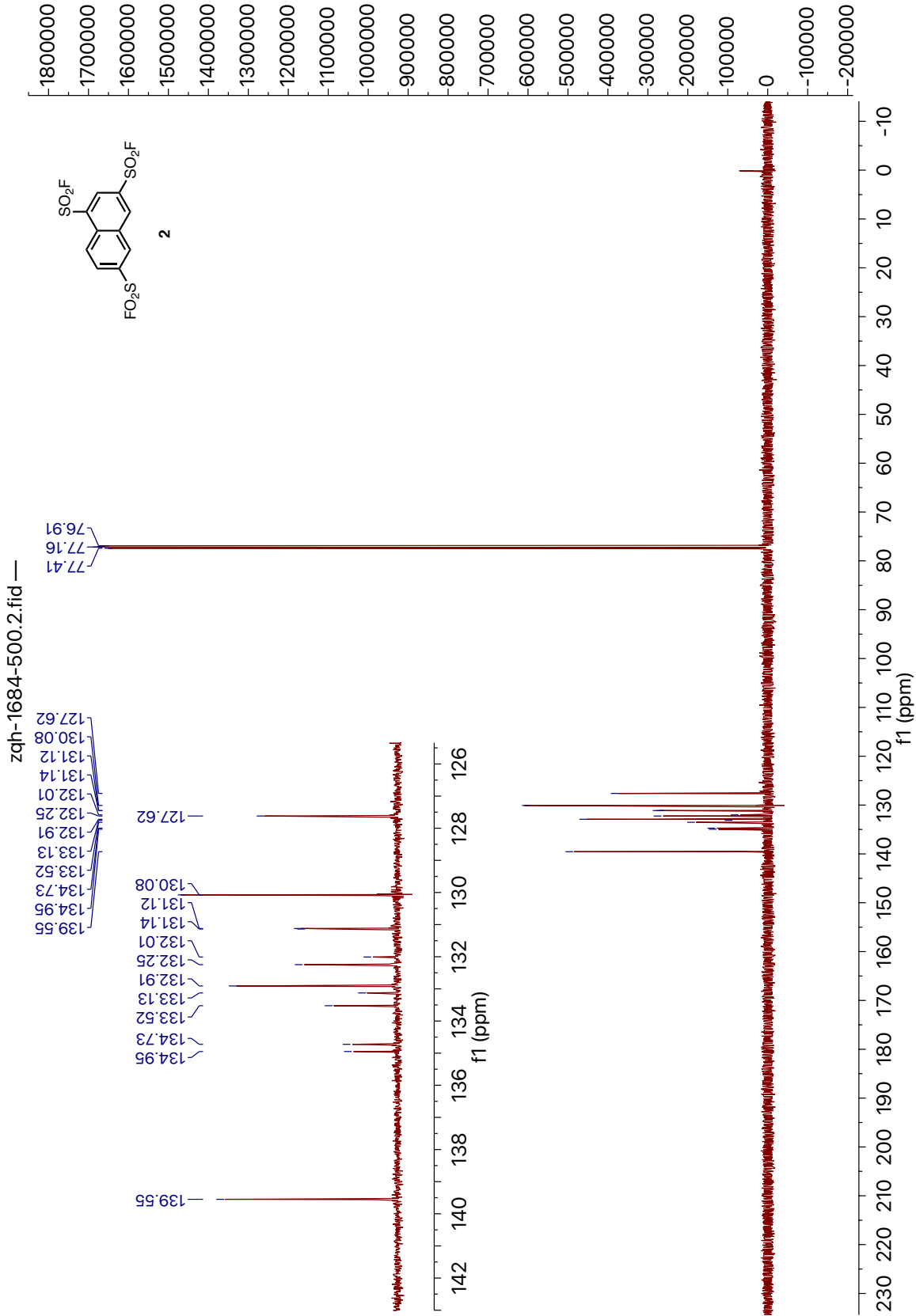
Entry	Electrophile	% remaining SM	Product (% HPLC yield)	Analytical method
7	 (xii) maleimide	0	 (27)  (73)	LC-MS
8	 (xiii) α-chloroketone	0	Unidentified mixture	LC-MS
9	 (xiv) fluorophosphate	11	 (55)  (34)	LC-MS

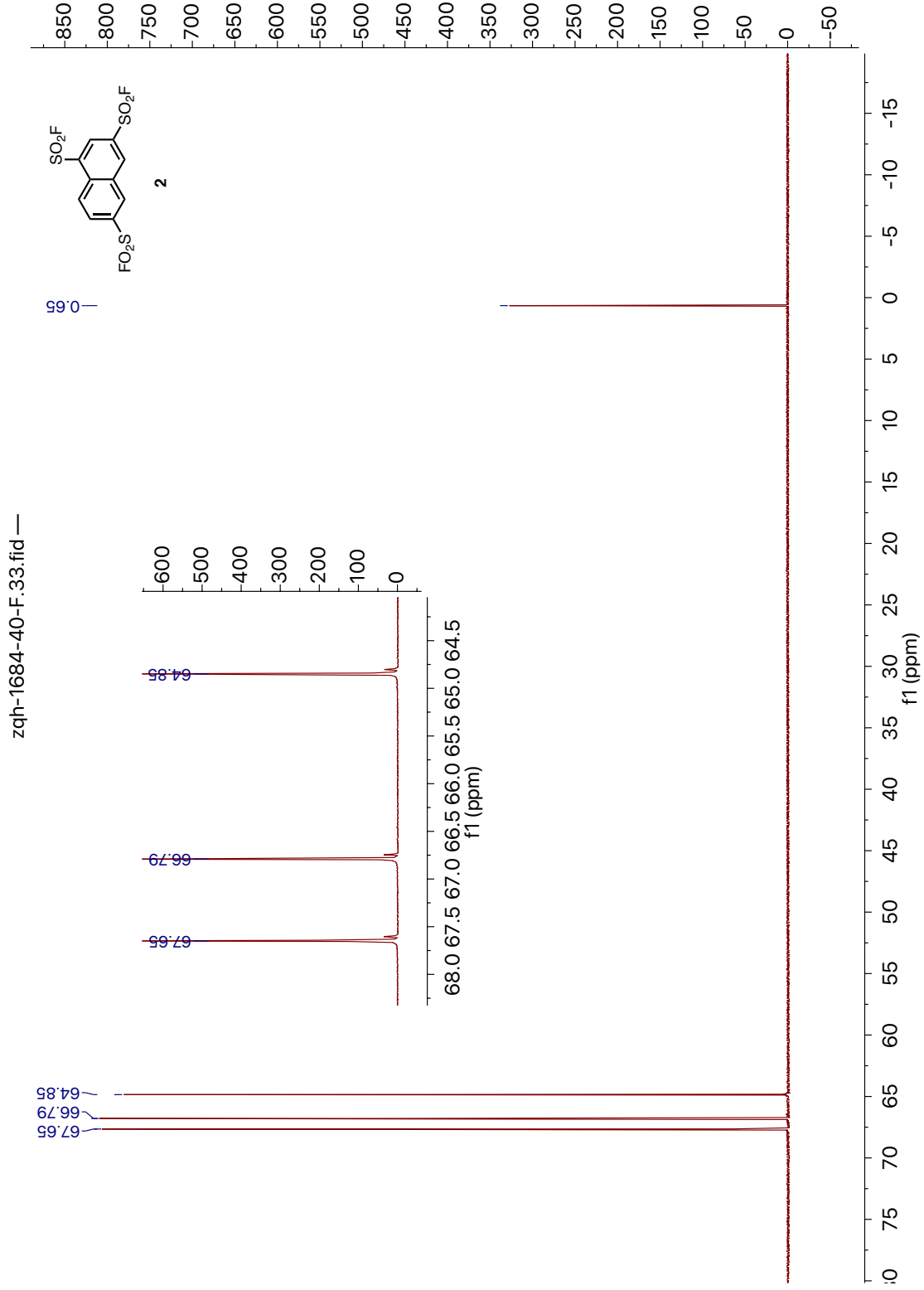
*“Refluxing aniline” test was performed by heat the neat mixture of respective electrophiles (1.0 mmol) with 1.3 mL aniline at 184 °C.

10. NMR spectra

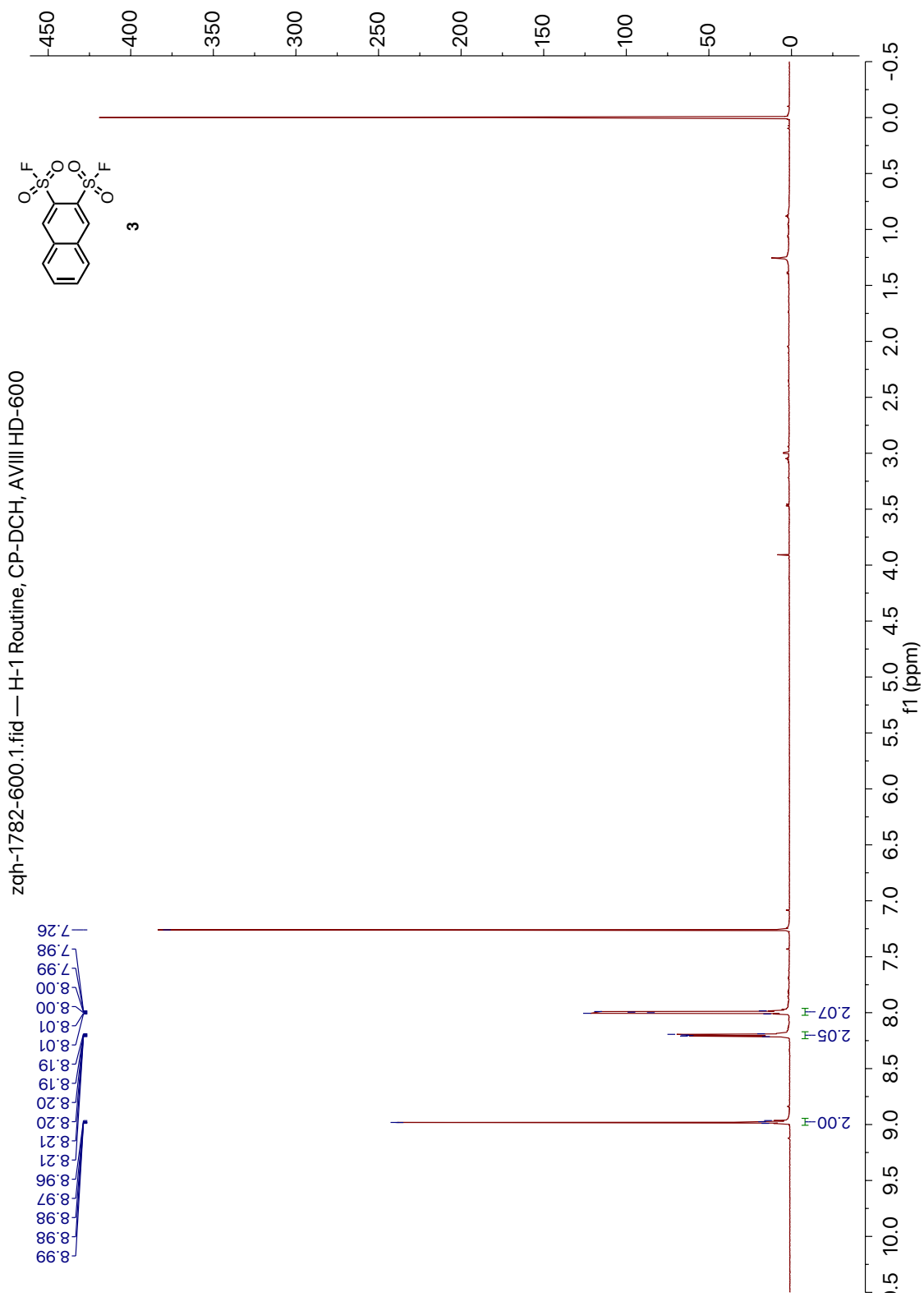
10.1. Naphthalene-1,3,6-trisulfonyl trifluoride (**2**)

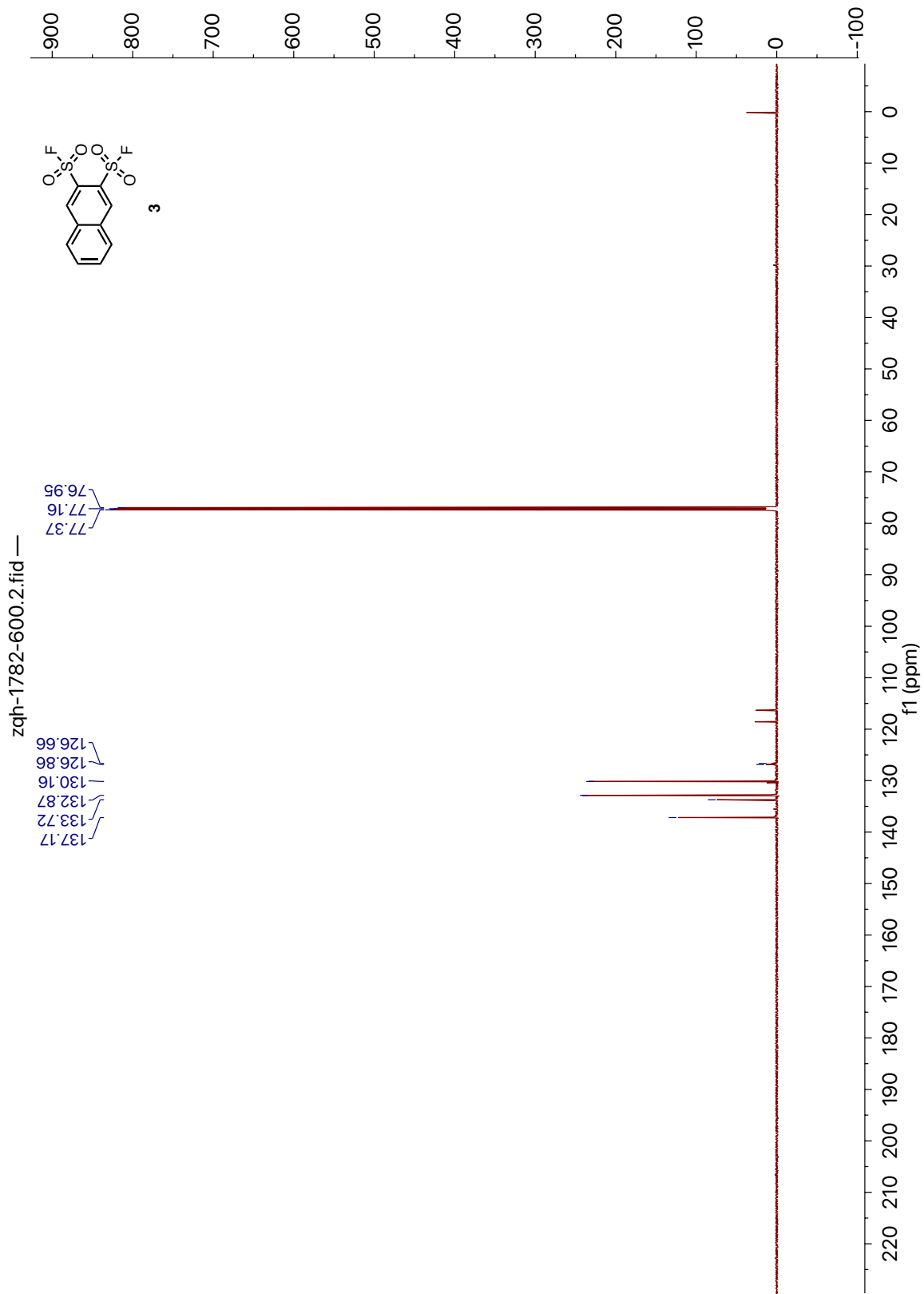




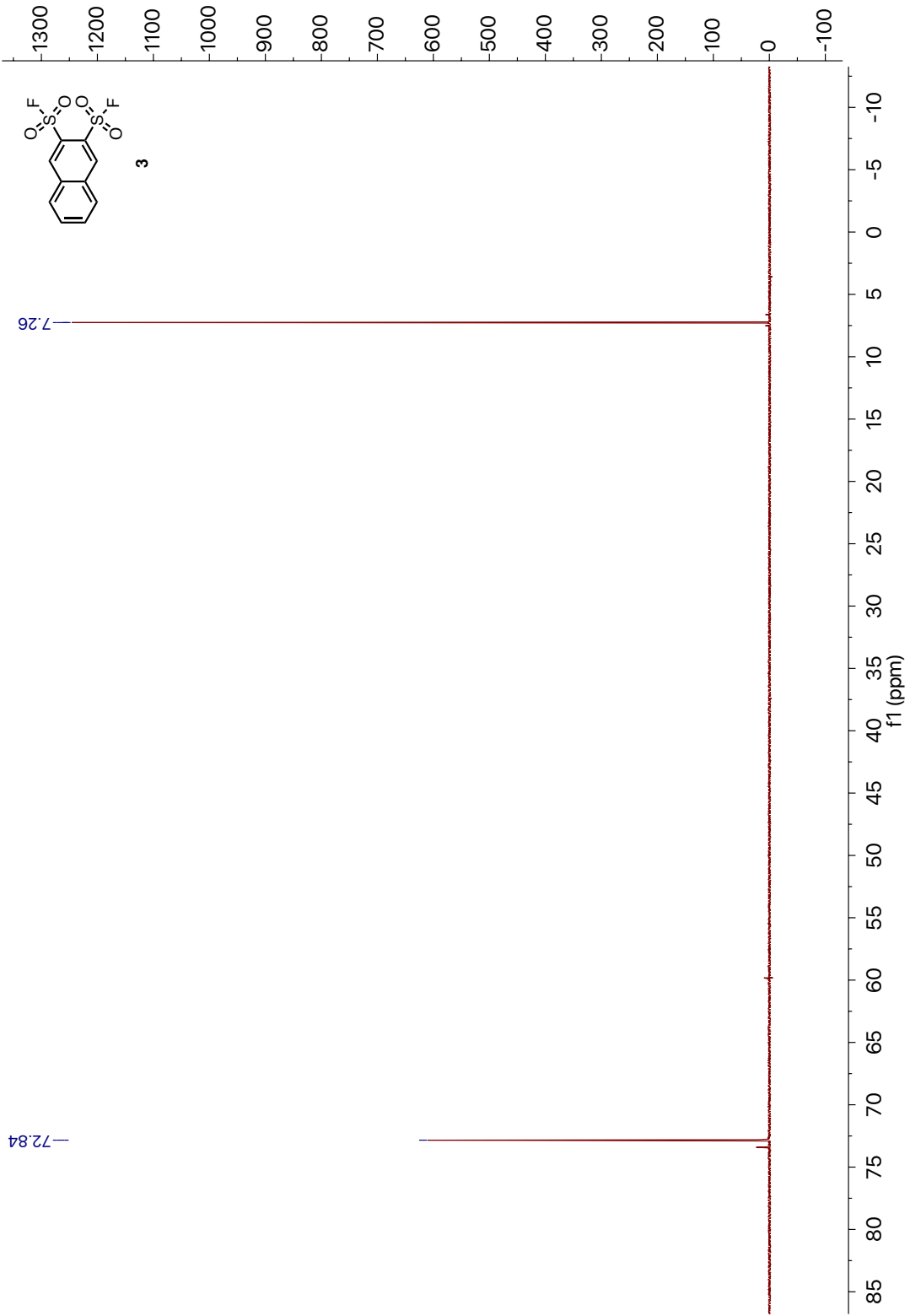


10.2. Naphthalene-2,3-disulfonyl difluoride (**3**)

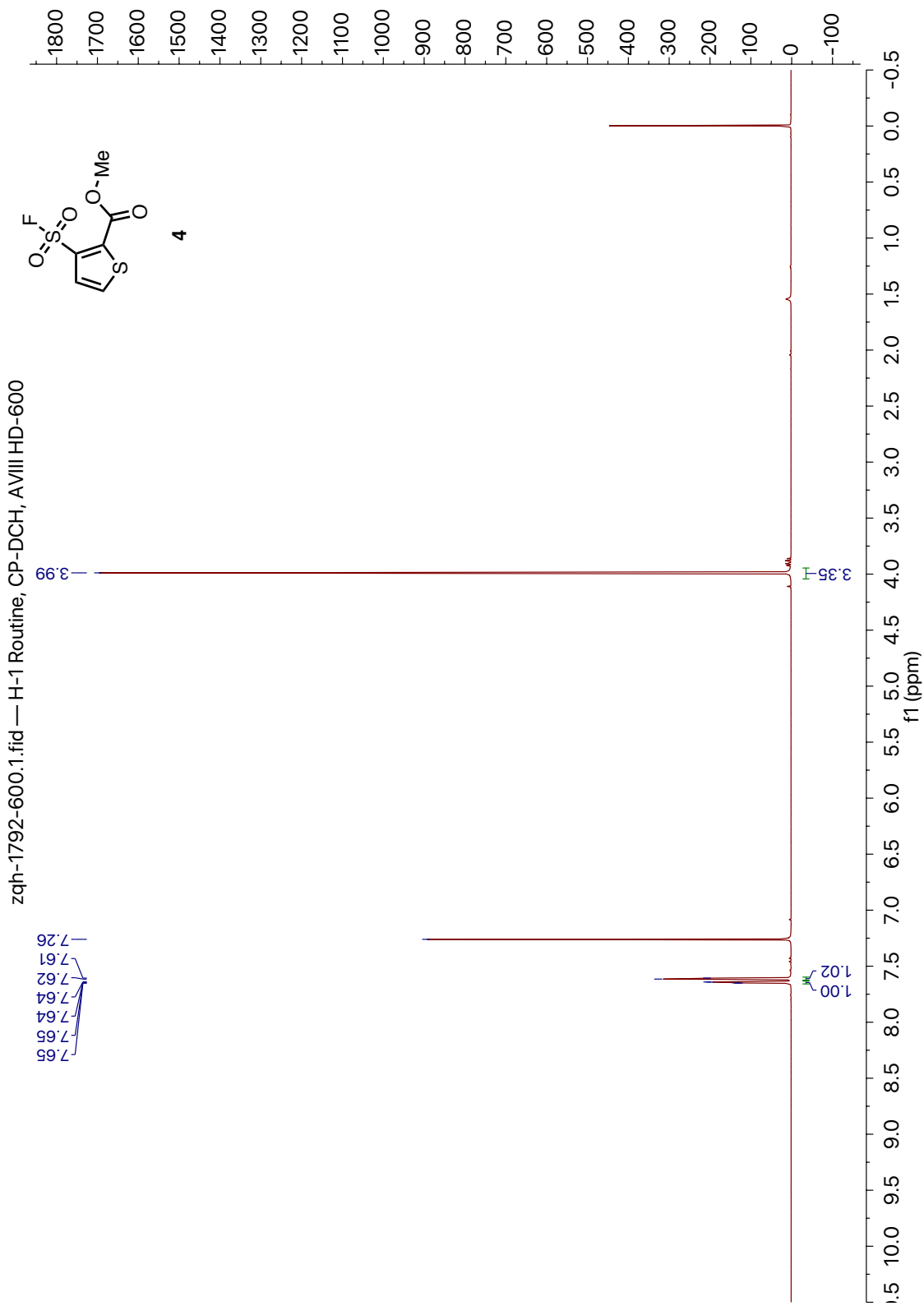


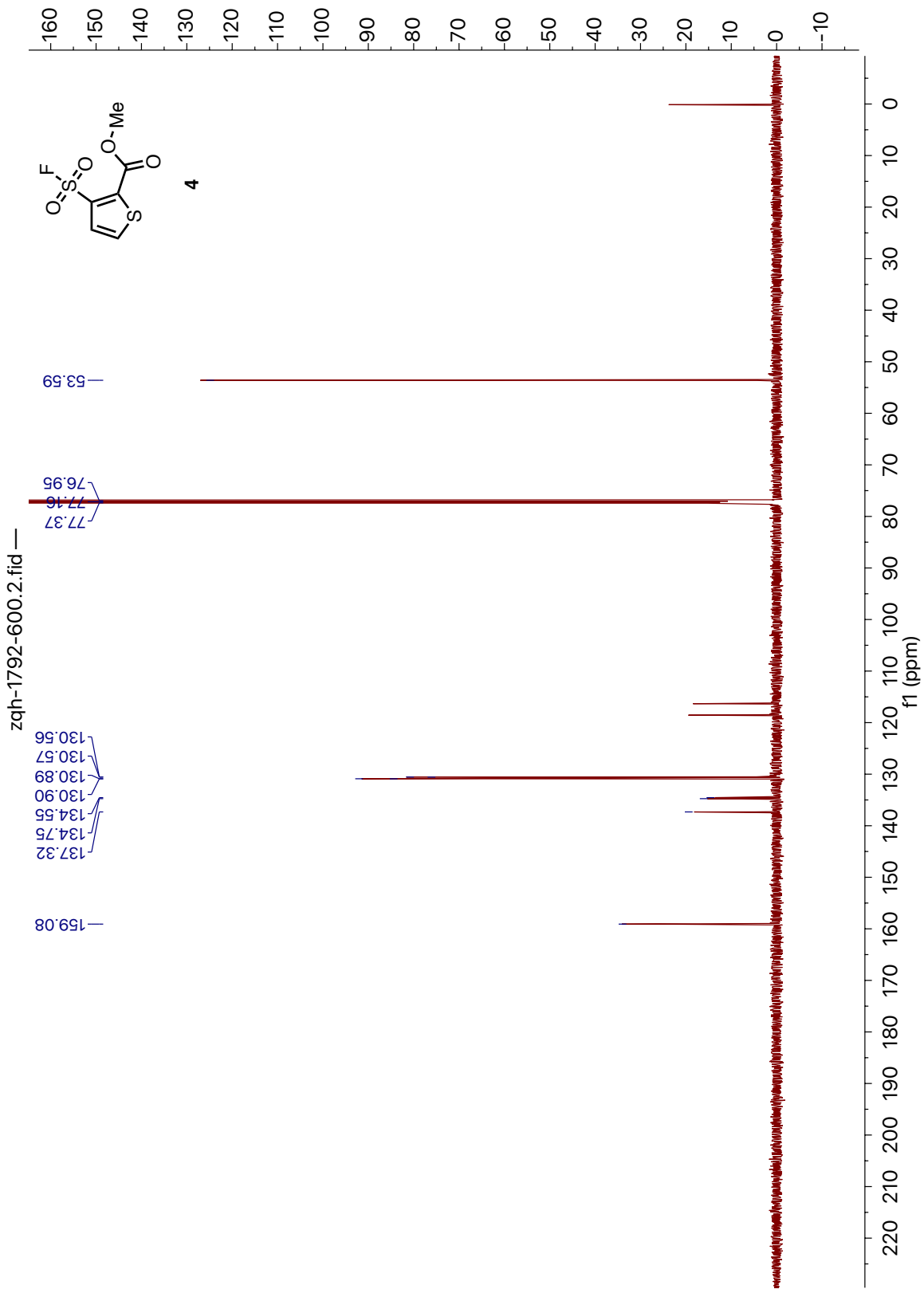


zqh-1782-400-F.1.fid — F-19, CDCI3, DPX-400 QNP Probe. CF3Cl as Ref at 0 ppm.

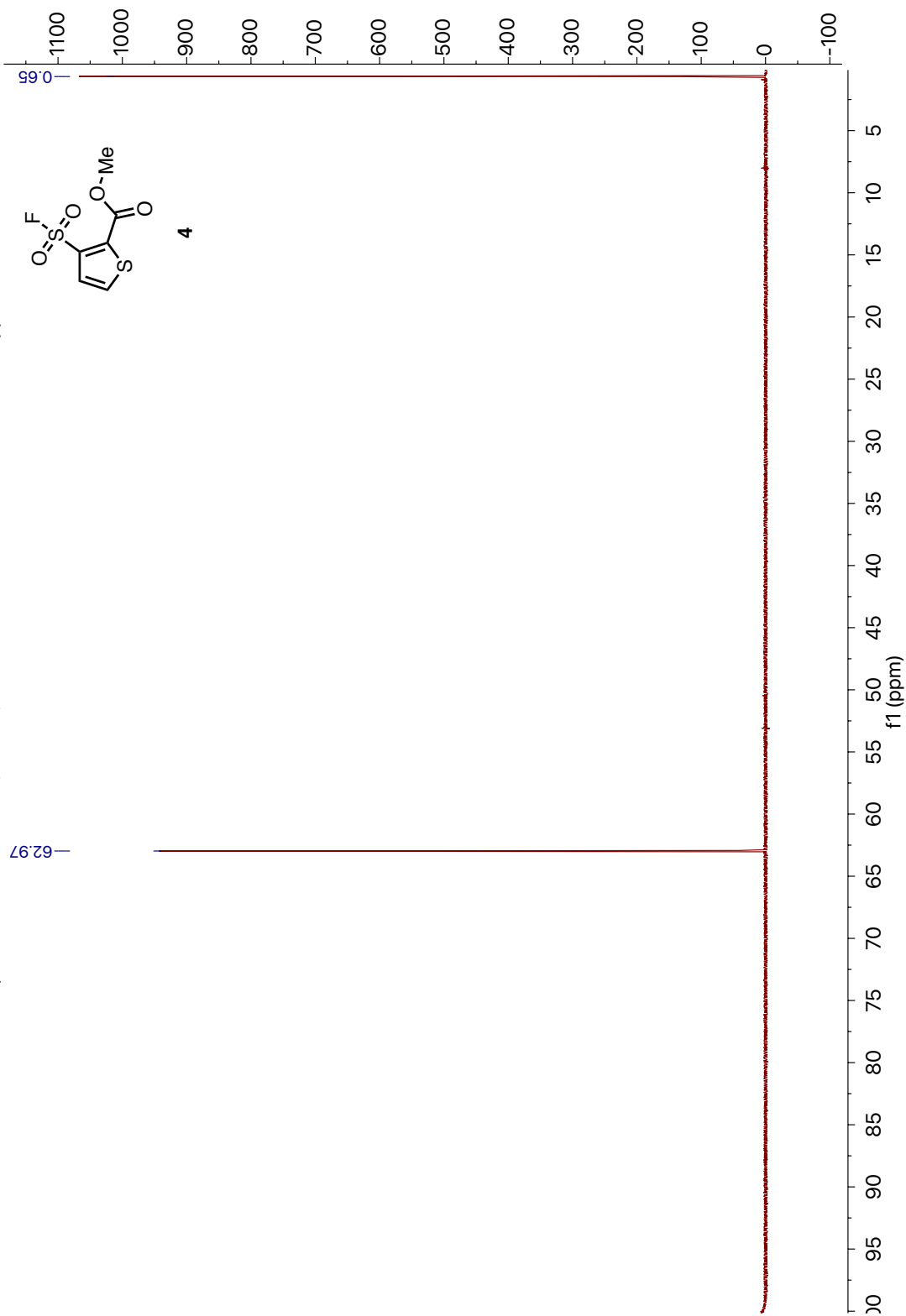


10.3. Methyl 3-(fluorosulfonyl)thiophene-2-carboxylate (**4**)

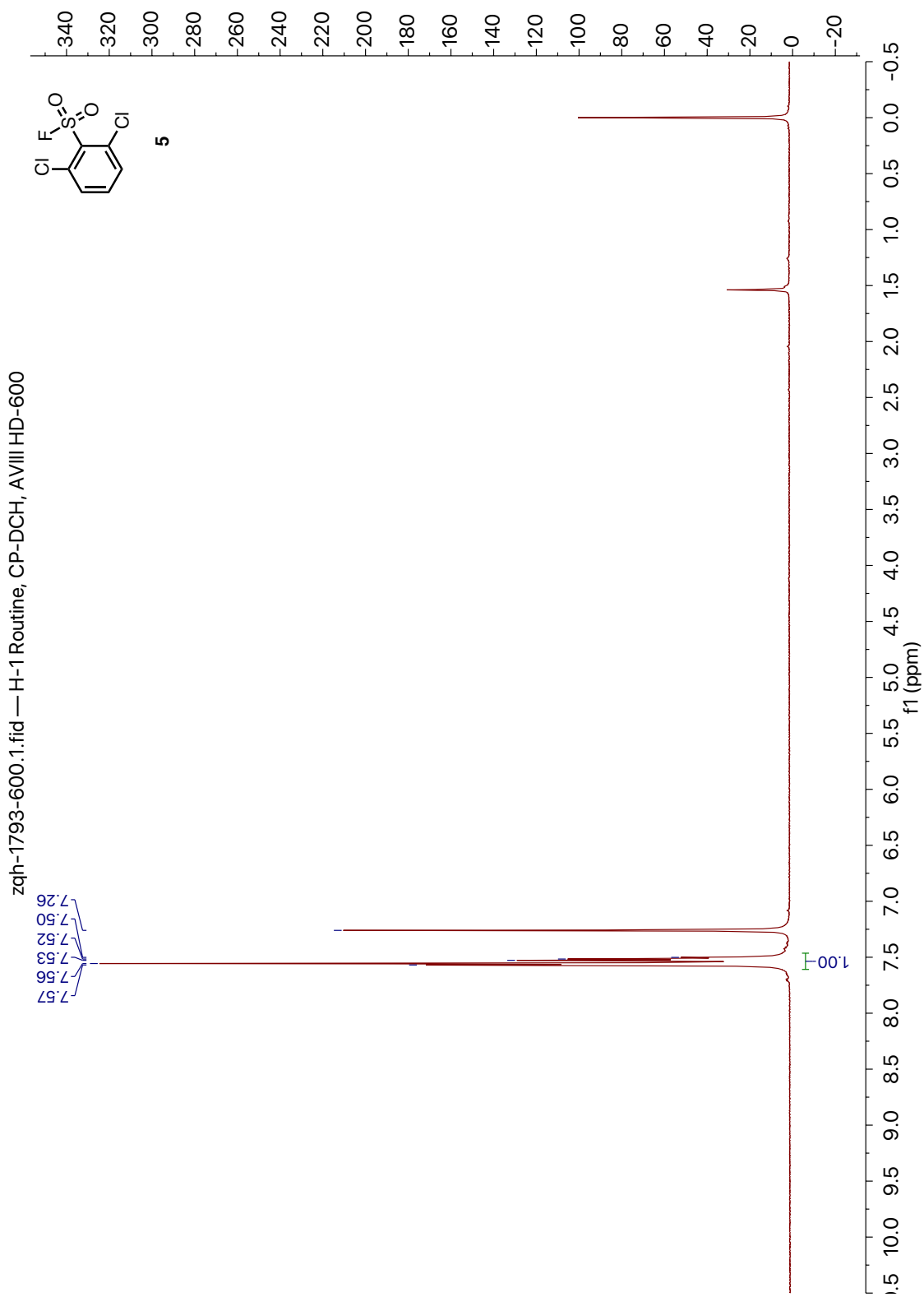




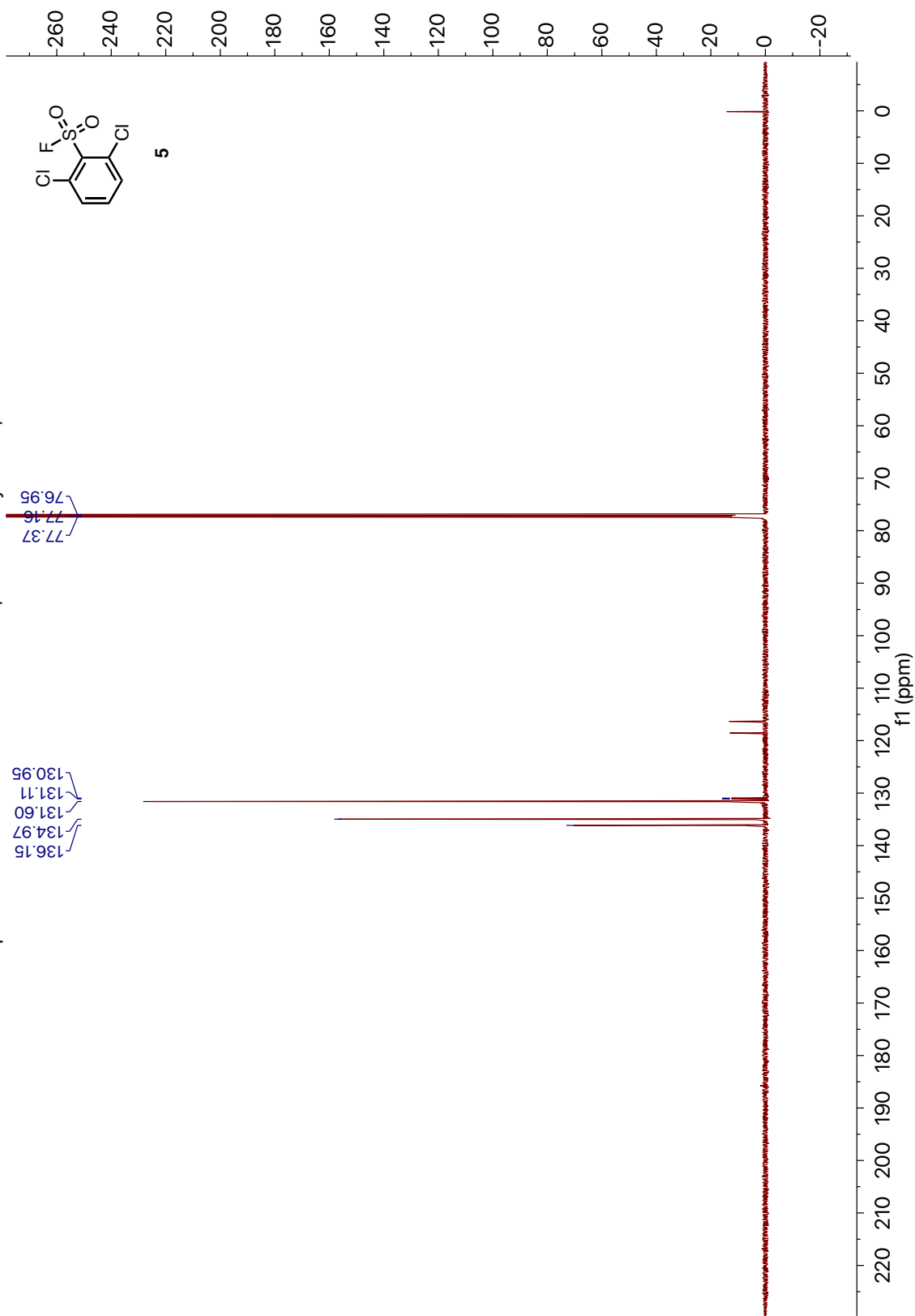
zqh-1792-F.1.fid — F-19, CDCl₃, DPX-400 QNP Probe. CF₃Cl as Ref at 0 ppm.



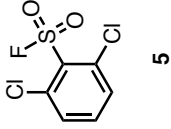
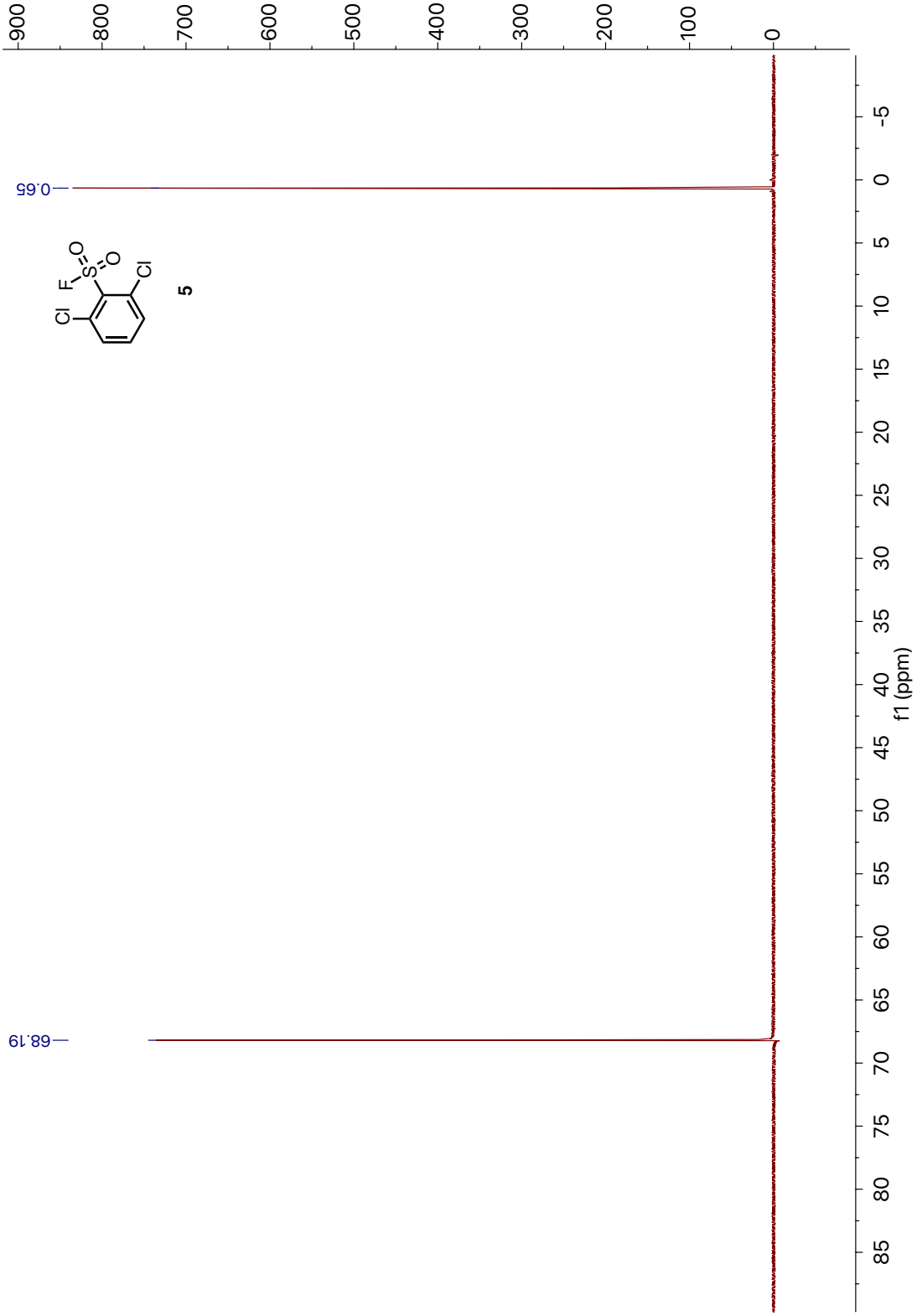
10.4. 2,6-dichlorobenzenesulfonyl fluoride (5)



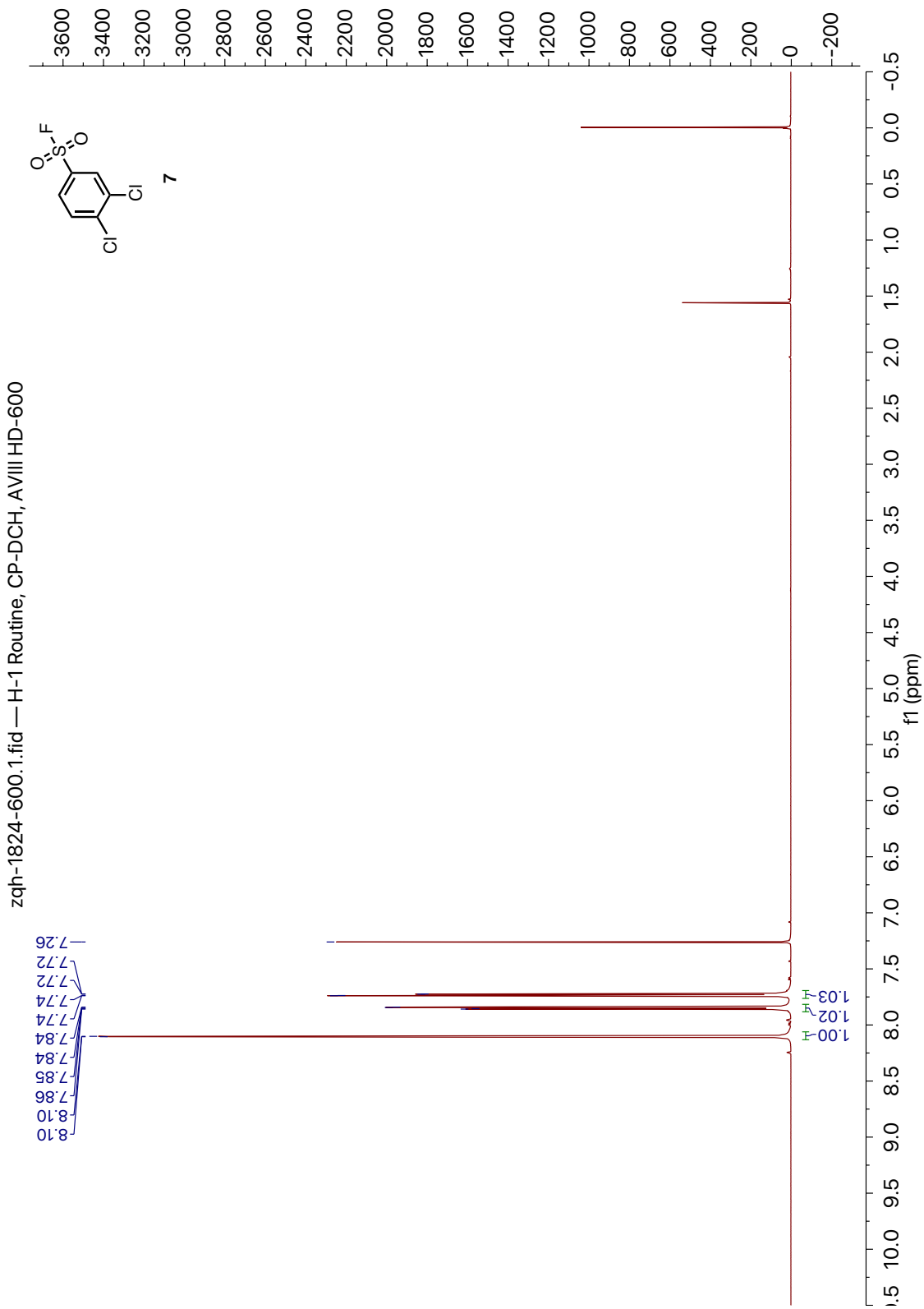
zqh-1793-600.2.fid — C-13 Routine 1D, CPDCH CryoProbe, AVIII-600

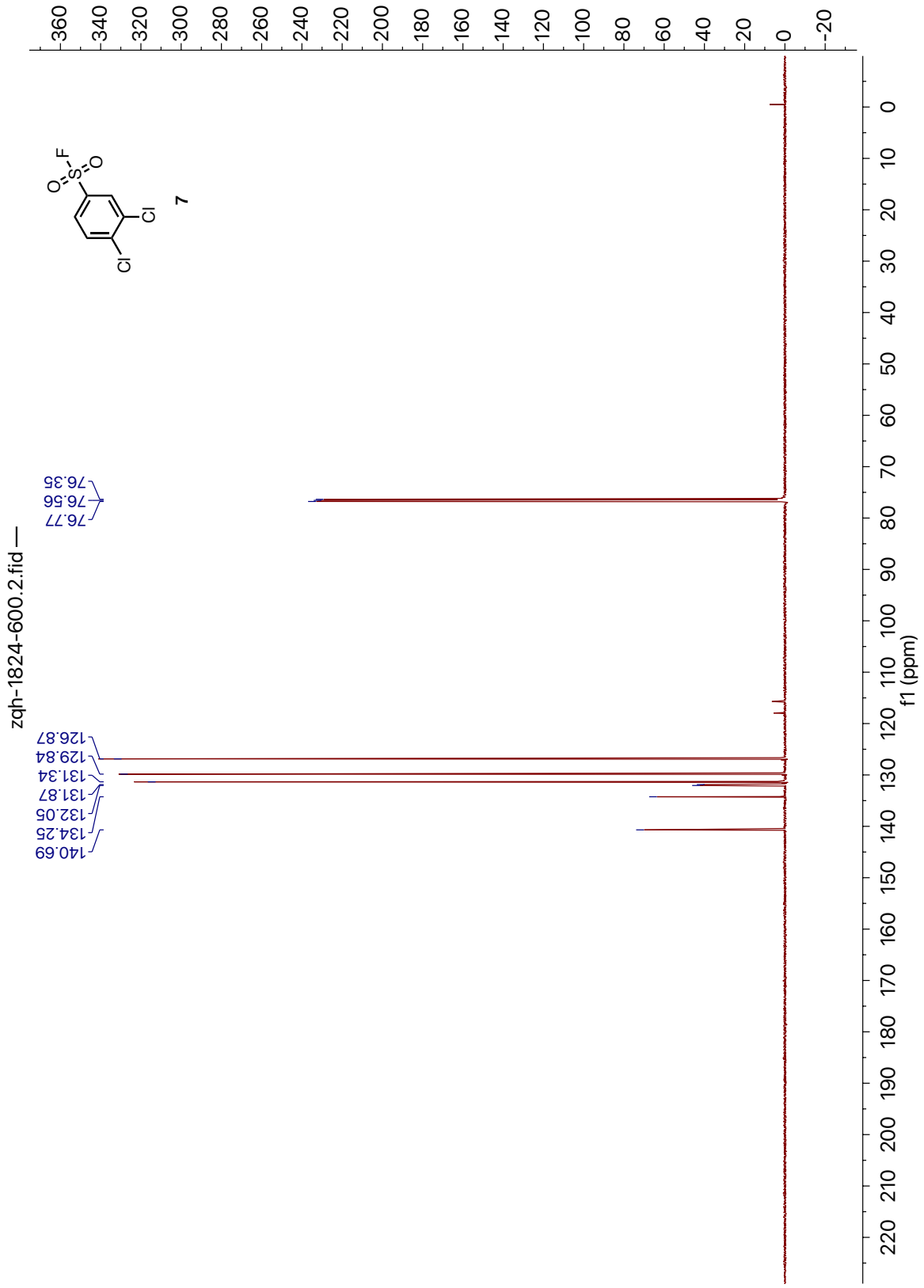


zqh-1793-F.1.fid — F-19, CDCl₃, DPX-400 QNP Probe. CF₃Cl as Ref at 0 ppm.

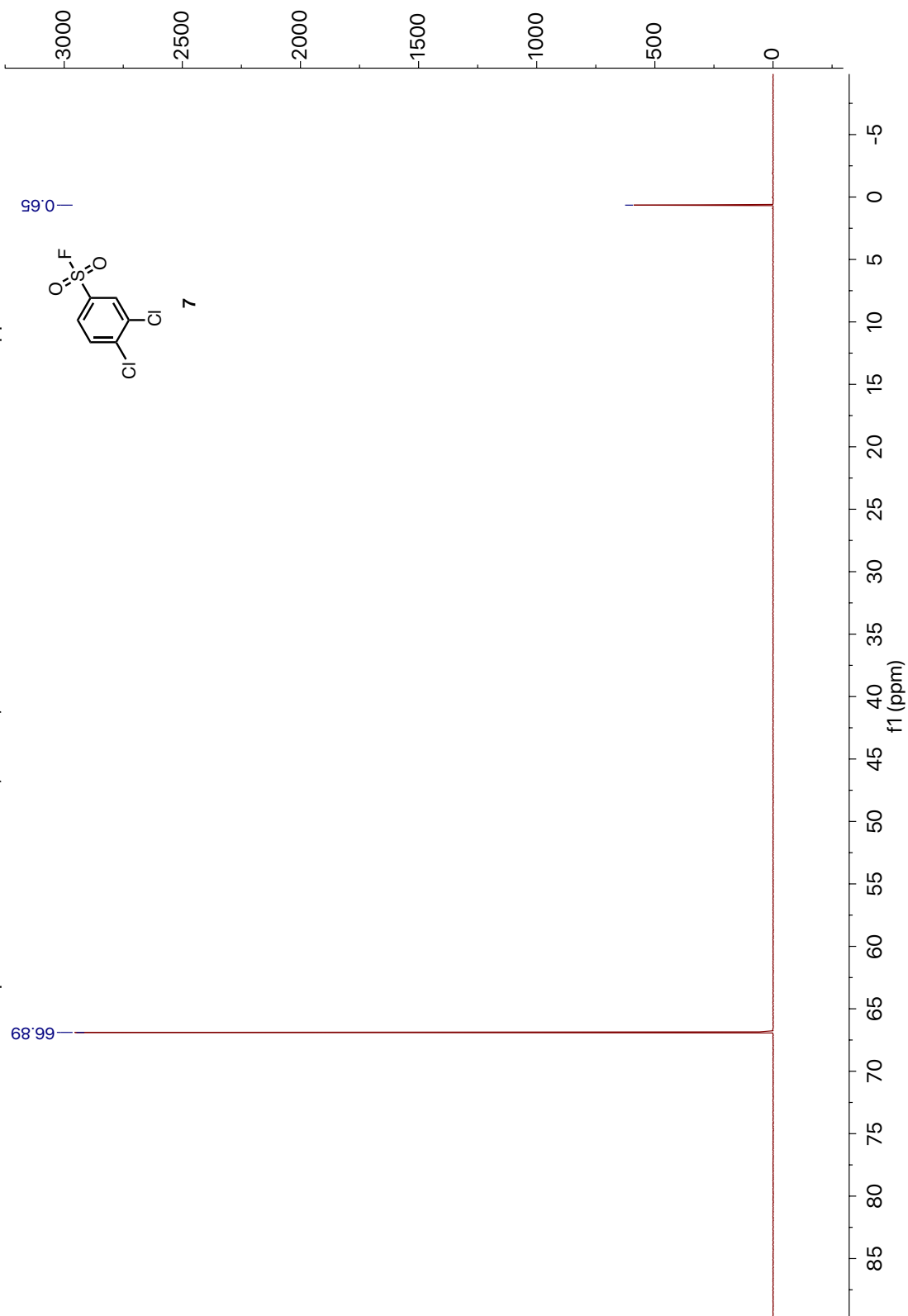


10.5. 3,4-dichlorobenzenesulfonyl fluoride (7)

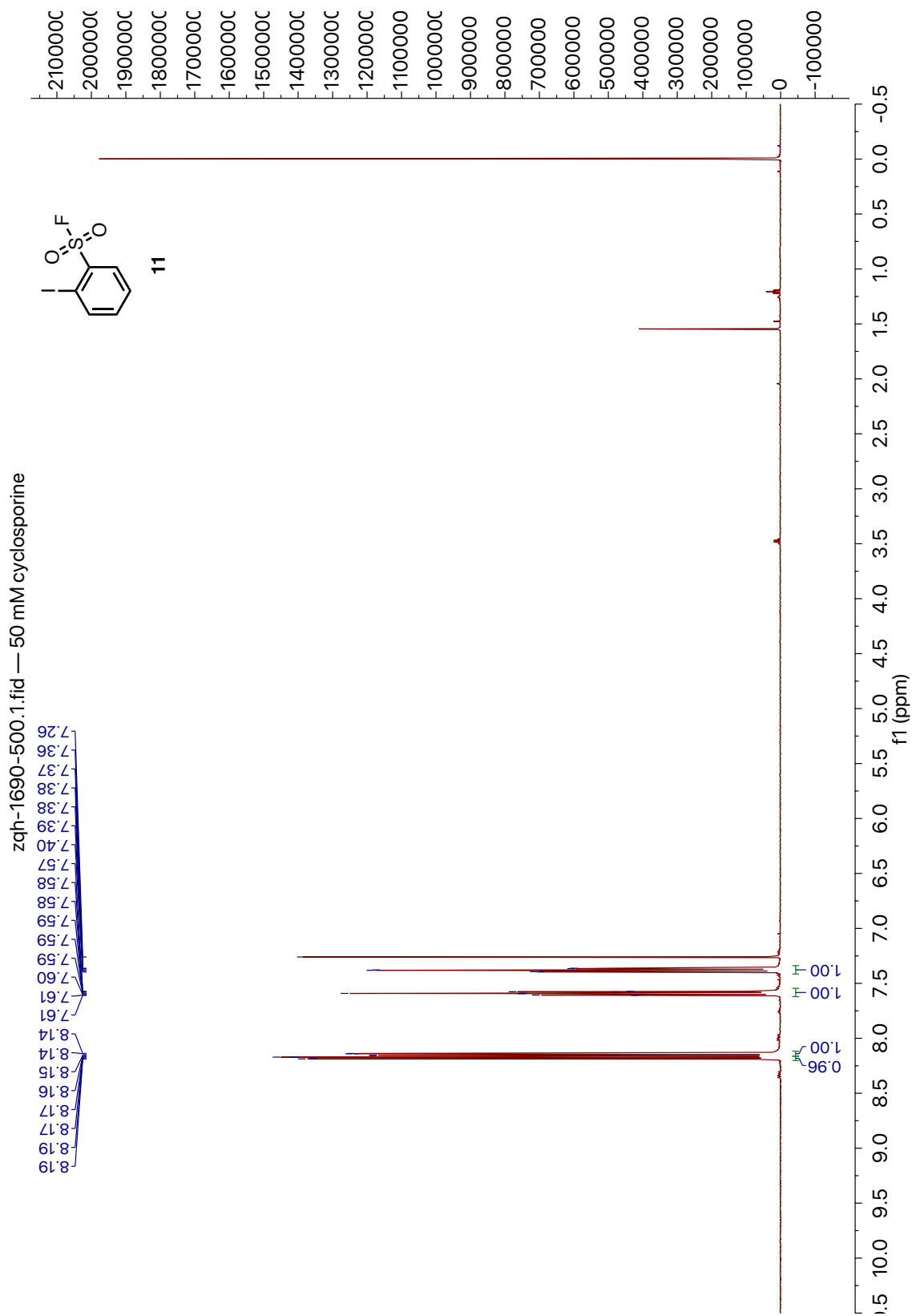




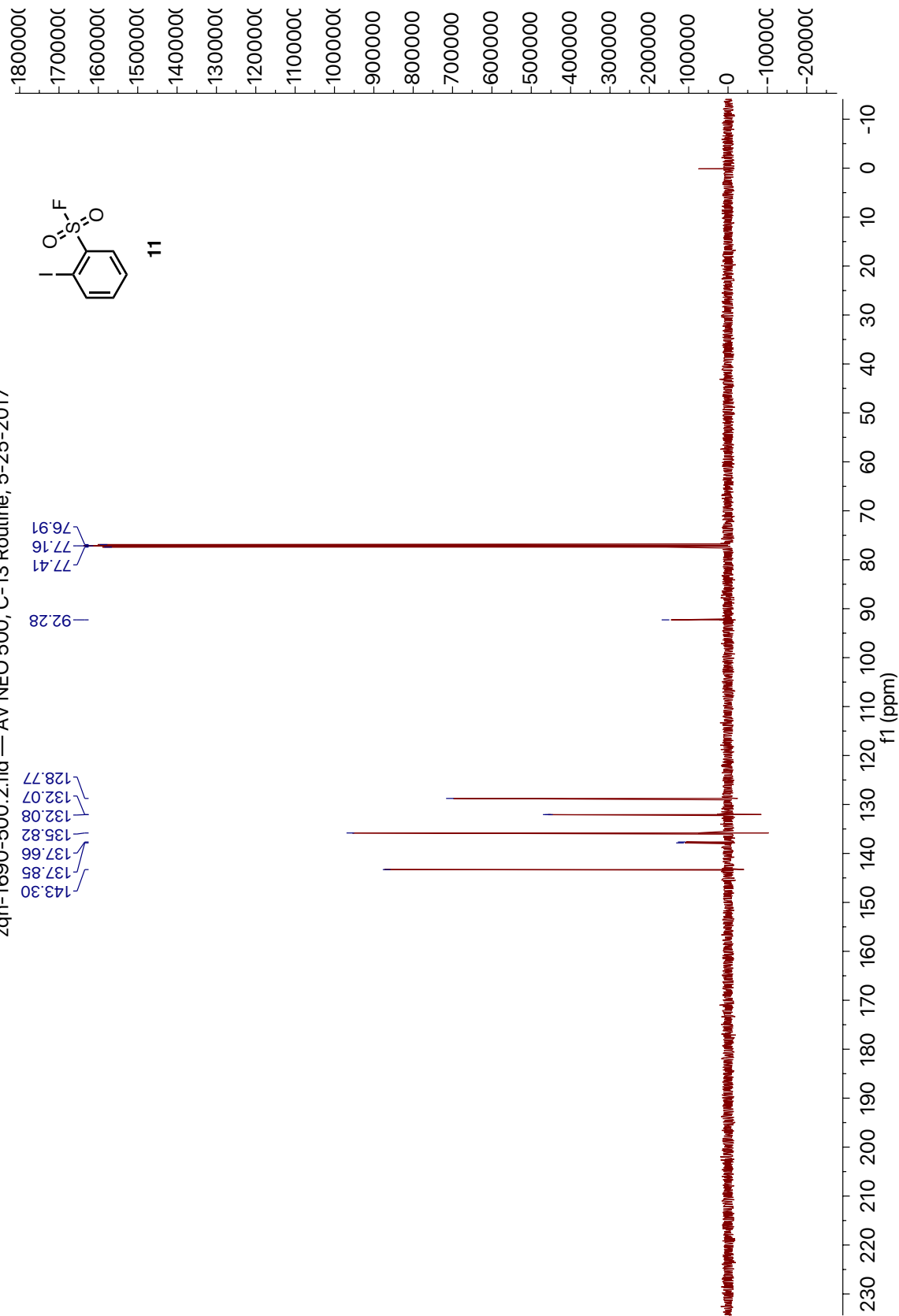
zqh-1824-F.1.fid — F-19, CDCl₃, DPX-400 QNP Probe. CF₃Cl as Ref at 0 ppm.



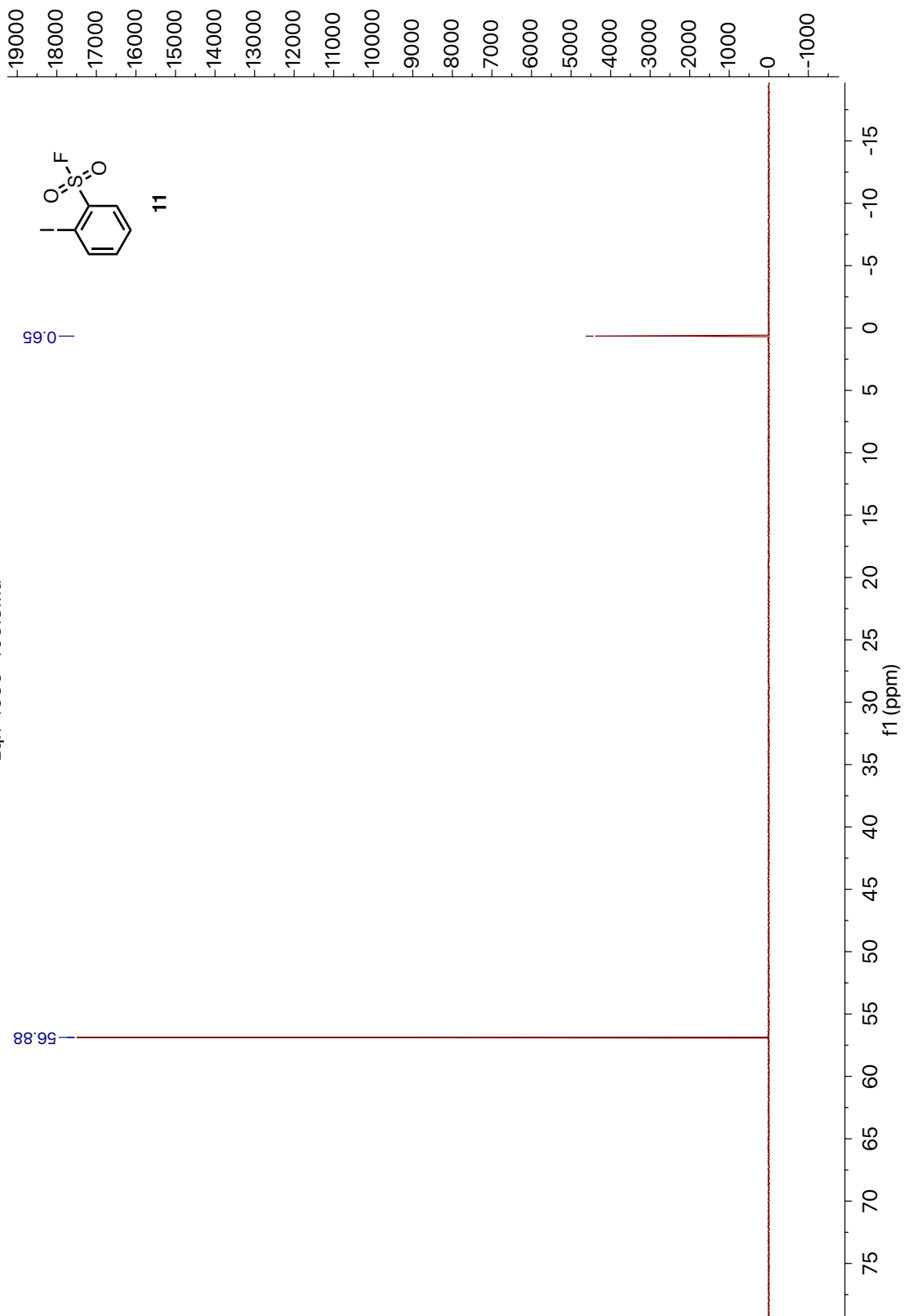
10.6. 2-Iodobenzenesulfonyl fluoride (**11**)



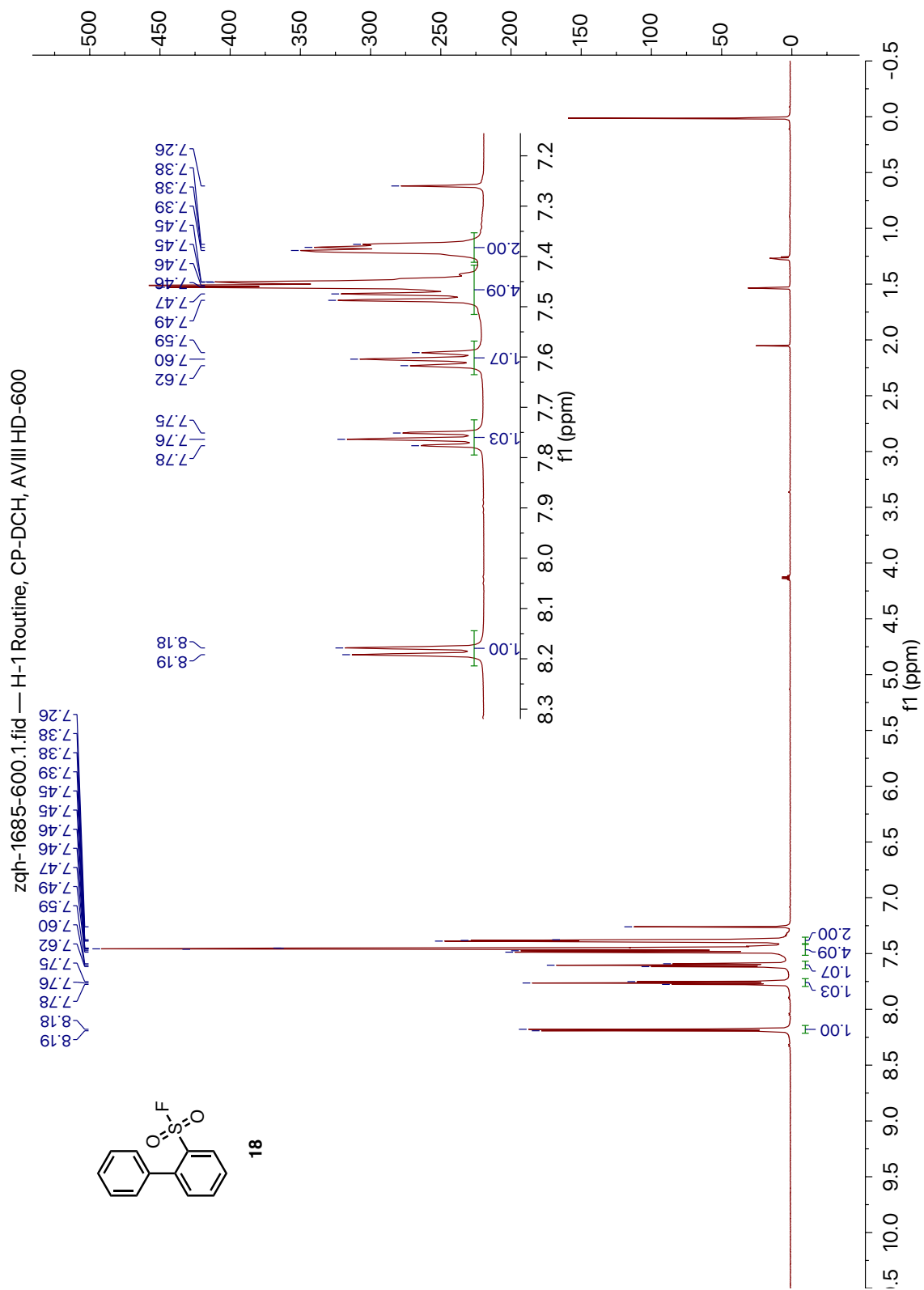
zqh-1690-500.2.fid — AV NEO 500, C-13 Routine, 5-25-2017



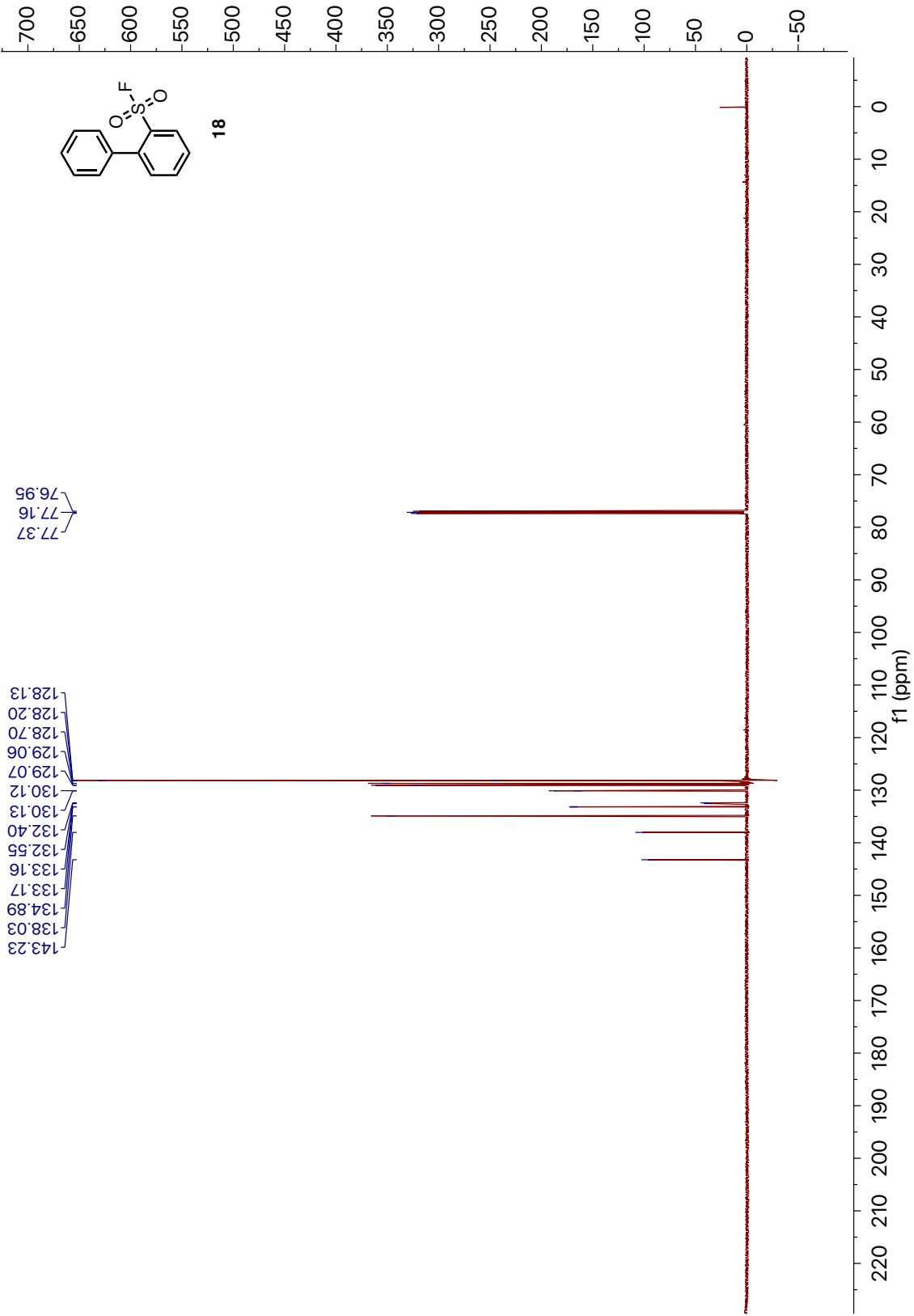
zqh-1690-400.3.fid

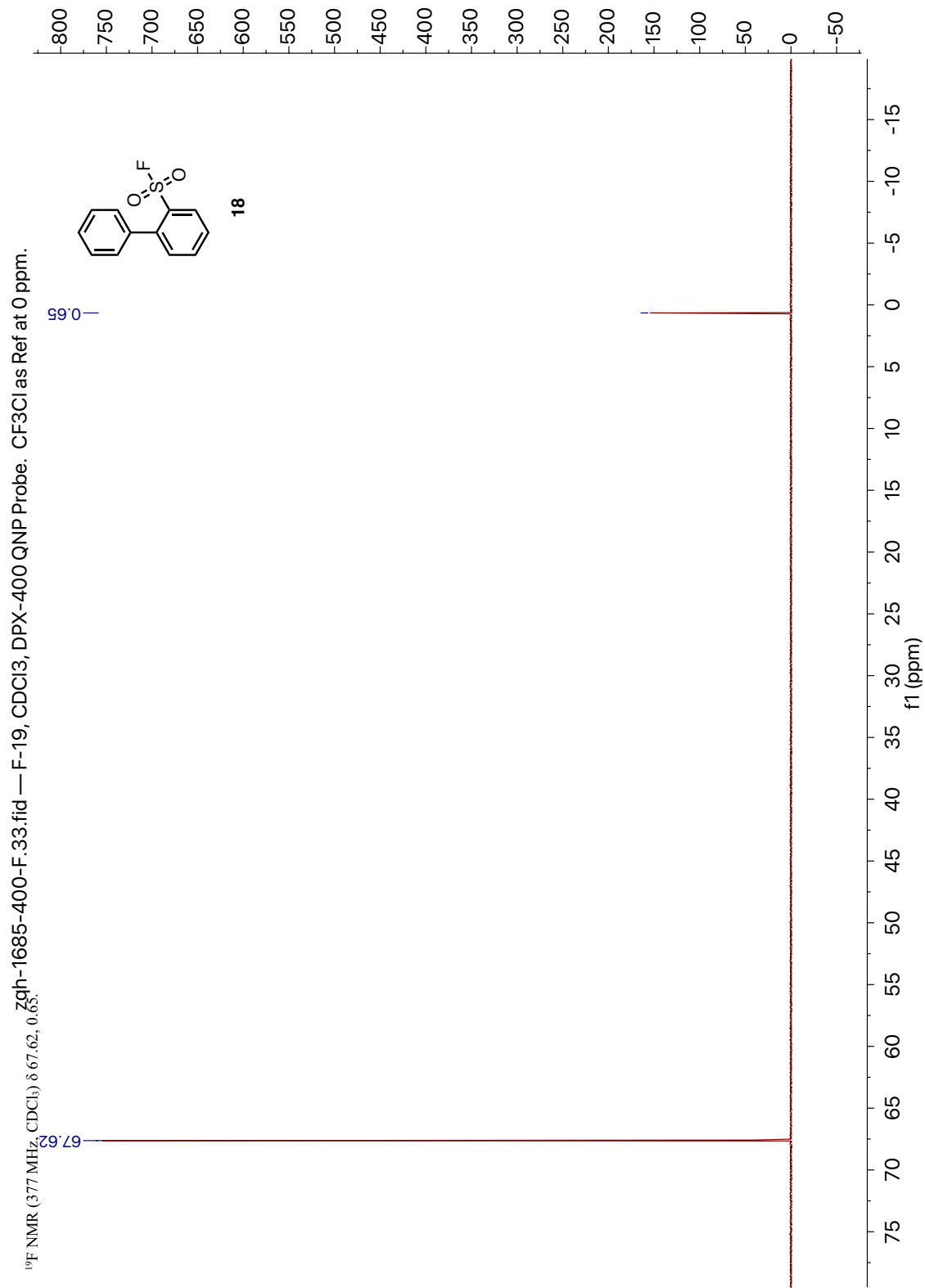


10.7. [1,1'-biphenyl]-2-sulfonyl fluoride (**18**)

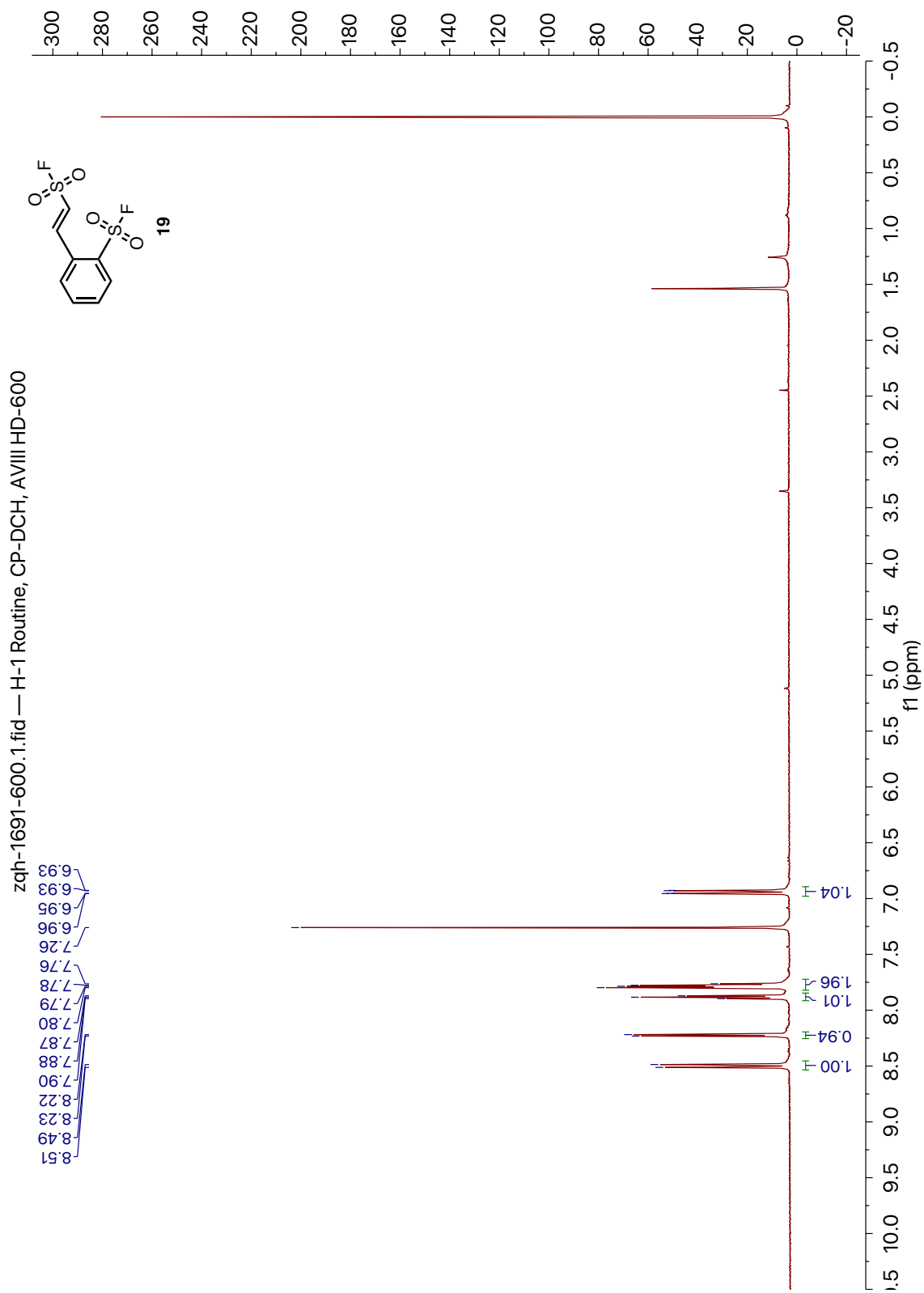


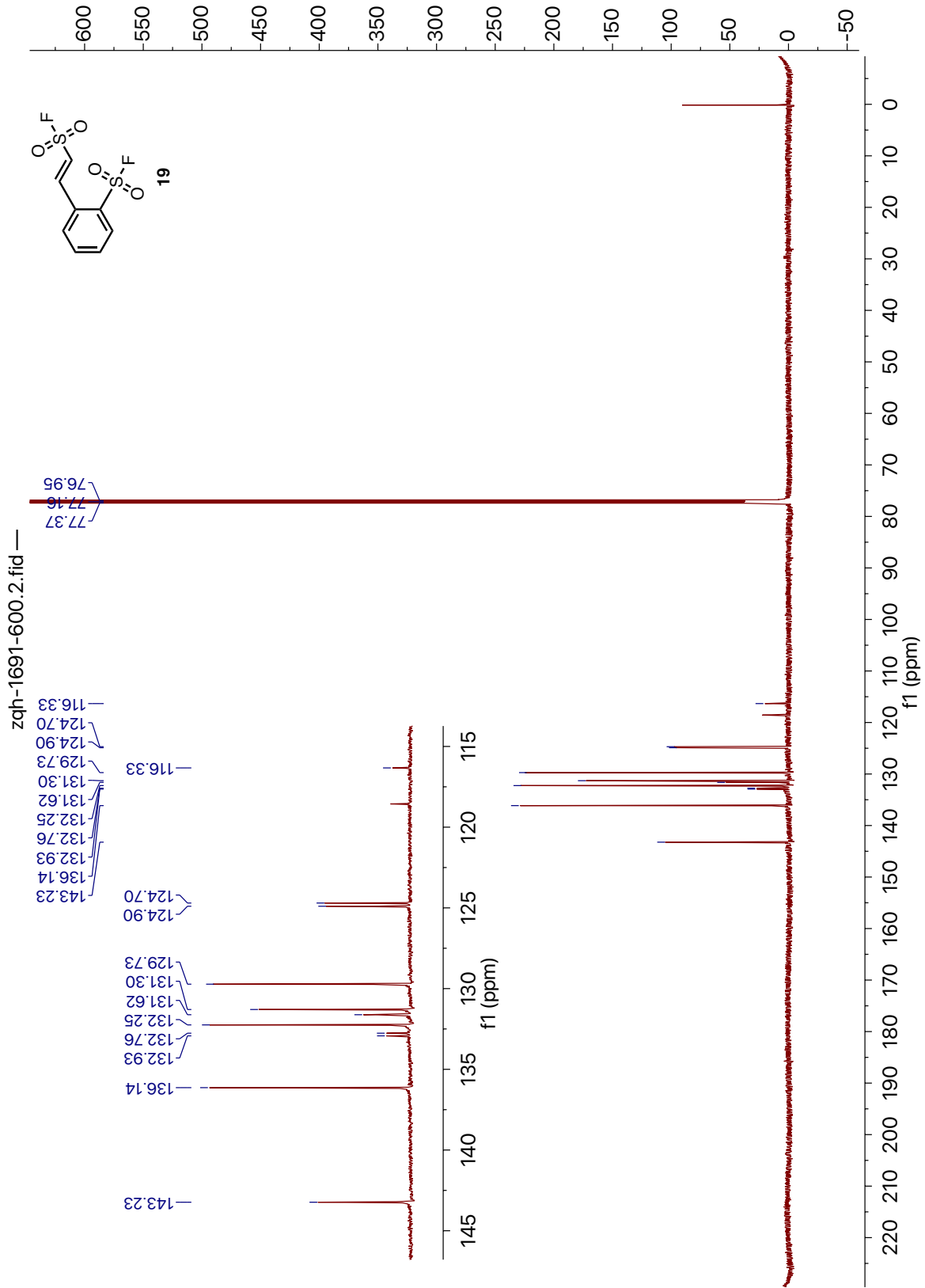
zqh-1685-600.2.fid — C-13 Routine 1D, CPDCH CryoProbe, AVIII-600



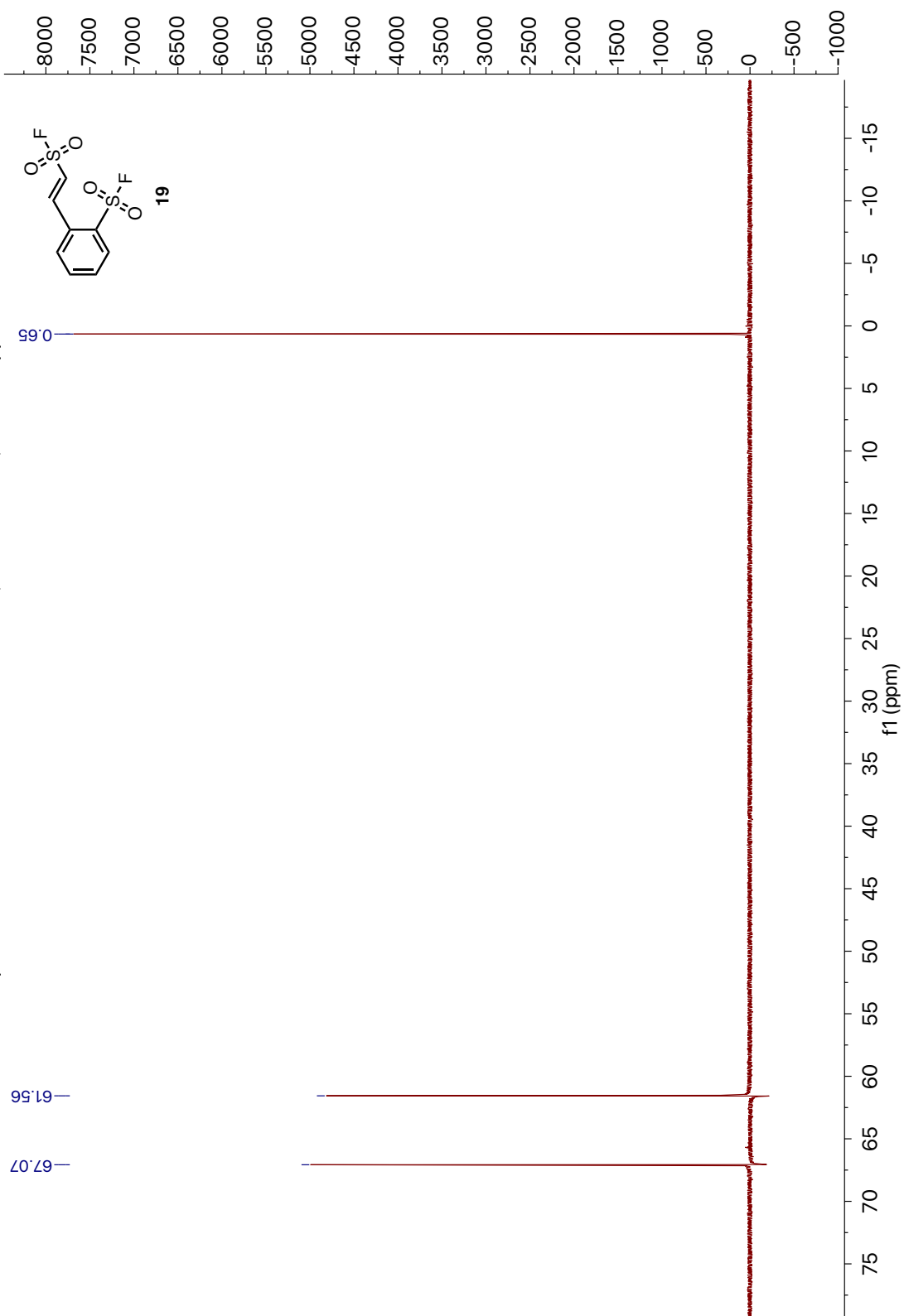


10.8. (E)-2-(2-(fluorosulfonyl)vinyl)benzenesulfonyl fluoride (19)

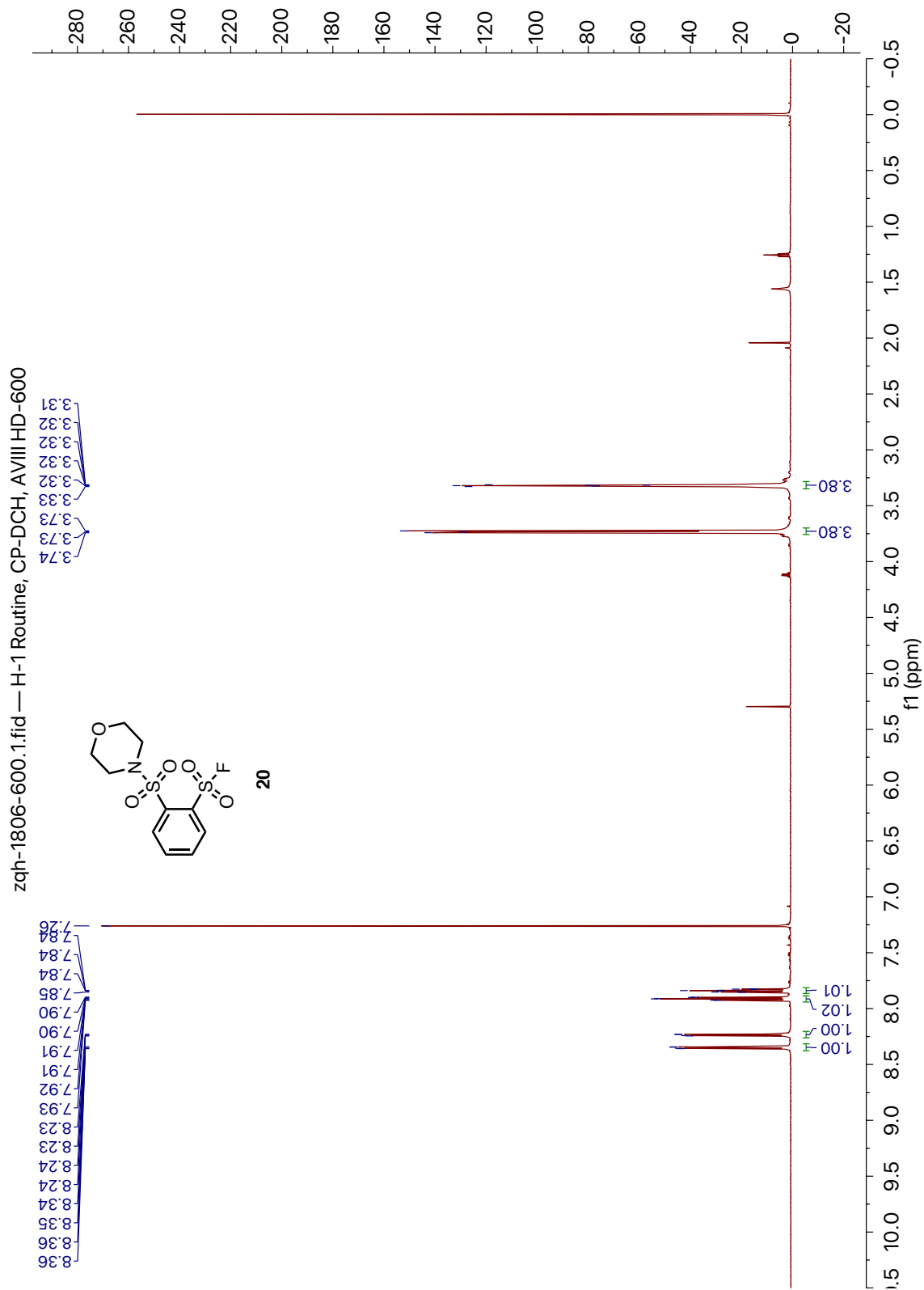




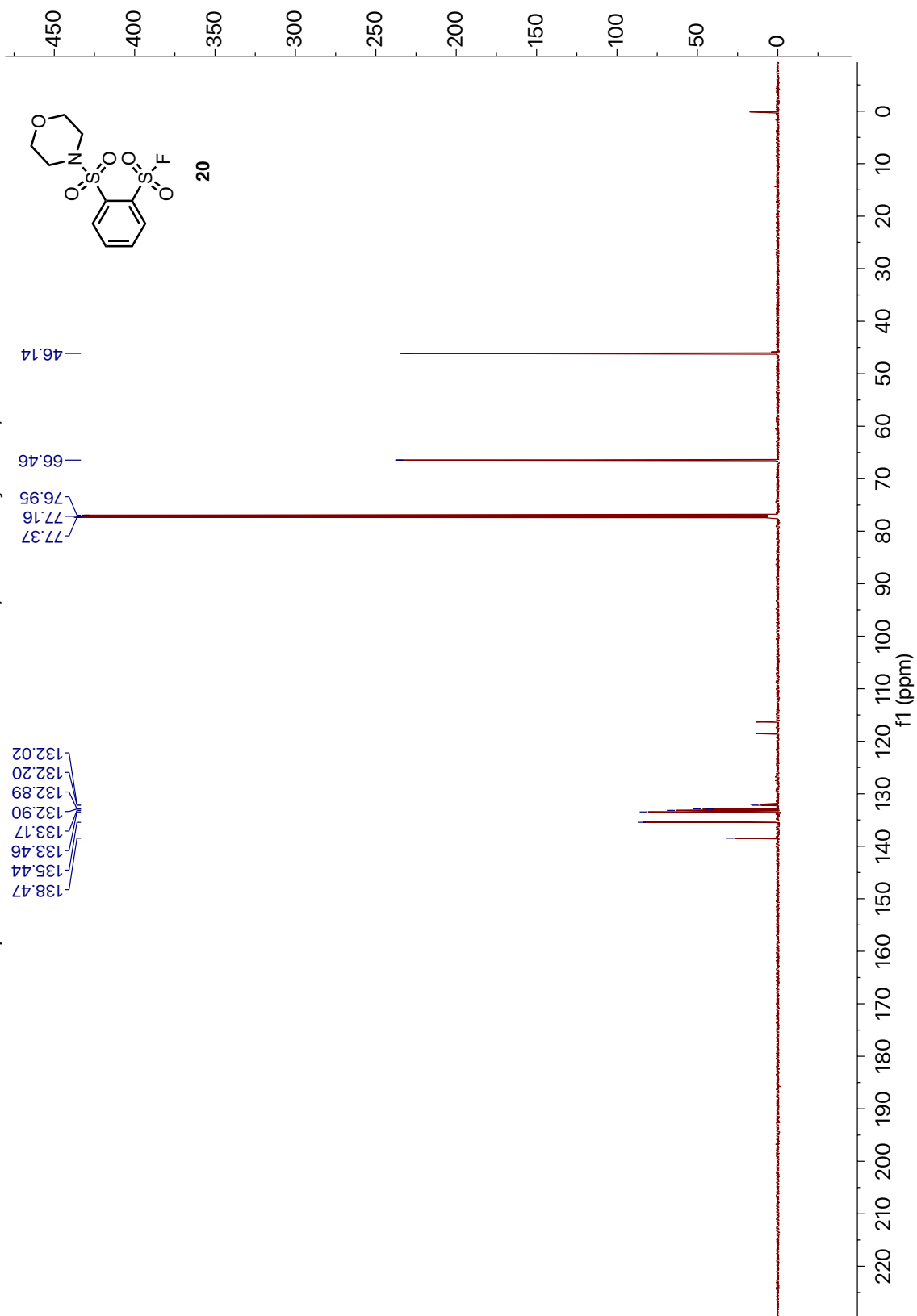
zqh-1691-400-F-3.fid — AV400 BBOF Probe, F-19 in CDCl₃, CFCI₃=0 ppm.



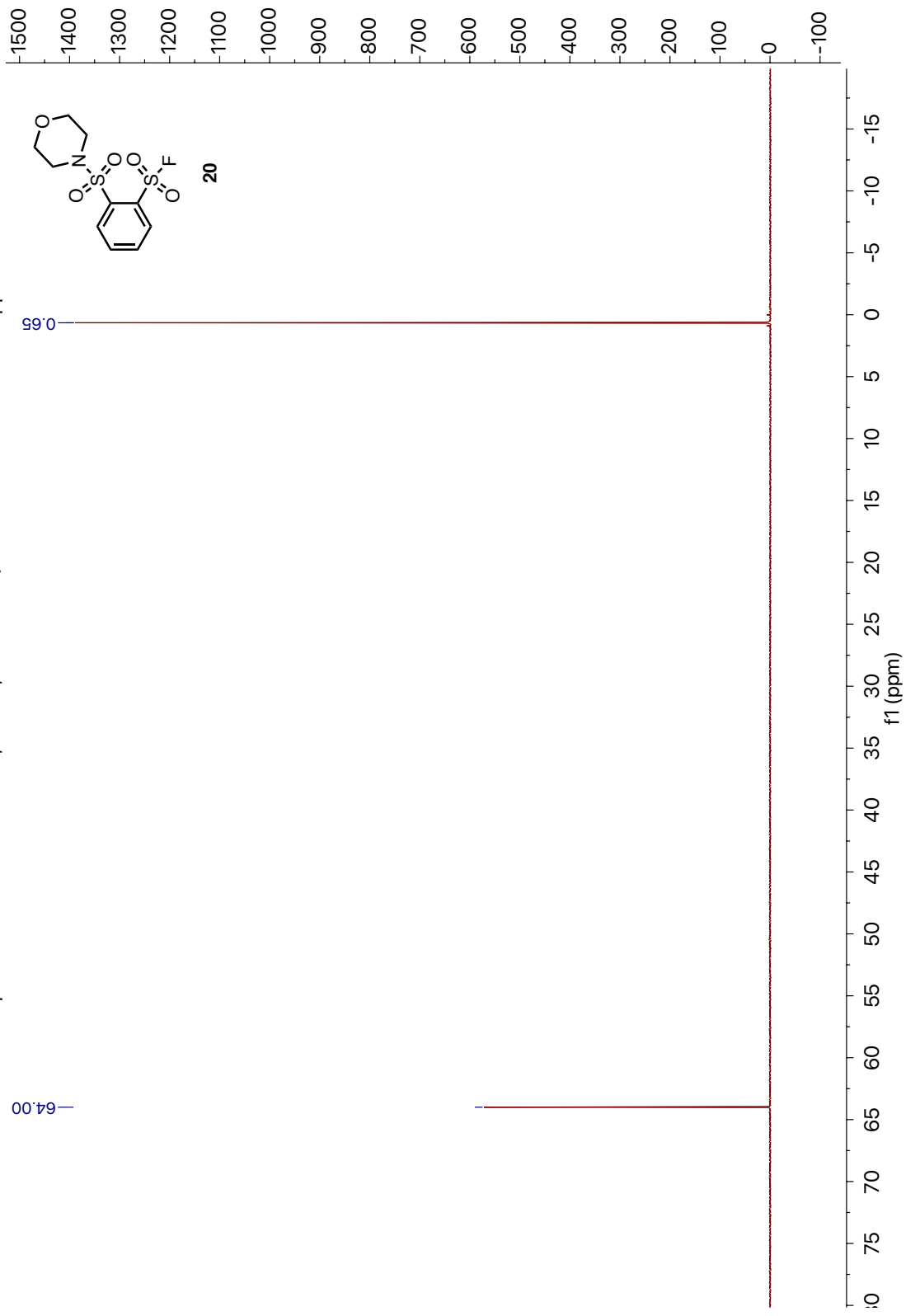
10.9. 2-(Morpholinosulfonyl)benzenesulfonyl fluoride (20)



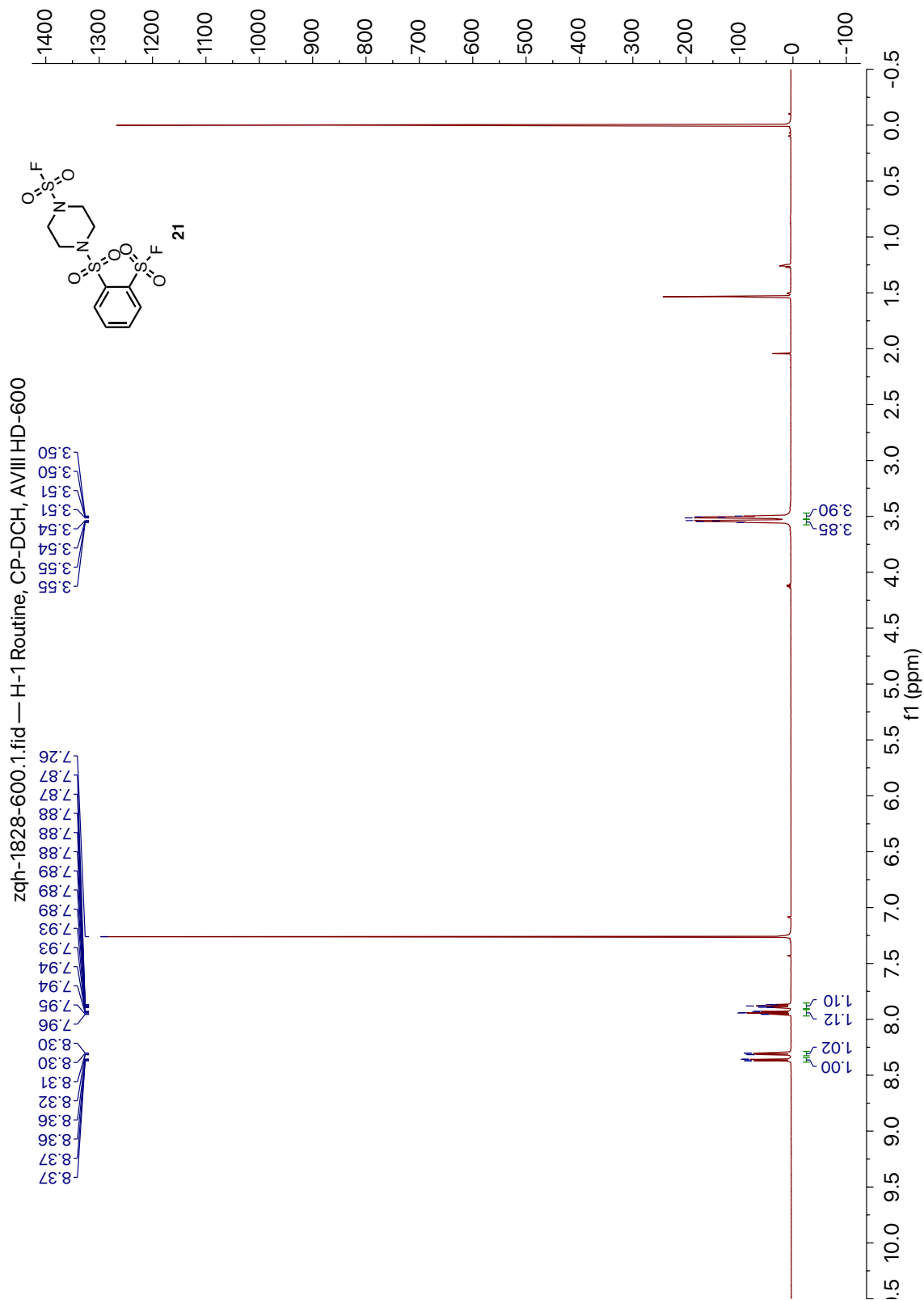
zqh-1806-600.2.fid — C-13 Routine 1D, CPDCH CryoProbe, AVIII-600



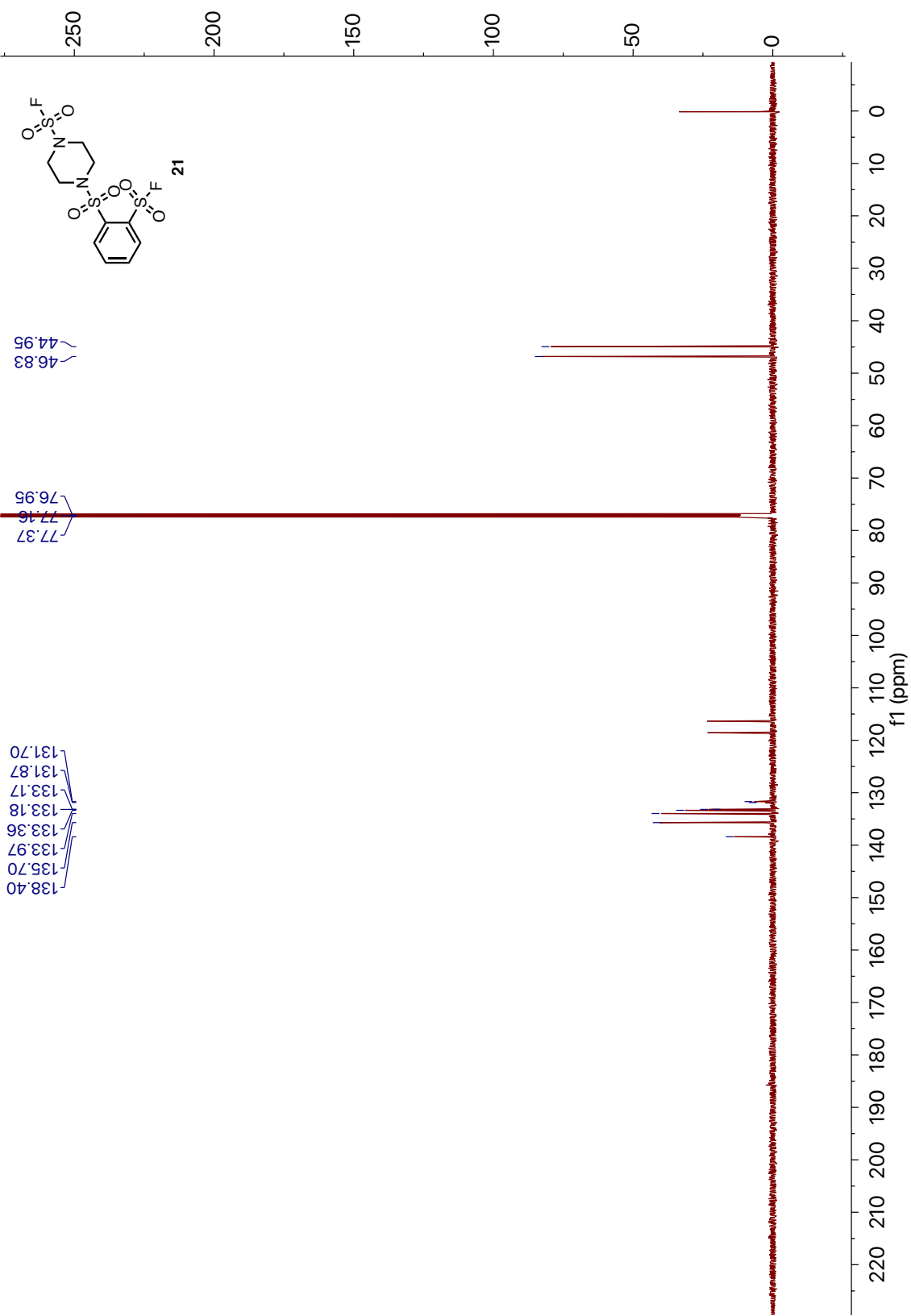
zqh-1806-400-f.1.fid — F-19, CDCI3, DPX-400 QNP Probe. CF3Cl as Ref at 0 ppm.

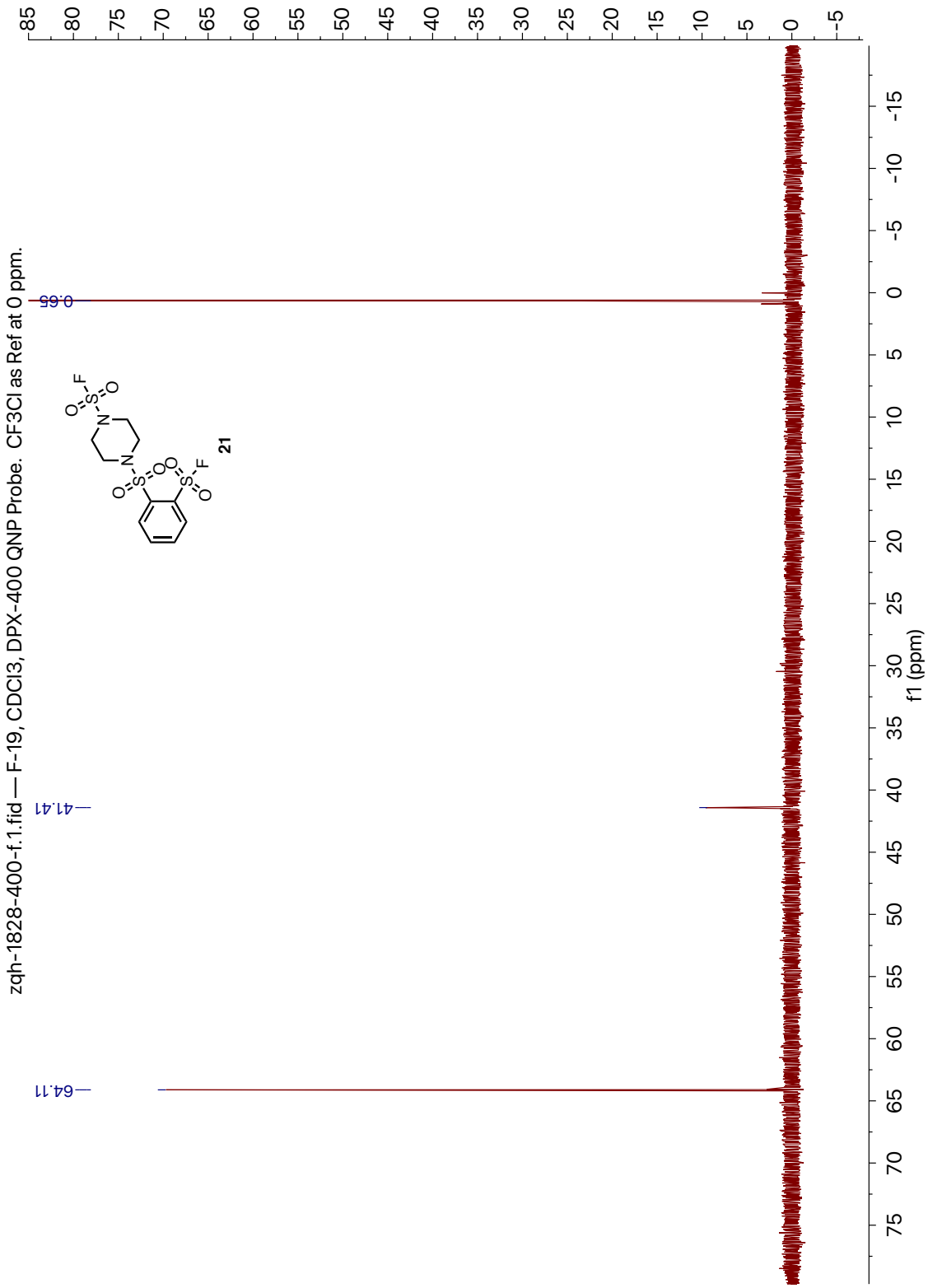


10.10. 4-((2-(Fluorosulfonyl)phenyl)sulfonyl)piperazine-1-sulfonyl fluoride (**21**)

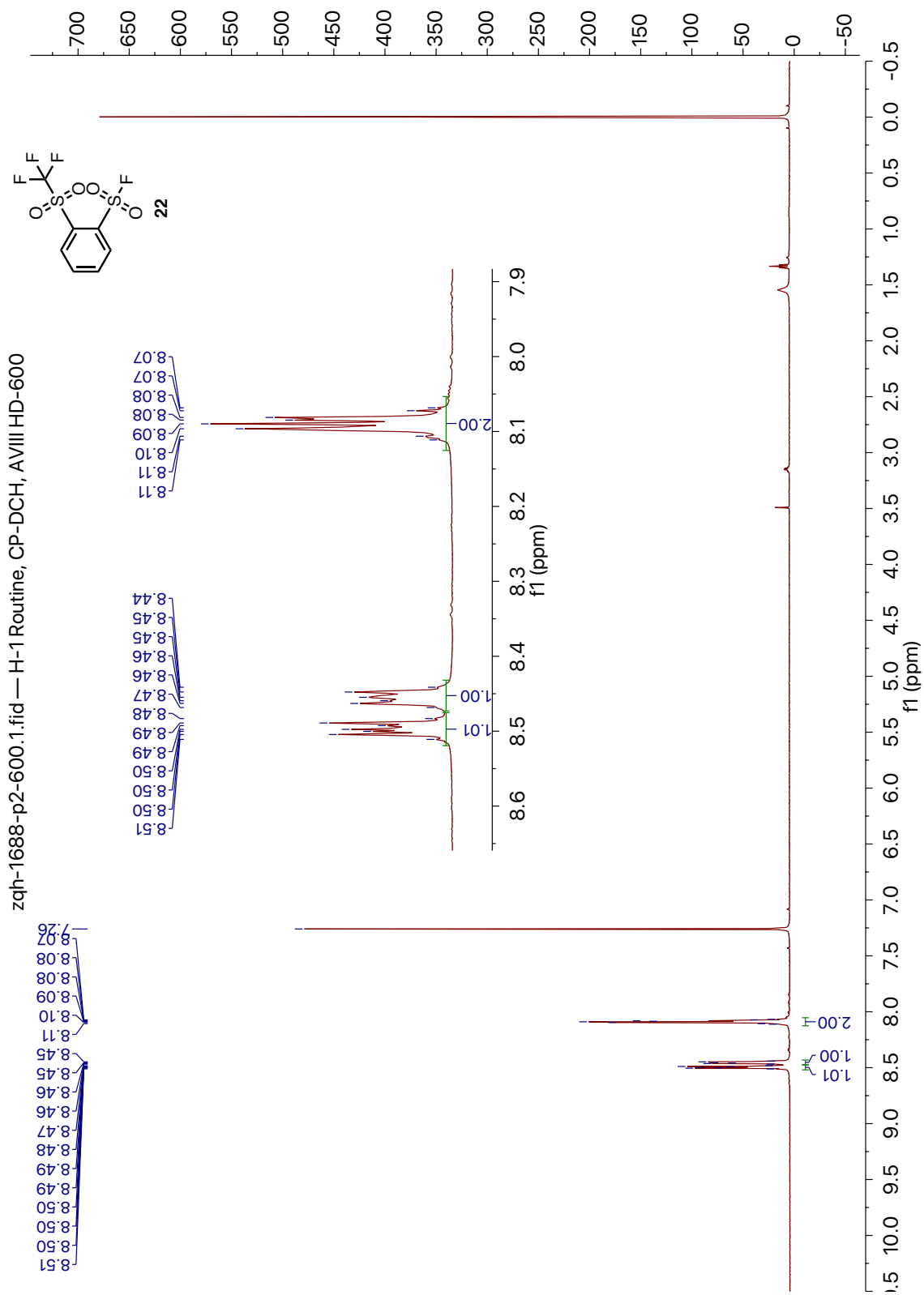


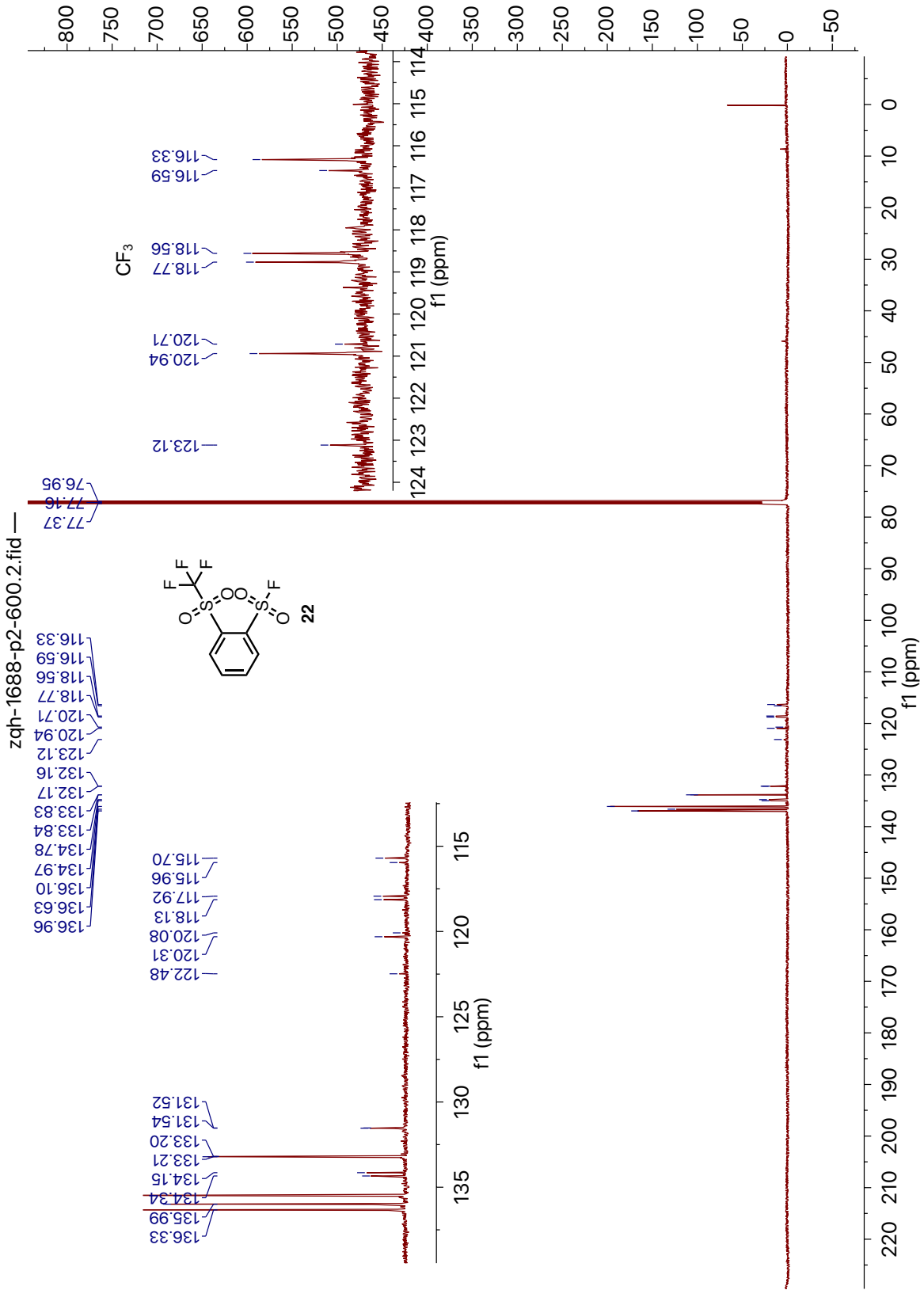
zqh-1828-600.2.fid — C-13 Routine 1D, CPDCH CryoProbe, AVIII-600



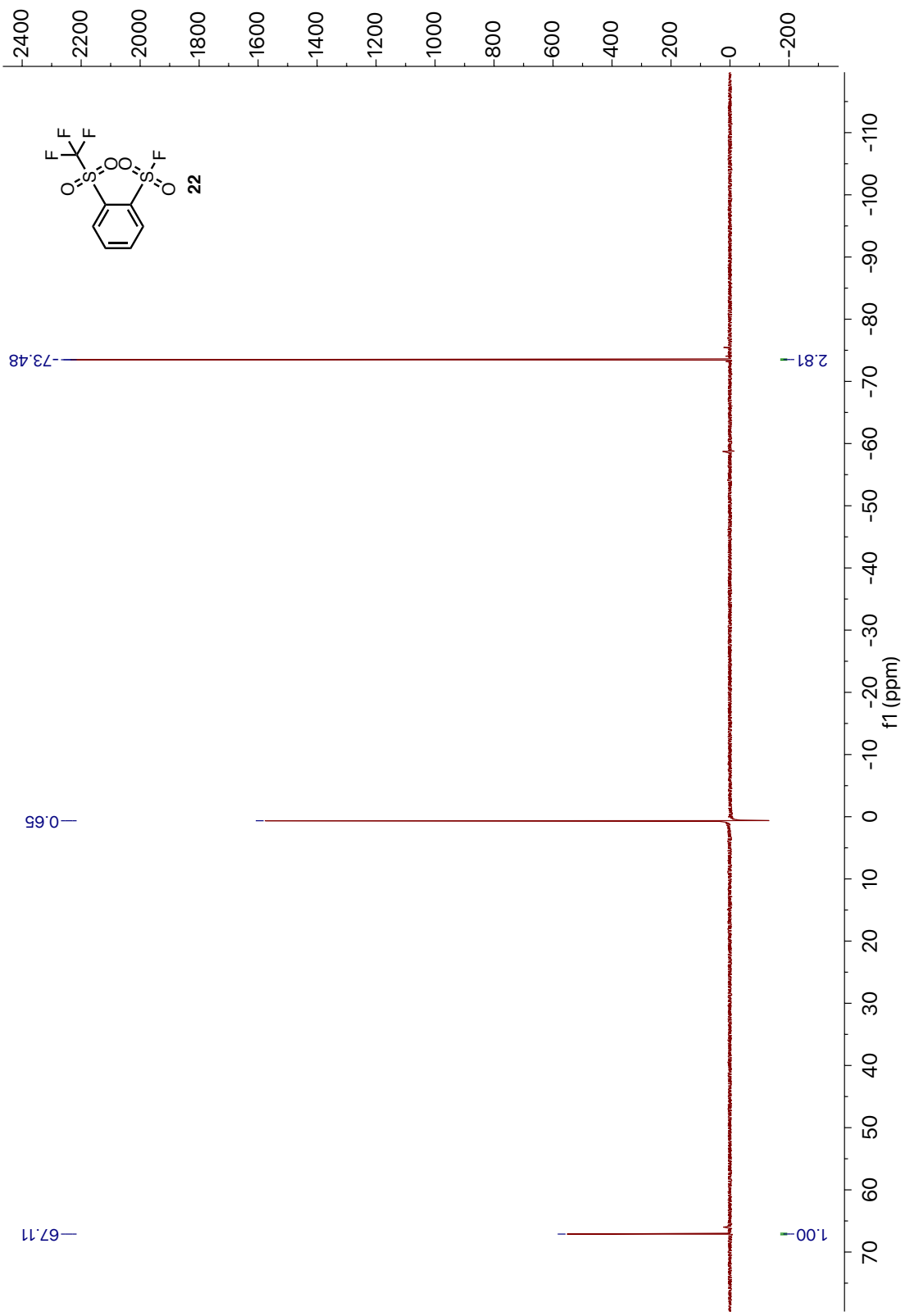


10.11. 2-((Trifluoromethyl)sulfonyl)benzenesulfonyl fluoride (22)

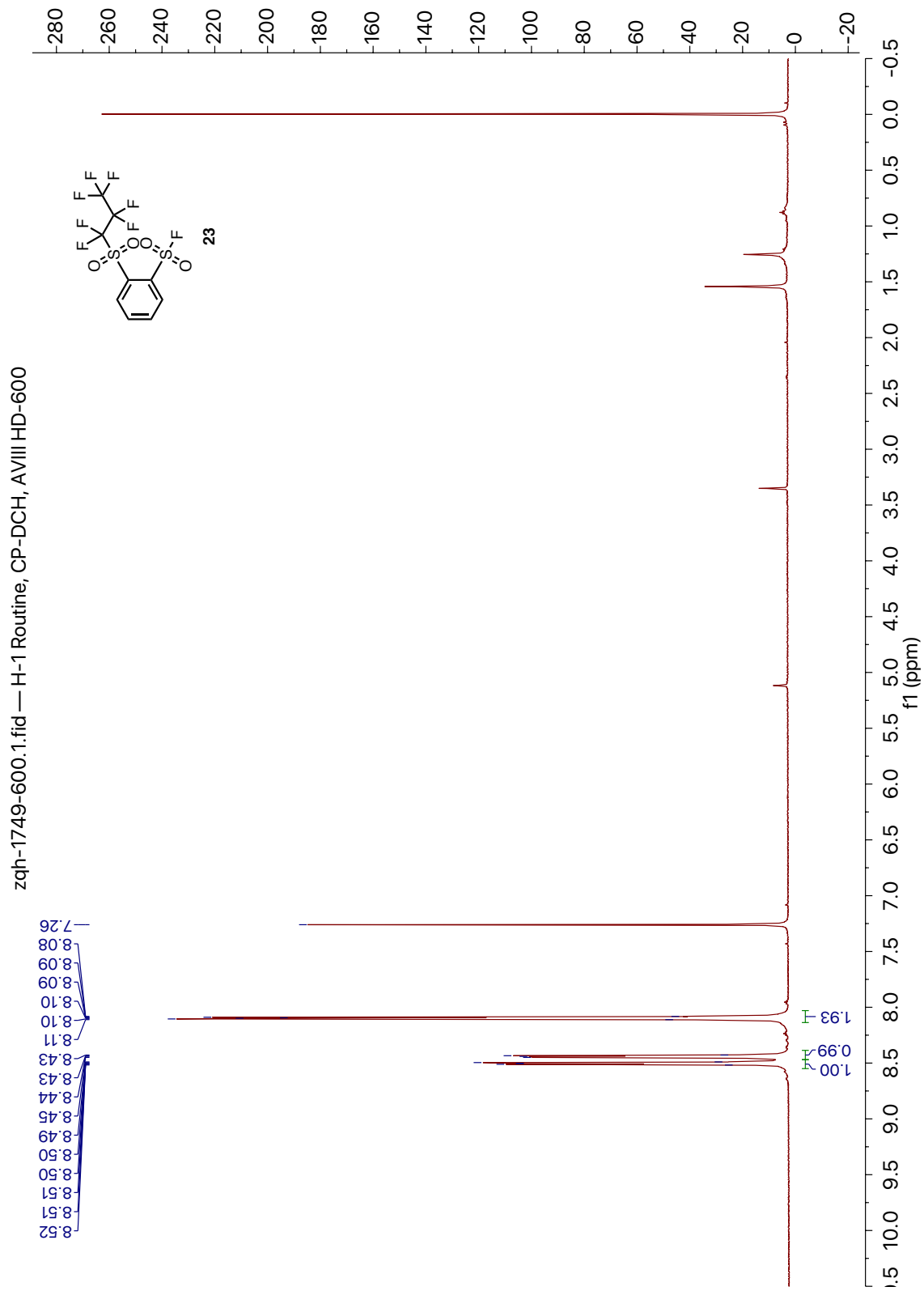




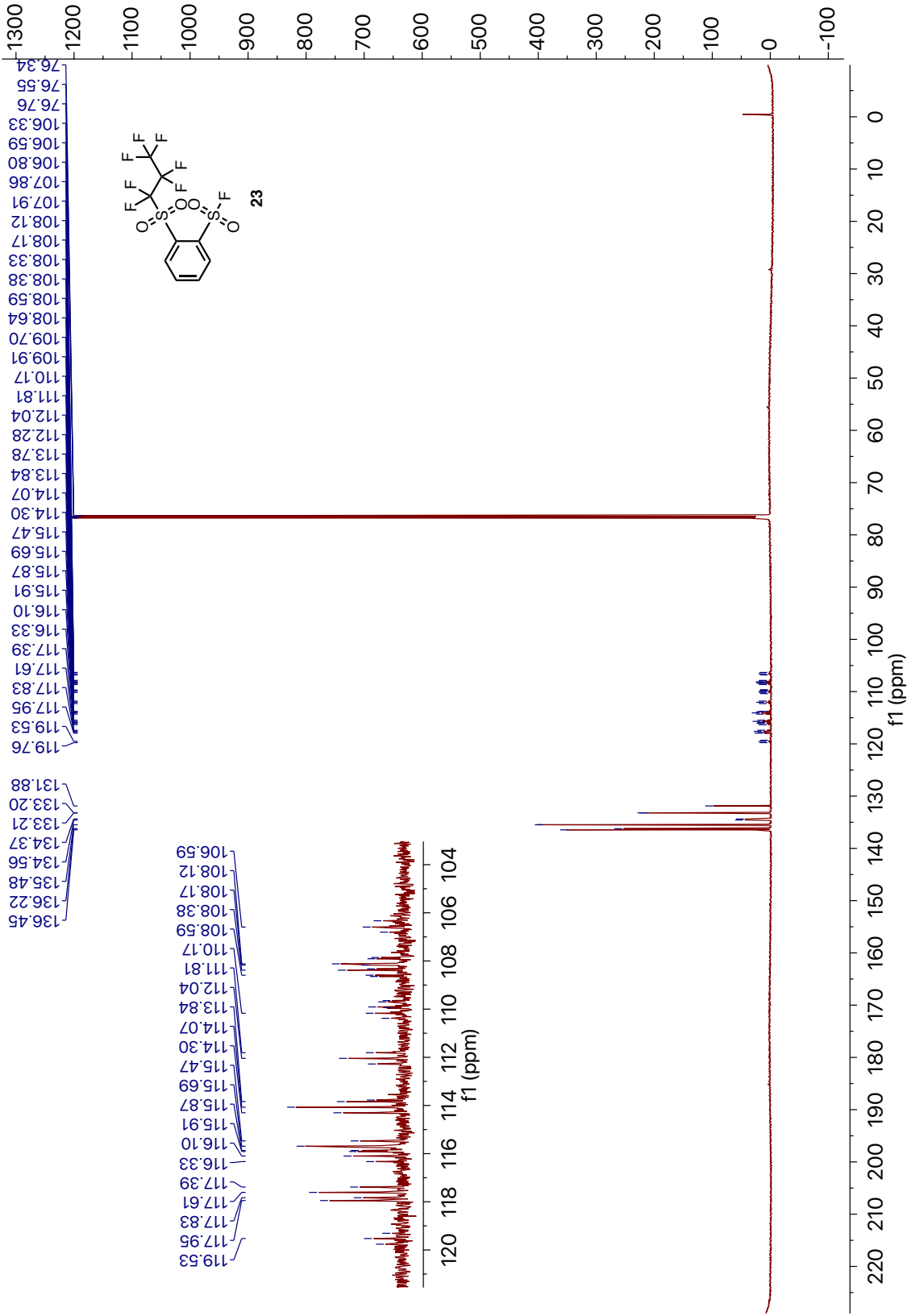
zqh-1688-p2-400.1.fid — F-19, CDCI3, DPX-400 QNP Probe. CF3Cl as Ref at 0 ppm.



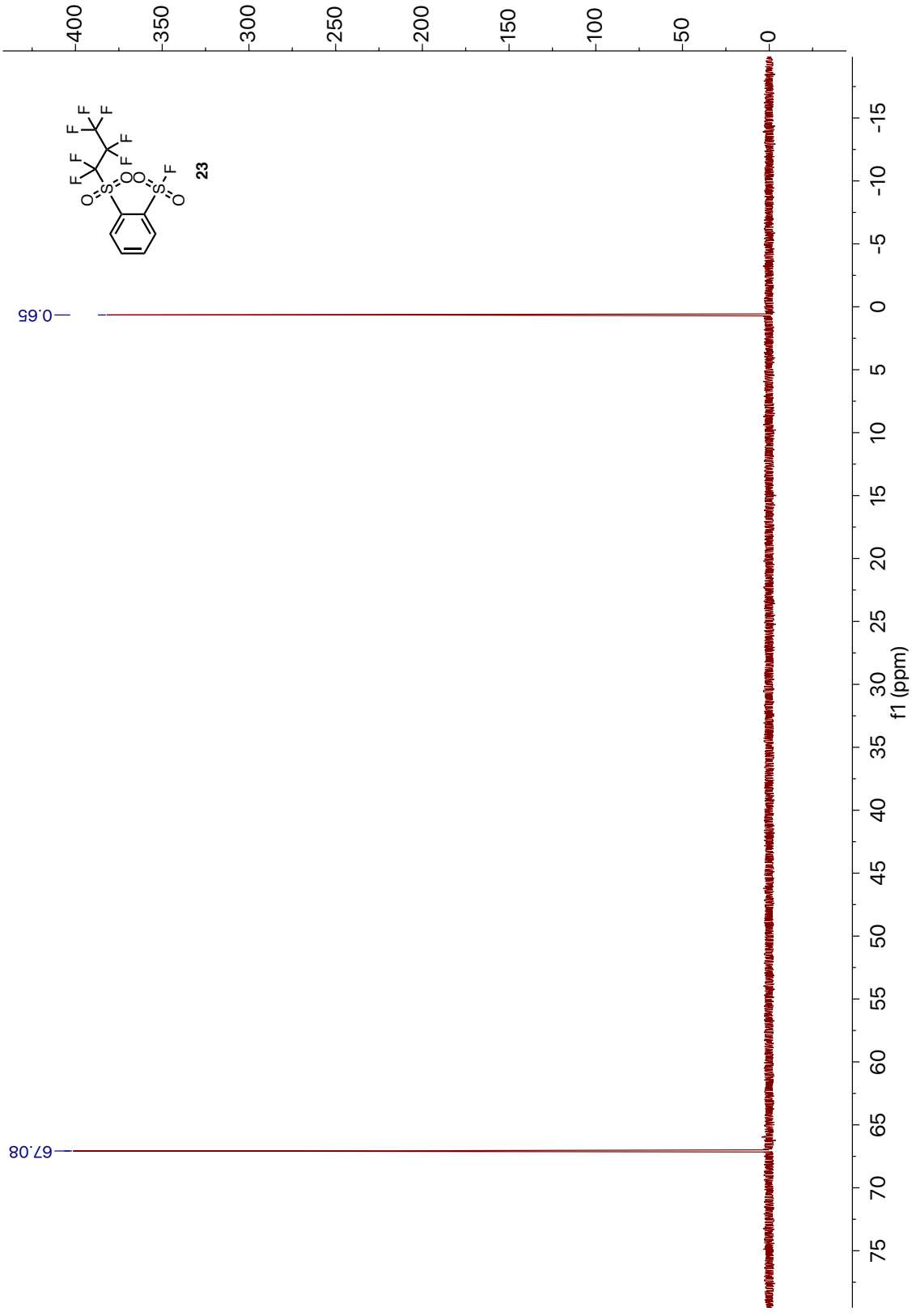
10.12. 2-((Perfluoropropyl)sulfonyl)benzenesulfonyl fluoride (23)



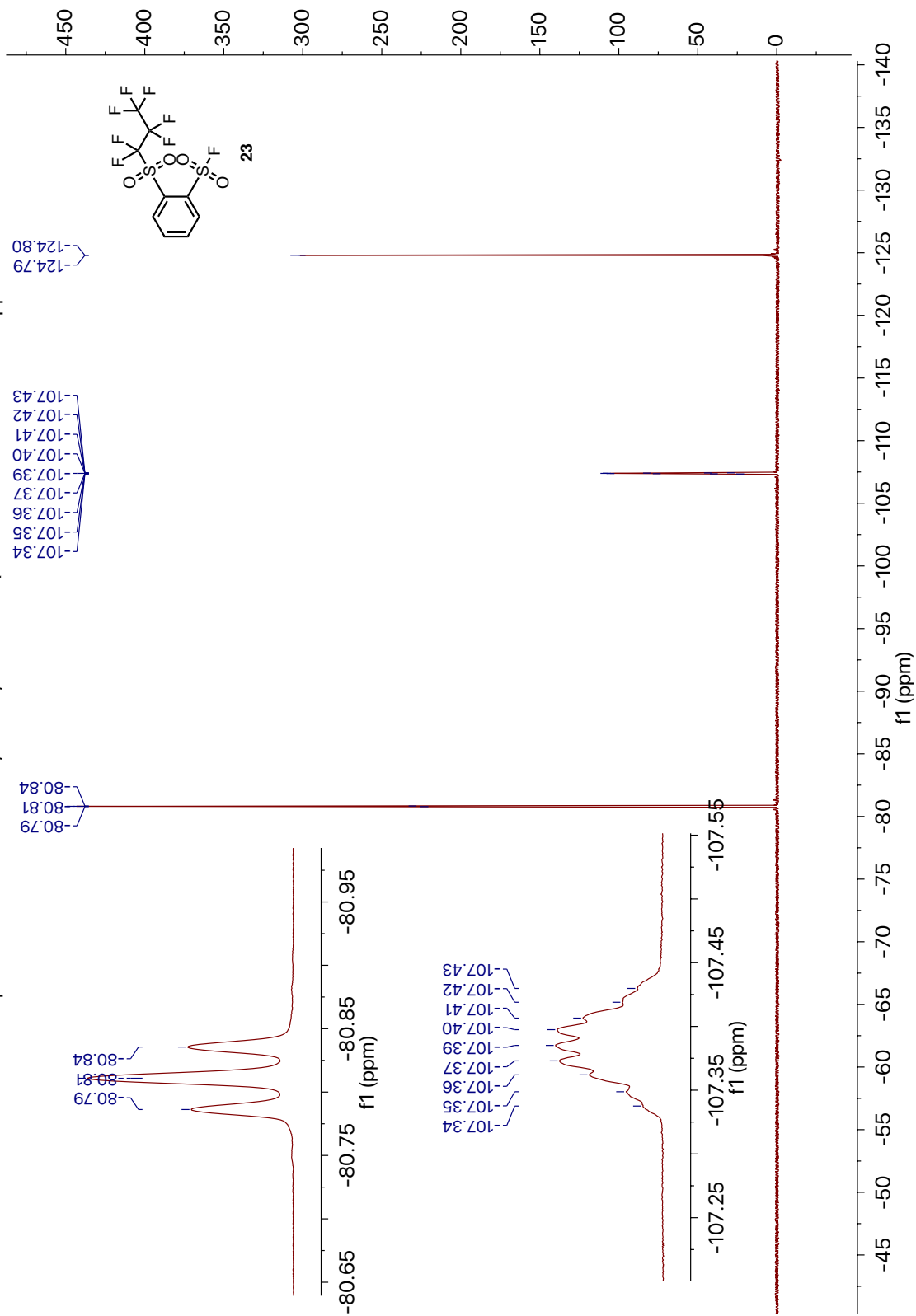
zqh-1749-600.2.fid — C-13 Routine 1D, CPDCH CryoProbe, AVIII-600



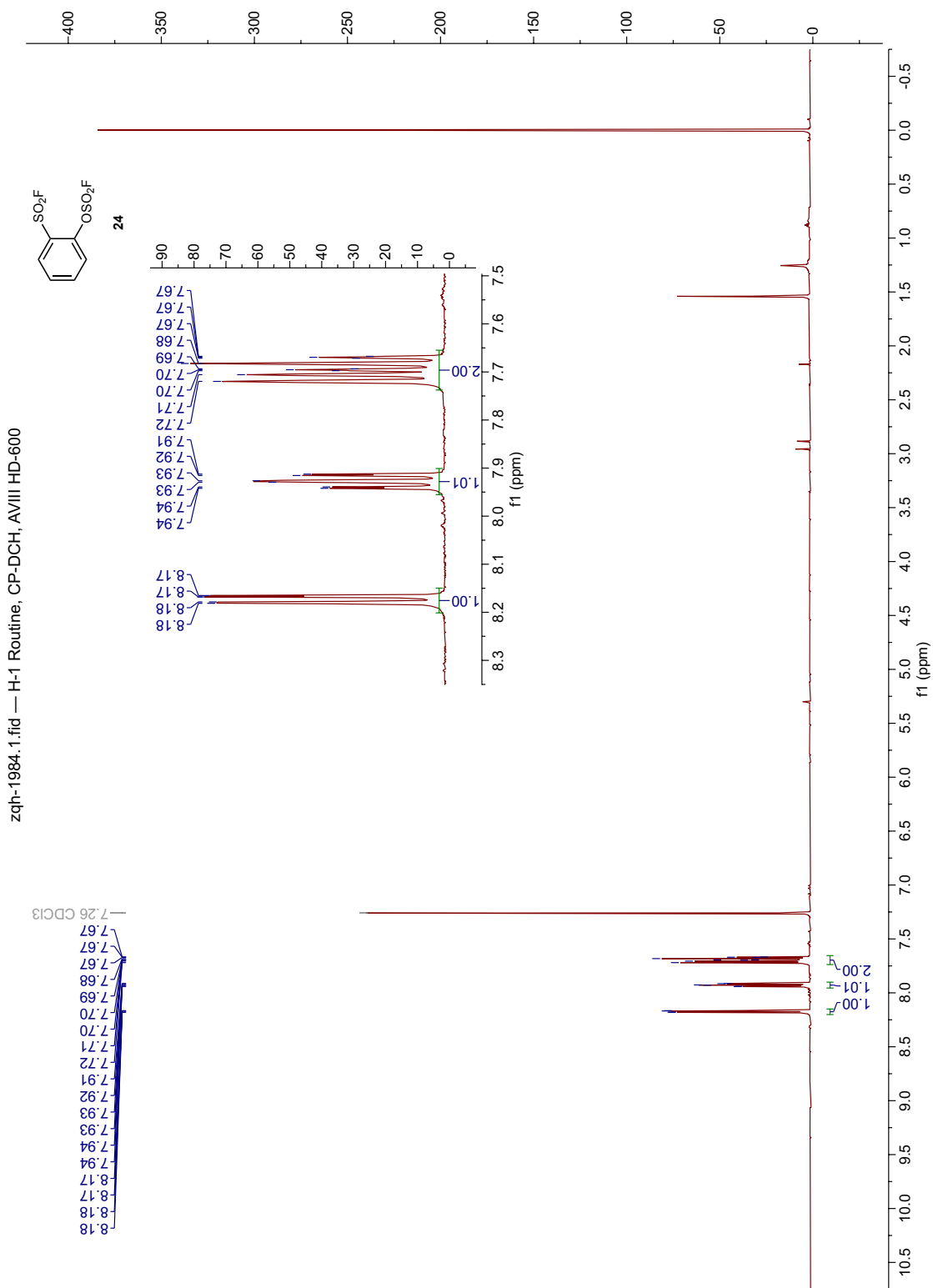
zqh-1749-400.1.fid — F-19, CDCl3, DPX-400 QNP Probe. CF3Cl as Ref at 0 ppm.



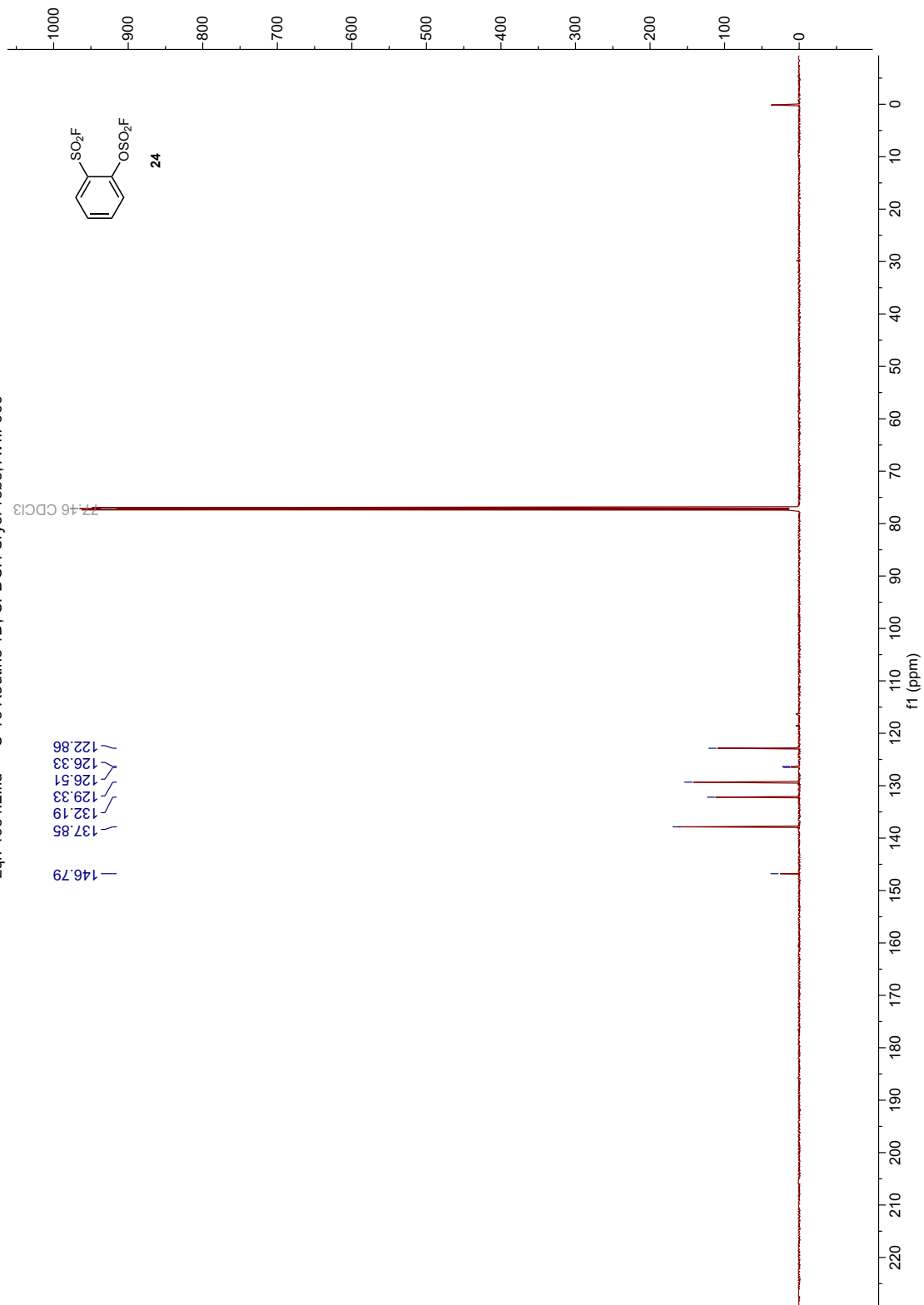
zqh-1749-400.4.fid — F-19, CDCl3, DPX-400 QNP Probe. CF3Cl as Ref at 0 ppm.

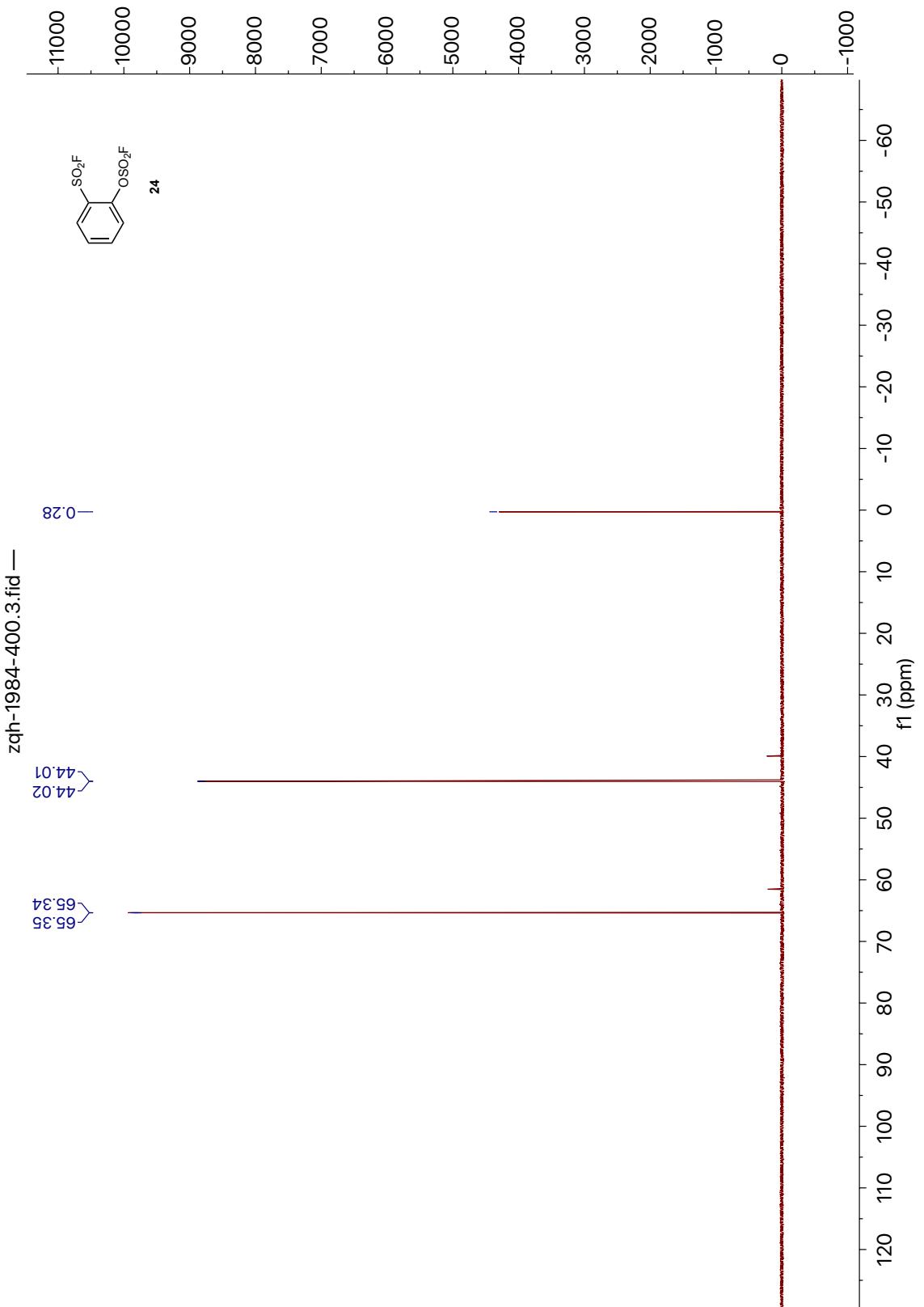


10.13. 2-(Fluorosulfonyl)phenyl fluorosulfate (**24**)



zqh-1984.2.fid — C-13 Routine 1D, CPDCH CryoProbe, AVIII-600





11. References

1. Rosenau CP, Jelier BJ, Gossert AD, & Togni A (2018) Exposing the Origins of Irreproducibility in Fluorine NMR Spectroscopy. *Angewandte Chemie-International Edition* 57(30):9528-9533.
2. Dong JJ, Krasnova L, Finn MG, & Sharpless KB (2014) Sulfur(VI) Fluoride Exchange (SuFEx): Another Good Reaction for Click Chemistry. *Angewandte Chemie-International Edition* 53(36):9430-9448.
3. Gakh AA, Romaniko SV, Ugrak BI, & Fainzilberg AA (1991) N-Fluorination with Cesium Fluoroxysulfate. *Tetrahedron* 47(35):7447-7458.
4. Nielsen MK, Ugaz CR, Li WP, & Doyle AG (2015) PyFluor: A Low-Cost, Stable, and Selective Deoxyfluorination Reagent. *Journal of the American Chemical Society* 137(30):9571-9574.
5. Tribby AL, Rodriguez I, Shariffudin S, & Ball ND (2017) Pd-Catalyzed Conversion of Aryl Iodides to Sulfonyl Fluorides Using SO₂ Surrogate DABSO and Selectfluor. *Journal of Organic Chemistry* 82(4):2294-2299.
6. Vanderpuy M (1988) Potassium Fluoride Catalyzed Fluorodesulfonylations of Aryl Sulfonyl Fluorides. *Journal of Organic Chemistry* 53(18):4398-4401.
7. Guo TJ, *et al.* (2018) A New Portal to SuFEx Click Chemistry: A Stable Fluorosulfonyl Imidazolium Salt Emerging as an "F-SO₂+" Donor of Unprecedented Reactivity, Selectivity, and Scope. *Angewandte Chemie-International Edition* 57(10):2605-2610.
8. Krutak JJ, Burpitt RD, Moore WH, & Hyatt JA (1979) Chemistry of Ethenesulfonyl Fluoride - Fluorosulfonylethylation of Organic-Compounds. *Journal of Organic Chemistry* 44(22):3847-3858.
9. Zha GF, *et al.* (2017) Palladium-Catalyzed Fluorosulfonylvinylation of Organic Iodides. *Angewandte Chemie-International Edition* 56(17):4849-4852.
10. Adolfsson H, Converso A, & Sharpless KB (1999) Comparison of amine additives most effective in the new methyltrioxorhenium-catalyzed epoxidation process. *Tetrahedron Lett* 40(21):3991-3994.
11. Smedley CJ, *et al.* (2019) Bifluoride Ion Mediated SuFEx Trifluoromethylation of Sulfonyl Fluorides and Iminosulfur Oxydifluorides. *Angew Chem Int Ed Engl* 58(14):4552-4556.

12. Stapels DAC, *et al.* (2014) Staphylococcus aureus secretes a unique class of neutrophil serine protease inhibitors. *Proceedings of the National Academy of Sciences of the United States of America* 111(36):13187-13192.
13. Stapels DAC, *et al.* (2018) Evidence for multiple modes of neutrophil serine protease recognition by the EAP family of Staphylococcal innate immune evasion proteins. *Protein Science* 27(2):509-522.
14. Hansen G, *et al.* (2011) Unexpected Active-Site Flexibility in the Structure of Human Neutrophil Elastase in Complex with a New Dihydropyrimidone Inhibitor. *Journal of Molecular Biology* 409(5):681-691.
15. McCoy AJ, *et al.* (2007) Phaser crystallographic software. *Journal of Applied Crystallography* 40:658-674.
16. Emsley P, Lohkamp B, Scott WG, & Cowtan K (2010) Features and development of Coot. *Acta Crystallographica Section D-Biological Crystallography* 66:486-501.
17. Adams PD, *et al.* (2010) PHENIX: a comprehensive Python-based system for macromolecular structure solution. *Acta Crystallographica Section D-Biological Crystallography* 66:213-221.
18. Laskowski RA, Moss DS, & Thornton JM (1993) Main-Chain Bond Lengths and Bond Angles in Protein Structures. *Journal of Molecular Biology* 231(4):1049-1067.
19. Hooft RWW, Vriend G, Sander C, & Abola EE (1996) Errors in protein structures. *Nature* 381(6580):272-272.
20. Davis IW, *et al.* (2007) MolProbity: all-atom contacts and structure validation for proteins and nucleic acids. *Nucleic Acids Research* 35:W375-W383.
21. de Garavilla L, *et al.* (2005) A novel, potent dual inhibitor of the leukocyte proteases cathepsin G and chymase - Molecular mechanisms and anti-inflammatory activity in vivo. *Journal of Biological Chemistry* 280(18):18001-18007.
22. Forli S, *et al.* (2016) Computational protein-ligand docking and virtual drug screening with the AutoDock suite. *Nature Protocols* 11(5):905-919.
23. Word JM, Lovell SC, Richardson JS, & Richardson DC (1999) Asparagine and glutamine: Using hydrogen atom contacts in the choice of side-chain amide orientation. *Journal of Molecular Biology* 285(4):1735-1747.

24. O'Boyle NM, *et al.* (2011) Open Babel: An open chemical toolbox. *Journal of Cheminformatics* 3.
25. Backus KM, *et al.* (2016) Proteome-wide covalent ligand discovery in native biological systems. *Nature* 534(7608):570-+.
26. Mortenson DE, *et al.* (2018) "Inverse Drug Discovery" Strategy To Identify Proteins That Are Targeted by Latent Electrophiles As Exemplified by Aryl Fluorosulfates. *Journal of the American Chemical Society* 140(1):200-210.
27. Wang N, *et al.* (2018) Genetically Encoding Fluorosulfate-l-tyrosine To React with Lysine, Histidine, and Tyrosine via SuFEx in Proteins in Vivo. *J Am Chem Soc* 140(15):4995-4999.
28. Suter C (1944) Derivatives of Aromatic Sulfonic Acids. 1 Sulfonyl Halides, Esters, and Anhydrides. *The Organic Chemistry of Sulfur: Tetravalent Sulfur Compounds*, (Wiley, New York), pp 452–458.